Discovering unknown Madagascar biodiversity: Integrative taxonomy of raft spiders (Pisauridae: *Dolomedes*)

Kuang-Ping Yu [1,2], Matjaž Kuntner [1, 3, 4, 5]

[1] Department of Organisms and Ecosystems Research, National Institute of Biology, Ljubljana, Slovenia

[2] Department of Biology, Biotechnical Faculty, University of Ljubljana, Ljubljana, Slovenia

[3] Jovan Hadži Institute of Biology, ZRC SAZU, Ljubljana, Slovenia

[4] Department of Entomology, National Museum of Natural History, Smithsonian Institution, Washington, DC, USA

[5] State Key Laboratory of Biocatalysis and Enzyme Engineering, and Centre for Behavioural Ecology and Evolution, School of Life Sciences, Hubei University, Hubei, China

Corresponding Author:
Kuang-Ping Yu [1]

[1] Department of Organisms and Ecosystems Research, National Institute of Biology, Večna pot 111, 1000 Ljubljana, Slovenia
Email address: Kuang-Ping.Yu@nib.si

Abstract

Madagascar is a global biodiversity hotspot, but its biodiversity continues to be underestimated and understudied. Of raft spiders, genus *Dolomedes* Latreille, 1804, literature only reports a single species on Madagascar. Our single expedition to humid forests of eastern and northern Madagascar, however, yielded a series of *Dolomedes* exemplars representing both sexes of five morphospecies. To avoid only using morphological diagnostics, we devised and tested an integrative taxonomic model for *Dolomedes* based on the unified species concept. The model first determines morphospecies within a morphometrics framework, then tests their validity via species delimitation using COI. It then incorporates habitat preferences, geological barriers, and dispersal related traits to form hypotheses about gene flow limitations. Our results reveal four new *Dolomedes* species described from both sexes as *Dolomedes gregoric* **sp. nov.**, *D. bedjanic* **sp. nov.**, *D. hydatostella* **sp. nov.**, and *D. rotundus* **sp. nov.** The range of *D. kalanoro* Silva & Griswold, 2013, now also known from both sexes, is expanded to eastern Madagascar. By increasing the known raft spider diversity from one to five, our results merely scratch the surface of the true *Dolomedes* species diversity on Madagascar. Our integrative taxonomic model provides the framework for future revisions of raft spiders anywhere.

Introduction

56 Madagascar is well known for its diverse and unique biota (Antonelli et al., 2022). The island's
57 diverse habitats, including humid forests, dry spiny forests, tapia woodlands, and coastal areas,
58 provide niches for an incredible variety of flora and fauna found nowhere else on the planet.
59 Madagascar is renowned for its iconic inhabitants, such as lemurs, chameleons, and baobab trees,
60 but the richness and endemicity extend to numerous other organisms, including insects, reptiles,
61 birds, and spiders. Although currently positioned close to continental Africa, Madagascar was
62 part of the Indian subcontinent for around 50 million years since the break off from Gondwana
63 (Sanmartín & Ronquist, 2004; Ali & Aitchison, 2008). The combination of a unique geological
64 history of Madagascar and its long isolation for around 84 million years has affected the
65 evolution of organisms inhabiting the island resulting in extremely high endemism rates (Buerki
66 et al., 2013; Antonelli et al., 2022). Despite a long and lively history of biodiversity research of
67 Madagascar its biota continues to be vastly underestimated. Bridging this knowledge gap is
68 critical for conservation of Madagascar's biodiversity that is undergoing major threats and losses
69 due to human activities (Ralimanana et al., 2022).
70   The globally distributed spider genus *Dolomedes* Latreille, 1804—known as raft- or
71 fishing spiders—contains around 100 species (World Spider Catalog, 2023). Being large and
72 iconic, with semi-aquatic lifestyles, and often predators of freshwater vertebrates in addition to
73 invertebrates, *Dolomedes* species are model organisms in diverse fields such as behavioral
74 ecology (Bleckmann & Bender, 1987; Suter & Gruenwald, 2000; Johnson, 2001; Johnson & Sih,
75 2007; Schwartz, Wagner & Hebets, 2013; Kralj-Fišer et al., 2016) and conservation biology
76 (Smith, 2000; Duffey, 2012; Leroy et al., 2013). While *Dolomedes* has been well surveyed in
77 some regions (Carico, 1973; Smith, 2000; Zhang, Zhu & Song, 2004; Tanikawa & Miyashita,
78 2008; Vink & Dupérré, 2010; Raven & Hebron, 2018), our knowledge of *Dolomedes* in the
79 tropics is much more limited. One region that stands out in this respect is Madagascar.
80   Strand's (1907) description of *Dolomedes saccalavus* Strand, 1907 from Nosy Be
81 (Nossibé) was the first *Dolomedes* record in Madagascar. However, Silva and Griswold (2013a)
82 considered the species as *nomen dubium* as the original description was based on a subadult
83 female and the type specimen was destroyed. *Dolomedes kalanoro* Silva & Griswold, 2013 is
84 currently the only valid *Dolomedes* species from Madagascar. Silva and Griswold (2013a)
85 described the species from two male specimens collected from rivers in dry and subhumid forests
86 in the west and the south of the island. Although the humid forests in the east and the north of
87 Madagascar harbor the highest biodiversity on the island (Antonelli et al., 2022), surprisingly, no
88 *Dolomedes* species have been described there. During our single expedition to two National
89 Parks, Marojejy in the north and Andasibe-Mantadia in the east of Madagascar, we discovered
90 several morphospecies of *Dolomedes*. These exemplars have proven to be difficult to assign to
91 species using conventional morphological diagnostics.
92   As in numerous other clades, defining clear species boundaries among closely related
93 *Dolomedes* species is difficult using a single line of evidence (see Tanikawa & Miyashita, 2008;
94 Vink & Dupérré, 2010). Recent taxonomic reviews of *Dolomedes* (Tanikawa, 2003; Zhang, Zhu
95 & Song, 2004; Tanikawa & Miyashita, 2008; Vink & Dupérré, 2010; Raven & Hebron, 2018)

96   have used different combinations of characteristics for species diagnostics (Table 1). The
97   characteristic that all prior studies had in common relate to habitus coloration and the
98   morphology of the male palpal retrolateral tibial apophysis (RTA) and the female epigynal
99   middle field (MF) (Table 1). These structures, however, can show intraspecific variation (see
100   Tanikawa & Miyashita, 2008; Vink & Dupérré, 2010) and may introduce ambiguity in species
101   taxonomy (see Zhang, Zhu & Song, 2004; Tanikawa & Miyashita, 2008). To avoid this problem
102   and to strengthen species boundaries, only two prior studies have added other types of evidence
103   such as DNA barcodes and habitat preferences (Table 1) (Tanikawa & Miyashita, 2008; Vink &
104   Dupérré, 2010). So far, these two are the only revisions of *Dolomedes* that have approached the
105   definition of integrative taxonomy (Dayrat, 2005).
106   To establish a comparative framework for future *Dolomedes* taxonomic discoveries (see
107   Schlick-Steiner et al., 2010; Bond et al., 2022), our study aims to: i) treat variation in
108   morphological features within a statistical framework in order to utilize the best combination of
109   the diagnostic characteristics among Madagascar *Dolomedes*; and ii) define robust species
110   boundaries among Madagascar *Dolomedes* using an integrative taxonomic model which includes
111   morphological, molecular, and ecological evidence.
112

Materials & Methods

Taxon sampling

115   We collected *Dolomedes* exemplars by hand both day and night (research permit issued by
116   Direction des Aires Protégées, des Ressources Naturelles renouvelables et des Ecosystèmes;
117   N°166/20/MEDD/SG/DGGE/DAPRNE/SCBE.Re). Specimens were preserved in 75% ethanol
118   for morphological examination. Two to four legs of each specimen were removed and preserved
119   separately in 96% ethanol for DNA extraction and molecular analyses. Specimens examined in
120   this study are held at the National Institute of Biology (NIB) in Slovenia (voucher code KPARA)
121   while the type series are deposited at the National Museum of Natural History, Smithsonian
122   Institution (USNM), Washington, DC, USA (voucher code USNMENT). We also included
123   original Madagascar sequences of a *Dolomedes* species that is being described from Réunion
124   (Cazanove et al., in prep.). In addition, we examined a male *Dolomedes* sp. collected by Pauly A.
125   in January of 1995 at forêt Analalava, Foulpointe, Tamatave, Madagascar deposited at the Royal
126   Museum for Central Africa (RMCA, voucher code: MT_207084). Representing an outgroup
127   clade to the Madagascar *Dolomedes*, we included a sequence of *Dolomedes raptor* Bösenberg &
128   Strand, 1906 from Taiwan (Yu & Kuntner, unpublished data).
129

Anatomical examination

131   We used Leica M205C stereomicroscope and Keyence digital microscope VHX7000 to examine,
132   measure, and image specimens. All the measurements given are in millimeters (mm). The
133   measurements of palps consisted of femur, patella, tibia, and tarsus or cymbium while those of
134   legs consisted of femur, patella, tibia, metatarsus, and tarsus. Variation values were presented as
135   "mean ± s.d.". Female epigyna were dissected and cleaned in Potassium hydroxide (KOH)

136   solution. Male right palps were expanded by repeatedly soaking in distilled water and KOH
137   solution for further morphological analyses.
138   Abbreviations used: AB: accessory bulb; AER: anterior eye row; AME: anterior median
139   eye; ALE: anterior lateral eye; BCA: basal cymbium apophysis; BS: base of spermathecae; Co:
140   conductor; CD: copulatory duct; Cy: cymbium; COp: copulatory opening; DTP: distal tegular
141   projection; DST: distal sclerotized tube of apical division; DTA: distal tegular apophysis; Eb:
142   embolus; EF: epignal fold; Fu: fulcrum; FD: fertilization duct; HS: head of spermathecae; LA:
143   lateral subterminal apophysis; LL: lateral lobe; MA: median apophysis; MF: middle field; MOA:
144   median ocular region; PER: posterior eye row; PME: posterior median eye; PLE: posterior
145   lateral eye; RTA: retrolateral tibial apophysis; Sa: saddle; T: tegulum.
146

Integrative taxonomy
148   Our integrative taxonomy model combined original morphological, molecular, and ecological
149   data (Fig 1) based on the unified species concept (de Queiroz, 2005, 2007; see also Schlick-
150   Steiner et al., 2010). Using morphological data as the primary evidence (morphology-first, see
151   Hedin & Milne, 2023), we first classified all specimens into groups by descriptive species
152   diagnosis. The observed differences and those commonly used diagnostic characteristics (Table
153   1) were put into detailed size comparisons and intragroup morphometric framework to facilitate
154   species hypotheses. We then tested the species hypotheses using a molecular phylogeny and
155   molecular species delimitation. We also included habitat preferences, potential geological
156   barriers, and dispersal-related traits in adding credits to the species hypotheses considering
157   potential geneflow limitations.
158   *Morphological comparisons and dispersal-related traits*
159   We compared the variation of sizes and shapes of the selected characteristics. For size
160   comparisons, we chose measurements of six characteristics: carapace width, relative length of
161   leg I (leg I length divided by carapace width), relative length of tarsus I (tarsus I length divided
162   by leg I length), relative length of male palp (palp length divided by carapace width), relative
163   length of male palp Cy (Cy length divided by palp tibia length), and diameter of the male
164   embolic ring (D_e, see Fig S1A). We used Photoshop 2022 to recalibrate the images of male DST
165   into one magnification. We then rotated the images until the tip and the outer basal point of the
166   embolus were positioned on the same horizontal reference line (baseline). A vertical and a
167   horizontal reference line were then added to define the maximum distance between the baseline
168   and the outer margin of the embolic ring. Such maximum distance was given as D_e (see Fig
169   S1A). D_e was then measured under the software ImageJ (Schneider, Rasband & Eliceiri, 2012).
170   We performed one-way Analyses of Variance (ANOVA) with hypothesized morphospecies as
171   the factor. If the results from the ANOVA are significant (p-value < 0.05), Tukey's honestly
172   significant difference (Tukey HSD) was followed to test whether the sizes of the selected
173   structures are different between pairs of morphospecies. We performed the above analyses in R
174   version 4.2.1 (R Core Team, 2022).

175   For shape comparisons, we chose ten structures to be included into morphometric
176   analyses, including three structures form the expanded male right palp, Eb (retrolateral view, Fig
177   S1A), Fu (retrolateral view, Fig S1B), and LA (retrolateral view, Fig S1C); four structures from
178   the male left palp, MA (ventral view, Fig S2A) , Eb (ventral view, Fig S2B), Fu (ventral view,
179   Fig S2C), and RTA (posterolateral view, Fig S2D); and three female genital structures, margin of
180   epigynum (ventral view, Fig S3A), MF (ventral view, Fig S3B), and vulva (dorsal view, Fig
181   S3C); see also Table S1 for descriptions of each landmarks. We then recalibrated the images into
182   the same magnification and resized them into 30 cm × 20 cm, 72 dpi in Photoshop 2022. Six
183   additional reference lines (see Fig S1A) were added to the images of male DST, on the basis of
184   those used in measuring D_e, to support the consistency of landmark plotting within embolus. We
185   first added the six reference lines at the same position as the baseline. With the intersection point
186   between the baseline and the vertical line as the center, we then rotated each line to equally
187   divide the embolus by 22.5 degrees.
188   We imported the images to the software ImageJ for landmark plotting. All the landmarks
189   chosen in this study are Type II landmarks determined by the following criteria: i) the maximum
190   or minimum curvatures, ii) the attach or intersection point between borders, or iii) the tip of the
191   structure. See Table S1 For details of landmarks in each structure. We performed Generalized
192   Procrustes analyses (GPA) to isolate the shape allometries caused by sizes. Each landmark
193   configuration was rotated and scaled by its centroid size. Via GPA, the shape component of the
194   structure of each specimen can be represented by a point projected in an n-dimensional space, in
195   which n equals the number of landmarks. We then performed principal component analyses
196   (PCA) to determine the two component axes that demonstrate the highest proportion of shape
197   variation. For details of this methodology, see Klingenberg (2016).
198   Because small sample sizes can introduce unwanted sampling error in morphometrics
199   (Cardini & Elton, 2007), we avoided the commonly used one-way multivariate analysis of
200   variance in determining whether the shape components are significantly different among species.
201   Instead, we investigated how shape components change along the first two PC axes (PC1, PC2).
202   Distribution patterns of the projection points on the first two PC axes were used to i) support
203   statistical evidence in facilitating morphospecies hypotheses, ii) compare shape variations of
204   different characteristics within and among morphospecies, and iii) support the species diagnosis
205   in the taxonomy section. All the morphometric analyses were performed in R version 4.2.1 using
206   the package "geomorph" (Adams & Otárola-Castillo, 2013).
207   We used the relative length of leg I and tarsus I from the above size comparison to
208   estimate the dispersal abilities of each species. Following the basic assumption that the length of
209   legs could refer to the ability of walking, species with relatively long leg I were considered to be
210   good terrestrial dispersers. On the other hand, *Dolomedes* are known for their rafting behavior
211   and aquatic dispersal (Suter, 1999; Suter, Stratton & Miller, 2004; Duffey, 2012). By linking the
212   morphology and habitat preferences among groups of wandering spiders, Lapinski and
213   colleagues (2015) indicated that the relatively longer tarsus may facilitate semi-aquatic

214 locomotion. Therefore, we considered species with relatively long tarsus I to be good aquatic
215 dispersers.

216 *Molecular phylogeny and species delimitation*

217 We extracted genomic DNA of Madagascar *Dolomedes* by Qiagen DNeasy Blood & Tissue Kit
218 (Qiagen, Valencia, CA, USA) following the manufacturer's instructions. We amplified
219 cytochrome c oxidase I (COI) from at least a pair of mature *Dolomedes* per morphospecies per
220 locality for the reconstruction of gene trees and for molecular species delimitation. PCR reaction
221 mixture (25 μL) contained 12.5 μL of EmeraldAmp MAX HS PCR Master Mix (Takara Bio Inc,
222 USA), 0.5 μL (10 pmol / μL) of the forward primer (LCO: 5'-
223 GGTCAACAAATCATAAAGATATTGG-3', Folmer et al., 1994) and the reverse primer
224 (Maggie: 5'- GGATAATCAGAATATCGTCGAGG-3', Hedin & Maddison, 2001), 8.0–9.0 μL
225 of distilled water, and 2.5–3.5 μL of genomic DNA. Sequence amplification protocols started at
226 94°C for 2 minutes followed by 35 cycles of 30 seconds of denaturation at 94°C, 30 seconds of
227 annealing started at 46°C, + 0.3°C per cycle until 52°C, and 120 seconds of polymerizing at
228 68°C. PCR products were sent to Macrogen Europe B.V. (Amsterdam, Netherlands) for
229 purification and sequencing. All sequences were edited and aligned in Geneious Pro 5.6.7 and
230 uploaded to GenBank (see Table S2).

231 We first performed Assemble Species by Automatic Partitioning (ASAP) (Puillandre,
232 Brouillet & Achaz, 2021) under Kimura 2 genetic distance substitution model (Kimura, 1980).
233 To obtain COI gene trees, we performed a maximum likelihood (ML) and a Bayesian inference
234 (BI) phylogenetic analysis on the CIPRES Science Gateway portal (Miller et al. 2010) with
235 sequences partitioned by codon. The ML analysis was done in RAxML with 1,000 bootstrap
236 replicates using the program's rapid bootstrapping algorithm (Stamatakis, 2014). The BI analysis
237 was performed in MrBayes (Huelsenbeck & Ronquist, 2001) under the substitution model GTR
238 + I + G, suggested by jModelTest (Posada, 2008), with 10 million generations ran independently
239 in two chains. Trees were sampled every 10,000 generations with 25% burn-in of the trees. We
240 then summarized the topologies of the two gene trees by SumTrees Version 4.0.0 (Sukumaran &
241 Holder, 2015) under DendroPy (Sukumaran & Holder, 2010) with the topology with overall
242 higher nodal supports set as the target tree. We then imported the summarized tree into a
243 Bayesian implementation of the Poisson tree process (bPTP) species delimitation under
244 maximum likelihood and Markov chain Monte Carlo (Zhang et al., 2013).

245 *Habitat preferences estimation and geological barriers*

246 Based on our field observations and the literature by Vink and Dupérré (2010), we chose canopy
247 coverage (open or dense) and water velocity (flowing or standing) as the factors in classifying
248 habitats. We then classified the localities where *Dolomedes* were collected into four categories
249 (Fig S4) to generate a rough estimation of the habitat preference of each species.

250 We estimated the geological barriers by the connectivity of rivers or waterbodies between
251 localities where *Dolomedes* specimens were collected. We obtained the information on river
252 drainages from the maps provided by the two national parks and the open online data sources on
253 DIVA-GIS (https://www.diva-gis.org). Localities were pinpointed to the map under QGIS

254   3.22.10 (QGIS.org, 2023). We considered those localities connected to the same river drainage to
255   represent only low geological barriers with relatively higher possibilities of gene flow.
256
257   **Nomenclatural acts**
258   The electronic version of this article in Portable Document Format (PDF) will represent a
259   published work according to the International Commission on Zoological Nomenclature (ICZN),
260   and hence the new names contained in the electronic version are effectively published under that
261   Code from the electronic edition alone. This published work and the nomenclatural acts it
262   contains have been registered in ZooBank, the online registration system for the ICZN. The
263   ZooBank LSIDs (Life Science Identifiers) can be resolved and the associated information viewed
264   through any standard web browser by appending the LSID to the prefix http://zoobank.org/. The
265   LSID for this publication is: urn:lsid:zoobank.org:pub:C9091268-EC61-41CD-A20C-
266   5C7DC08DAD46. The online version of this work is archived and available from the following
267   digital repositories: PeerJ, PubMed Central SCIE and CLOCKSS.
268

269   # Results

270   Of the collected 69 *Dolomedes* individuals in Parc National de Marojejy and Parc National
271   d'Andasibe-Mantadia, Madagascar, 29 were females, 21 were males, and 19 were juveniles. We
272   initially classified these exemplars into two groups, the "Kalanoro" group, and the
273   "Hydatostella" group, based on the habitus coloration (see also Taxonomy) and the
274   measurements of the carapace width (see Fig 2A–B). The female and male carapace width of the
275   "Kalanoro" group exceeded 7 mm and 6.5 mm, respectively, whereas in the "Hydatostella"
276   group they were below these values. Within the "Kalanoro" group, we identified one
277   morphospecies as *D. kalanoro*, and hypothesized two additional morphospecies, tentatively
278   named "gregoric", and "bedjanic" based on their genital anatomy (see Taxonomy). Individuals of
279   the "Hydatostella" group were more uniform, but based on constant genital differences (see
280   Taxonomy), we hypothesized two morphospecies, "hydatostella" and "rotundus".
281

282   **Morphological comparisons**
283   *Somatic characters*
284   Comparisons in the carapace width and relative length of leg I, tarsus I, and palp together support
285   the two-group classification stated above but cannot fully separate the morphospecies within
286   groups (Fig 2, see also Table S3, S4). The morphospecies of the "Kalanoro" group in general
287   have a wider carapace (Fig 2A–B), and longer appendages (Fig 2C–H) compared to the
288   "Hydatostella" group. Such differences in leg I and tarsus I also refer to better abilities in
289   walking and aquatic locomotion in the "Kalanoro" group (Fig 2C–F). Carapace width of male
290   and female "gregoric" are the only exception failing to fit the two-group classification as they are
291   not significantly wider than the "Hydatostella" group (see Table S4). Only the width of the
292   female carapace (Fig 2A) and the relative length of the male palp (Fig 2H) can partially separate
293   the morphospecies of the "Kalanoro" groups. The "gregoric" females have narrower carapace

294   than the other two morphospecies of the group (Fig 2A). The "bedjanic" males have longer
295   palps than *D. kalanoro* (Fig 2H).
296   *Male genital characters*
297   The shape of LA (Fig 3) and the ventral view of the Eb (Fig 4A–B) can well separate males of all
298   morphospecies in both groups. The measurements and the shapes of the other male palpal
299   structures can only partially support the separation of the morphospecies within their group (Fig
300   4C–D, 5, 6, 7, 8). Within the "Kalanoro" group, the three morphospecies are well separated by i)
301   the length (Fig 4A, PC1) and the width (Fig 4A, PC1 & 2) of the basal Eb in both the ventral and
302   the retrolateral view after palp expansion (Fig 4C, PC1); ii) D_e (Fig 5A, se also Table S3, S4); iii)
303   the curvature of the retrolateral edge of the MA (Fig 6A, PC1 & 2); and iv) the curvature of the
304   posterior (Fig 3A, PC1) and the dorsal edge (Fig 3A, PC2) of LA. The relative length of Cy (Fig
305   5B, see also Table S3, S4), shapes of Fu in both views (Fig 7), and RTA (Fig 8A) can only help
306   distinguish *D. kalanoro* from "bedjanic" while "gregoric" can match either of the other two
307   morphospecies. The two morphospecies within the "Hydatostella" group differ in i) curved
308   versus strait retrolateral arc of the Eb in ventral view (Fig 4B, PC1); ii) the shape and relative
309   size of the dorsal lobe of the RTA (Fig 8B, PC1); and iii) the curvature of the dorsal edge of the
310   LA (Fig 3B, PC1). However, D_e (Fig 5A, see also Table S3, S4), relative length of Cy (Fig 5B,
311   see also Table S3, S4), MA (Fig 6B), retrolateral view of Eb (Fig 4C), and Fu in both views (Fig
312   7) cannot fully separate "hydatostella" from "rotundus".
313   *Female genital characters*
314   The shape of MF can well separate all morphospecies in both groups (Fig 9). The margin of the
315   epigynum (Fig 10) and the vulva (Fig 11) can only support partial or no separation among
316   morphospecies within their group. Within the "Kalanoro" group, all three analyses of the female
317   genital structures agree that *D. kalanoro* and "bedjanic" are different (Fig 9A, 10A, 11A). The
318   morphospecies "gregoric", however, has an epigynal margin in the shape between those of the
319   other two morphospecies (Fig 10A) and a vulva similar to *D. kalanoro* (Fig 11A). All three
320   morphospecies are different in the shape of MF (Fig 9A), mainly in the presence or absence of
321   the horn extension at the MF (PC1), the aspect ratio of the MF (PC1 & 2), and the length of the
322   EF (PC2). Within the "Hydatostella" group, the two morphospecies are well separated by the
323   margins of epigynum (Fig 10B) and the MF (Fig 9B). The morphospecies "hydatostella" has a
324   pentagon-shaped epigynal margin (Fig 10B, PC1) with shorter EF (Fig 9B, PC1) while
325   "rotundus" has a round or triangular epigynal margin with relatively longer EF.
326   *Morphometric summary*
327   The first two PC axes in all the analyses explain more than half of the shape variations (Table
328   S5). Separation of the five hypothesized morphospecies is supported by different combinations
329   of the characteristics (Fig 12–14). Measurement of the somatic characteristics in general cannot
330   support the separation of morphospecies but can support the two species groups. Only shape
331   differences of the three structures out of ten, LA, Eb (ventral view), and MF, can separate all the
332   morphospecies in both groups (Fig 12–14). Degrees of variation in the shape of the other seven
333   structures and the measurements of male genitalia differ between groups; these features can only

334 provide evidence for some, but not all, morphospecies (Fig 2–11). The shapes of the Fu, in both
335 views, show higher variation compare to that of the other structures and fail to separate most
336 morphospecies (Fig 7). However, the shape of Fu can potentially help to diagnose the major
337 clades across *Dolomedes* phylogeny (see Taxonomy).
338

Phylogenetic and species delimitation analyses
340 We amplified 46 COI sequences with 1192 base pairs from eight *D. kalanoro*, five "gregoric",
341 16 "bedjanic", four "hydatostella", five "rotundus", and eight juveniles of the "Kalanoro" group.
342 Both ML and BI analyses recover monophyly of our morphospecies, and these are well
343 supported at least in one, if not both, analyses (Fig 15). The two species groups, "Kalanoro" and
344 "Hydatostella", are also well-supported as sister clades (Fig 15). Within the "Kalanoro" group,
345 the morphospecies "bedjanic" is sister to the clade uniting *D. kalanoro* and "gregoric" (Fig 15).
346 Genetic distances among these morphospecies hover between 3 and 5% (Fig 15). Analyses show
347 a weak population structure within "bedjanic" with specimens from Marojejy differing from
348 those from Analamazoatra + Andasibe-Mantadia by less than 2% (Fig 15). Genetic distances
349 between morphospecies of the "Hydatostella" are closer to 3% (Fig 15). Both ASAP and bPTP
350 support the five morphospecies (Fig 15).
351

Habitat preferences and geological barriers
353 We observed coexistence of several *Dolomedes* species in the same river drainage and even in
354 the same river sections or water bodies (Fig 16, Table 2). Namely, "bedjanic" and "hydatostella"
355 shared waterbodies at Marojejy (Fig 16C–D). The three morphospecies of the "Kalanoro" group
356 and "rotundus" were collected in the connected river system (Fig 16, see also Fig 1 in Kramer et
357 al., 1997) in Andasibe-Mantadia and Analamazoatra. Their coexistence in highly connected river
358 and water systems would estimate low levels of geological barriers. However, as explained
359 below, even the species that coexist occupy different types of habitats (Fig 17).
360 Estimations of the habitat preferences suggest the morphospecies of the "Kalanoro"
361 group occupy different types of habitats with partial overlaps; while "hydatostella" and
362 "rotundus" inhabit similar habitats (Table 2, Fig 17). The three morphospecies of the "Kalanoro"
363 group coexist and can all occupy flowing water with a dense canopy coverage, but in addition,
364 *D. kalanoro* and "bedjanic" also occupy flowing water with an open canopy as well as standing
365 water with a dense canopy respectively (Table 2, Fig 17). The two morphospecies of the
366 "Hydatostella" group show similar habitat preferences, both inhabiting standing water with dense
367 canopy (Table 2, Fig 17) but in two localities without connections of waterbodies.
368

Discussion
370 Our model demonstrates how an integrative approach can improve spider taxonomy. *Dolomedes*
371 contains extremely widespread as well as locally endemic species that often coexist in any
372 biogeographic region (World Spider Catalog, 2023; see also Raven & Hebron, 2018). Therefore,
373 regional reviews could result in conflicting species boundaries based on different combinations

374   of morphological evidence (see Zhang, Zhu & Song, 2004; Tanikawa & Miyashita, 2008). By
375   investigating variations of both the commonly used and the observed differences in the
376   diagnostic characteristic under an integrative taxonomic model, our study, albeit only focusing
377   on the Madagascar *Dolomedes* species, facilitates a comparative framework potentially
378   applicable to any *Dolomedes* taxonomic discoveries.
379   In this study, two groups of *Dolomedes*, the "Kalanoro" and the "Hydatostella" group,
380   show continuous or minor differences in the genital structures among exemplars. It was therefore
381   difficult to define whether these differences are intra or interspecific. We found our
382   delimitations, based on molecular and ecological, in addition to the morphological evidence, to
383   be decisive in solving this taxonomic problem. Our integrative model can well separate
384   *Dolomedes kalanoro* and the hypothesized four morphospecies collected from the humid forest
385   of north and east Madagascar. The species boundaries receive support from all three types of
386   evidence and could form preliminary hypotheses of their speciation, as we discuss below. We
387   hence consider the four hypothesized morphospecies as new species, *D. gregoric* **sp. nov.**, *D.*
388   *bedjanic* **sp. nov.**, *D. hydatostella* **sp. nov.**, and *D. rotuntus* **sp. nov.** (see Taxonomy).
389   Based solely on very few characteristics when identifying *Dolomedes* can be risky. Our
390   results suggest that the combinations of diagnostic characteristics are different even among
391   closely-related *Dolomedes*. In this study, only the female median field, male lateral subterminal
392   apophysis and embolus, are valid in diagnosing both groups of Madagascar *Dolomedes*.
393   Therefore, we recommend male palp expansion for examining the lateral subterminal apophysis,
394   a structure rarely described in *Dolomedes* taxonomy. Our model strongly suggests that multiple
395   types of evidence should be considered when facilitating species boundaries among *Dolomedes*.
396   Structures involved in copulation are under strong selection pressure (Kuntner et al.,
397   2009, 2016) and should therefore show stability in size and shape within species. In this study,
398   embolus and copulatory opening (shaped by the epigynal folds and median field) are such
399   structures related to sperm transfer, and as such maintain relatively low intraspecific variation.
400   They can diagnose well species in both groups of Madagascar *Dolomedes*. In some taxa, RTA is
401   responsible for anchoring the male palp into the correct position during copulation (Gering,
402   1953; Jäger, 2020; Poy et al., 2023) and is considered a critical diagnostic characteristic.
403   However, RTA in *Dolomedes* sometimes presents relatively high degrees of variation (Tanikawa
404   & Miyashita, 2008; Vink & Dupérré, 2010; see also Silva et al., 2015). Where and how RTA
405   anchors on the female genitalia in *Dolomedes* remains unknown. Indeed, our knowledge of how
406   each genital structure functions and interacts during copulation in *Dolomedes* is very limited.
407   More basic research is needed to further study the genital variation and its utility in species
408   diagnosis.
409   A combination of habitat preferences, geological barriers, and dispersal-related traits can
410   facilitate preliminary hypotheses of the speciation among the five Madagascar *Dolomedes*
411   species. Based on the relative length of leg I and tarsus I, morphospecies of the "Kalanoro"
412   groups are good dispersers with better walking abilities and aquatic locomotion compared to the
413   "Hydatostella" group. They also prefer flowing water which provides better chances of over

414 water dispersal. Therefore, the "Kalanoro" might be able to maintain gene flow across longer
415 geological barriers among unconnected river drainages. This generalization has already shown to
416 be accurate in *Dolomedes bedjanic* **sp. nov.**, which we collected in disjunct parts of north and
417 east Madagascar. Despite having good dispersal abilities and higher chances of dispersal,
418 adaptation to different habitats may support the gene flow limitation among the three
419 morphospecies of the "Kalanoro" group. On the other hand, the "Hydatostella" group is a
420 relatively poor disperser and dwells in standing waterbodies under a dense canopy. Therefore,
421 isolation may easily form between unconnected water bodies at a distance.
422   Our discoveries in Madagascar *Dolomedes*, albeit incomplete, include both wide ranging
423 species like *D. kalanoro* and *D. bedjanic* **sp. nov.**, as well as local endemics, *D. gregoric* **sp.**
424 **nov.**, *D. hydatostella* **sp. nov.**, and *D. rotundus* **sp. nov.** Such pattern is known in many other
425 organisms on Madagascar, such as lemurs (Wilmé, Goodman & Ganzhorn, 2006), geckos
426 (Pearson & Raxworthy, 2009), as well as in other spiders (Agnarsson & Kuntner, 2005;
427 Agnarsson et al., 2015; Jäger, 2020; Griswold et al., 2022). The two major biogeographic
428 scenarios behind the high local endemism rates are the climatic gradient hypothesis (Smith et al.,
429 1997; Schneider et al., 1999) and the watershed hypothesis (Wilmé, Goodman & Ganzhorn,
430 2006). The former considers the complex climate gradient across the island to shape high levels
431 of local endemism (see also Antonelli et al., 20222). The second hypothesis suggests that the
432 isolated humid refuges formed by rivers originated from the high mountains during Quaternary
433 climate shifts affected the evolution of local endemism (Wilmé, Goodman & Ganzhorn, 2006).
434 These hypotheses are not mutually exclusive, but could in combination explain the observed
435 contemporary distribution patterns of much of the biodiversity on Madagascar (Pearson &
436 Raxworthy, 2009; Brown et al., 2014). Considering that freshwater-associated organisms are
437 sensitive to spatial pattern changes in water bodies and river drainages, be it natural (e.g.,
438 Griffiths, 2006; Huang & Lin, 2011; Dias et al., 2013; Ye et al., 2018; Chen et al., 2021) or
439 artificial (Raharimalala et al., 2012), the two hypotheses could well explain the biogeography
440 and speciation of Madagascar *Dolomedes*.
441   Our research largely increases our knowledge of the semi-aquatic fauna in Madagascar.
442 Despite recent advances in pisaurid taxonomy in Madagascar (Silva & Griswold, 2013a,b; Silva
443 & Sierwald, 2013), only a single species of *Dolomedes* has been known prior to our study. Our
444 addition of four new species on the island—a result from only surveying two national parks—
445 only points to how incomplete the taxonomy of *Dolomedes* in Madagascar really is. Their rarity
446 in collections is likely due to nocturnal and semi-aquatic lifestyles. Indeed, the species described
447 here strictly adhere to water bodies and are never found on trails. In addition, these *Dolomedes*
448 species are cryptic and inactive during the day, but can be more easily located at night.
449 Consequently, arachnologists routinely overlook *Dolomedes* species if they do not engage in
450 targeted sampling along water bodies at night. Considering all above, we expect that future
451 targeted work in yet unexplored parts of this vast island will uncover many more *Dolomedes*
452 species. This suggests how important it is to protect aquatic habitats in Madagascar and
453 elsewhere, however small. Considering their poor dispersal abilities and narrow habitat

454 preferences, the locally endemic *Dolomedes*, especially the two "Hydatostella" species, could
455 rapidly go extinct in the face of small water body degradation.
456
457 **Taxonomy**
458
459   **Family Pisauridae Simon,1890**
460
461   ***Dolomedes* Latreille, 1804**
462   *Cispiolus* Roewer, 1955. **Type species:** *C. upembensis* Roewer, 1955. Synonymized by
463   Blandin (1979)
464   *Teippus* Chamberlin, 1924. **Type species:** *T. lamprus* Chamberlin, 1924. Synonymized
465   by Carico (1973), after Gertsch (1934)
466   **Type species:** *Araneus fimbriatus* Clerck, 1757: 106; plate 5, fig 9.
467   Clerck's (1757) description of a male "*Araneus fimbriatus*" from Sweden is the first
468   description of any *Dolomedes* species. When Latreille (1804) established the genus
469   *Dolomedes*, *Araneus fimbriatus* became its type species.
470
471 **Diagnosis:** *Dolomedes* can be separated from all the other pisaurid genera except *Mangromedes*
472 Raven & Hebron, 2018, *Megadolomedes* Davies & Raven, 1980, *Tasmomedes* Raven & Hebron,
473 2018, *Bradystichus* Simon, 1884, *Caledomedes* Raven & Hebron, 2018, and *Ornodolomedes*
474 Raven & Hebron, 2018, by the combination of the following characters:
475 Male palp (see also Sierwald, 1990; Santos, 2007)
476 1.  The presence of Sa, a round shaped and sclerotized part of upper T. The structure is
477   considered as a reduced DTA in Santos' (2007) cladistic analyses (Fig 18, red arrow).
478 2.  The presence of LA, which originated from the DST together with the Eb and Fu (Fig 19).
479 Female epigynum (see also Sierwald, 1989)
480 1.  Small knob, bulb, or horn shaped HS, which is also called as AB (Fig 20A–E, red arrows).
481   Head of spermathecae in other pisaurids is usually extended and elongated.
482 2.  Relatively long and usually vertically coiled FD that started with a tubular part and end up
483   with a flat flake. (Fig 20A–E)
484   *Dolomedes* can be diagnosed from *Mangromedes* by i) the strait and none pseudo-
485 segmented leg tarsus (but, see Santos, 2007); ii) the female COp positioned at the middle or the
486 posterior part of epigynum and anteriorly or laterally opened (Fig 20F–J); iii) the Eb and Fu that
487 are positioned at the retrolateral side of the palp and near vertically curved or coiled (Fig 18A–
488 E); and iv) the male palp RTA that does not deeply divide into two branches (Fig 18F–I, Fig 21,
489 see also Raven & Hebron, 2018).
490   *Dolomedes* can be diagnosed from *Megadolomedes* by i) the strait and none pseudo-
491 segmented leg tarsus (but, see Santos, 2007); ii) the simply curved or coiled Eb and Fu with less
492 than one loop (Fig 19, but see *D. bistylus* Roewer, 1955) and the embolic ring does not extend

493   anteriorly to near the tip of the Cy (Fig 18A–E); and iii) the broad female CD (Fig 20A–E)
494   without broken male embolus as mating plug (Davies & Raven, 1980; Raven & Hebron, 2018).
495   *Dolomedes* can be diagnosed from *Tasmomedes* by i) the simply curved or coiled Eb and
496   Fu (Fig 19) that does not extend anteriorly to near the tip of the Cy (Fig 18A–E); ii) the strong
497   and fully developed male palp RTA (Fig 21); and iii) vertically coiled female FD (Fig 20A–E).
498   *Dolomedes* can be diagnosed from *Bradystichus* by i) the unmodified abdomen (Fig 22);
499   ii) the absence of high contrast ventral abdominal coloration (see Raven & Hebron, 2018); iii)
500   denser leg femur spines, five pairs in *Dolomedes* while only three in *Bradystichus* (see Raven &
501   Hebron, 2018); iv) fully developed unpaired tarsal claw (Platnick & Forster, 1993; Raven &
502   Hebron, 2018), and v) the absence of prodorsal scopula on male Cy (Fig 18) (Platnick & Forster,
503   1993; Raven & Hebron, 2018).
504   *Dolomedes* can be diagnosed from *Caledomedes* by i) the AER that is wider than the
505   posterior width of MOA (see Taxonomy); and ii) the shorter male palp RTA (Raven & Hebron,
506   2018).
507   *Dolomedes* can be diagnosed from *Ornodolomedes* by i) the relatively simple carapace
508   color pattern (Fig 22, see also Raven & Hebron, 2018); and ii) the shorter leg tarsal and
509   metatarsal spines that do not overlapping each other (see Raven & Hebron, 2018).
510
511   **Remarks.** Subfamilies of Pisauridae are still debated (Simon, 1898; Petrunkevitch, 1928;
512   Sierwald, 1990; Griswold, 1993; Santos, 2007; Murphy & Roberts, 2015; Polotow, Carmichael
513   & Griswold, 2015; Silva, Gibbons & Sierwald, 2015; Albo et al., 2017; Wheeler et al., 2017;
514   Piacentini & Ramírez, 2019) and have not been comprehensively analyzed under phylogenetic
515   framework. More recent phylogenetic studies suggest that *Dolomedes* and the New Caledonia
516   endemic *Bradystichus* form a clade that is sister to all the other pisaurids (Wheeler et al., 2017;
517   Piacentini & Ramírez, 2019). Following the literature and the similarities in their genital
518   morphology (see genus diagnosis), perhaps *Dolomedes* and its close relatives can be argued to
519   form a subfamily (Dolomedinae). However, a well sampled, robust phylogeny and a taxonomic
520   review at a global scale are needed to detect phylogenetic proximities and synapomorphies of
521   pisaurid subfamilies.
522
523   **Key to known *Dolomedes* species of Madagascar**
524   1.   Large and long-legged *Dolomedes*, female carapace width above 7 mm, and male carapace
525   width above 6.5mm (Fig 2). Habitus uniformly brown to dark brown with light-colored, but
526   usually indistinct margins (Fig 22A–F). A few individuals have distinct but thin white
527   lateral bands that do not expand to the edge of the carapace (Fig 22G–I): **"Kalanoro"**
528   **group**
529   Female…………………………………………………………………………2
530   Male…………………………………………………………………………4

531   Small and short-legged *Dolomedes*, female carapace width below 7 mm, and male carapace
532   width below 6.5mm (Fig 2). Habitus dark brown to black with distinctively broad white
533   lateral bands that expand to the edge of the carapace (Fig 22I–M): **"Hydatostella" group**
534   Female……………………………………………………………………………6
535   Male………………………………………………………………………………7
536 2.   Epigynum MF with a horn extension (Fig 9A, 14, 20F):   ***D. kalanoro*** (Silva &
537   Griswold, 2013)
538   Epigynum MF without a horn extension (Fig 9A, 14, 20G–H) ………………………3
539 3.   Epigynum MF long and narrow; CD long and connect to the BS ventrally; Ab laterally
540   positioned (Fig 9A, 14, 20B):   ***D. gregoric* sp. nov.**
541   Epigynum MF short and wide; CD short and connect to the BS anteriorly; Ab anteriorly
542   positioned (Fig 9A, 14, 20C):   ***D. bedjanic* sp. nov.**
543 4.   Palp long, over twice the carapace width (Fig 2H); Cy shorter than palp tibia (Fig 5B); RTA
544   dorso-laterally positioned (Fig 18G) without dorsal lobe (Fig 8A, 13, 21C); MA with a
545   broad base (Fig 6A, 13, 18C); Eb short (Fig 4A–B, 12, 19C), D_e below 1.0 (Fig 5A); LA
546   with a broad tip (Fig 3A, 12, 19C):   ***D. bedjanic* sp. nov.**
547   Palp shorter than twice the carapace width (Fig 2H); Cy longer that palp tibia (Fig 5B);
548   RTA laterally positioned with dorsal lobe (Fig 8A, 13, 21A–B); MA with a narrow base
549   (Fig 6A, 13, 18A–B); D_e above 1.0 (Fig 5A); LA with a narrow tip (Fig 3A, 12, 19A–B)
550   …………………………………………………………………………………5
551 5.   Embolus long with narrow base (Fig 4A–B, 12, 19A), D_e above 1.2 (Fig 5A); Cy large, at
552   least 1.2 times longer than the palp tibia (Fig 5B); MA expands gradually from the base to
553   the middle part (Fig 6A, 13A, 18A); base of the dorsal edge of LA with a strait section (Fig
554   3A, 12, 19A):   ***D. kalanoro*** (Silva & Griswold, 2013)
555   Embolus long with broadened base (Fig 4A–B, 12, 19B), D_e between 1.0 and 1.2 (Fig 5B);
556   MA distinctly expands at the middle part (Fig 6A, 13, 18B); base of the dorsal edge of LA
557   without a strait section (Fig 3A, 12, 19B):   ***D. gregoric* sp. nov.**
558 6.   Epigynum pentagon-shaped with short EF, posterior MF relatively long (Fig 9B, Fig 14,
559   20I):   ***D. hydatostella* sp. nov.**
560   Epigynum round or triangular shaped with long EF that extend to near the anterior edge of
561   the epigynum; posterior MF relatively short (Fig 9B, 14, 20J): ***D. rotundus* sp. nov.**
562 7.   Dorsal and ventral lobes of RTA similar sized (Fig 8B, 13, 21D); In the ventral view,
563   retrolateral arc of the Eb straight (Fig 4B, 13, 18D); LA with a distinct narrow base (Fig 3B,
564   12, 19D): ***D. hydatostella* sp. nov.**
565 8.   Dorsal lobe of RTA round and broadened, larger than the ventral lobe (Fig 8B, 13, 21E); In
566   the ventral view, retrolateral arc of the Eb bent (Fig 4B, 13, 18E); LA without a distinct
567   narrow base (Fig 3B, 12, 19E–F):   ***D. rotundus* sp. nov.**
568
569 **Species group "Kalanoro"**

570   **Diagnosis.** *Dolomedes* species of the "Kalanoro" species group can be distinguished from all the
571   other known *Dolomedes*, except the Madagascar *Dolomedes* species of the group "Hydatostella",
572   by the combination of the following characters:
573   Male: The presence of a lateral lobe at the retrolateral edge of the Fu in the ventral view (Fig 18,
574   29, black arrows; see also species descriptions).
575   Female: i) epigynum longer than wide, without lateral extensions at the posterior edges (Fig
576   20F–J); ii) two fully separated, medially positioned, relatively small, and triangular or square-
577   shaped MF windows (Fig 20 F–J); iii) CD wider than the first loop of the FD, or similar in the
578   width (Fig 20A–E); and iv) FD simply and vertically coiled without any contrary flexure or
579   horizontal spiral (Fig 20A–E).
580   *Dolomedes* of the group "Kalanoro" can be diagnosed from those of the "Hydatostella"
581   group by i) larger body sizes, ii) longer legs, and iii) brownish coloration without distinct white
582   lateral bands; the lateral bands of the white banded morph do not extend to the edge of the
583   carapace.
584   **Composition.** *Dolomedes kalanoro*, *D. gregoric* **sp. nov.**, *D. bedjanic* **sp. nov.**
585
586   ### *Dolomedes kalanoro* Silva & Griswold, 2013
587   (Fig 16A, 18A & F, 19A, 20A & D, 21A, 22A–B & G–H, 23, 24)
588   *Dolomedes kalanoro* Silva & Griswold, 2013: 462; fig 2–12 (Description of male).
589   **Material examined.** MADAGASCAR: Toamasina Province: 2 female, 2 males, and 2 juveniles,
590   the river next to Hotel Feon'ny Ala (18°56'49.9"S, 48°25'8.8"E, 942 m), 4 IV 2022, Kuang-Ping
591   Yu (KPY) leg., KPARA00183–187, 00201 (NIB); 1 female, 2 males, and 4 juveniles, the
592   streams around Lac Vert, Reserve Analamazoatra (18°56'14.2"S, 48°25'12.5"E, 939 m), 4–8 IV
593   2022, KPY leg., KPARA00193–196, 00212–213, 00228, 00231 (NIB); 1 female, 1 male, and 1
594   juvenile, the river along Circuit Tsakoka, Parc national d'Andasibe-Mantadia (18°47'54.5"S,
595   48°25'34.8"E, 959 m), 6 IV 2022, KPY leg., KPARA00207–208, 00214 (NIB).
596   **Diagnosis.** Male *D. kalanoro* differs from the other two *Dolomedes* species of the "Kalanoro"
597   group by i) the MA expands gradually with a narrow base (Fig 18A, 23C & E); ii) the long and
598   narrow-based Eb (Fig 18A, 19A, 23C & E); and iii) the LA with a narrow ventral tip and a
599   straight section at the basal part of the dorsal edge (Fig 19A). Female *D. kalanoro* can be
600   separated from all the other *Dolomedes* species by a narrow, horn shaped extension on the
601   epigynal MF (Fig 20D, 24C–E; but see Remark).
602   **Description. Male (KPARA00185).** Total length 15.18: carapace length 7.89, width 7.11,
603   anterior height 2.78, posterior height 3.42; abdomen length 7.29, width 3.33. Length of palp and
604   legs: palp 13.81 (5.64, 2.21, 2.61, 3.35); leg I 41.89 (10.81, 3.35, 11.16, 10.47, 6.10); leg II 41.47
605   (11.01, 4.13, 10.41, 10.61, 5.31); leg III 31.58 (10.02, 3.79, 8.87, 8.90, NA); leg IV 43.33 (11.10,
606   4.13, 10.67, 11.40, 6.03). Leg formula 4123. Carapace pear-shaped, light brown bearded with
607   dense black short setae that form series of radial black markings pointing towards the distinct
608   fovea (Fig 22B, 23A). A pair of triangular black markings positioned anterior to the fovea (Fig
609   22B, 23A). The margin of the carapace covered with sparse milky white short setae that form

indistinct lateral bands (Fig 22B, 23A). Eight eyes ringed with black (Fig 23B). Eyes arranged in two rows. AER weakly recurved while PER strongly recurved. MOA dark brown with several black setae (Fig 23B). Diameters of AME 0.34, ALE 0.24, PME 0.48, PLE 0.54; MOA length 1.04, anterior width of MOA 0.74, posterior width of MOA 1.23; interval of AMEs 0.10, interval of PMEs 0.19, interval between AME and ALE 0.13, interval between PME and PLE 0.16. Clypeus 1.01, brownish covered with dark short setae. Chelicerae length 3.18, chestnut-brown covered with black long setae (Fig 23B). Chelicerae with three promarginal and four retromarginal teeth, both fang and marginal teeth black. Endite length 2.52, width 1.23; labium length 1.43, width 1.45; sternum near round, length 3.10, width 3.38; all endite, labium, and sternum yellowish-brown. Abdomen long oval with a distinct brownish cardiac mark; dorsum bearded with dense, dark brown short setae (Fig 22B, 23A). Lateral abdomen covered with grayish short setae that form irregular and indistinct lateral bands. A series of white lines and spots distribute on the dorsal abdomen (Fig 22B, 23A). Venter abdomen brown. Legs yellowish-brown, covered with dark blackish setae in different densities, regions with sparser setae form light-colored linear markings. Palp tibia with a highly sclerotized RTA which divided into a sharp, larger ventral lobe and a smaller blunt dorsal lobe (Fig 21A). Basal retrolateral edge of the ventral Cy with an oval shaped BCA (Fig 18A, 23C & E). T sclerotized with a membranous upper edge, the prolateral side attached to the DTP and the retrolateral side attached to the membranous Co (Fig 18A, 23C & E). T + DTP + Co forms a "U" shaped tegular ring (Fig 18A, 23C & E). A highly sclerotized Sa sits at the lower center of the ring, attached to the T (Fig 18A, 23C & E). MA hook-shaped, gradually expands from the narrow base and sits retrolaterally to the Sa (Fig 18A, 23C & E). Fu hook shaped, retrolateral side with a broad and distinct lateral lobe (Fig 18A, 23C & E). Ventral edge of the Fu folded and forms a groove that contains the long, narrow, and curved Eb (Fig 18F, 19A, 23D & F). LA trapezoid with a blunt and narrow ventral tip (Fig 19A). Dorsal edge of the LA with straight basal section (Fig 19A). All Fu, Eb, and LA originated from the DST (Fig 19A).

Female (KPARA00193). Total length 20.28: carapace length 10.31, width 9.32, anterior height 3.35, posterior height 4.17; abdomen length 9.97, width 5.78. Length of palp and legs: palp 14.51 (5.20, 2.12, 2.91, 4.28); leg I 43.23 (11.84, 4.99, 11.62, 9.45, 5.33); leg II 45.16 (12.73, 5.15, 11.65, 10.19, 5.44); leg III 40.05 (11.55, 4.41, 10.20, 9.17, 4.72); leg IV 46.26 (12.18, 4.88, 11.25, 11.79, 6.16). Leg formula 4213. Diameters of AME 0.44, ALE 0.29, PME 0.59, PLE 0.62; MOA length 1.32, anterior width of MOA 0.89, posterior width of MOA 1.45; interval of AMEs 0.16, interval of PMEs 0.25, interval between AME and ALE 0.20, interval between PME and PLE 0.57. Clypeus 1.56. Chelicerae length 3.87. Chelicerae with three promarginal and four retromarginal teeth. Endite length 3.03, width 1.50; labium length 1.59, width 1.64; sternum near round, length 4.31, width 4.40. Female similar to male, but larger, darker in the coloration, and with relatively shorter legs (Fig 24A–B). Epigynum pentagon shaped, longer than wide and highly sclerotized; divided into two LLs by the narrow rectangular MF with two distinct membranous windows (Fig 20D, 24C). Posterior half ventrally protruded with a narrow horn extension pointed anteriorly (Fig 20D, 24C–D). CD long and ventrally bent (Fig 20A, 24E). AB

650   small, knob shaped, and laterally positioned (Fig 20A, 24E). FD begins with a coiled and tubular
651   part; ended with a triangular flake (Fig 20A, 24E).
652   **Variation.** Given as variation of four females followed by variation of five males in parentheses.
653   Total length 21.35 ± 1.06 (16.98 ± 1.17): carapace length 10.31 ± 0.93 (8.65 ± 0.64), width 9.15
654   ± 0.95 (7.85 ± 0.64), anterior height 3.39 ± 0.45 (2.83 ± 0.14), posterior height 4.23 ± 0.52 (3.75
655   ± 0.31); abdomen length 11.04 ± 0.81 (8.34 ± 0.74), width 6.92 ± 0.89 (4.73 ± 1.08). Palp 14.88
656   ± 1.55 (15.06 ± 0.79); leg I 44.03 ± 4.06 (46.21 ± 2.59); leg II 44.66 ± 3.85 (45.43 ± 2.31); leg
657   III 40.44 ± 3.39 (40.00 ± 2.00); leg IV 48.74 ± 5.45 (46.65 ± 2.06). Diameters of AME 0.41 ±
658   0.06 (0.36 ± 0.03), ALE 0.29 ± 0.03 (0.25 ± 0.01), PME 0.56 ± 0.05 (0.51 ± 0.03), PLE 0.63 ±
659   0.02 (0.55 ± 0.02); Clypeus 1.48 ± 0.18 (1.10 ± 0.09). Chelicera length 3.96 ± 0.20 (3.34 ± 0.15).
660   Endite length 3.06 ± 0.28 (2.58 ± 0.18), width 1.59 ± 0.19 (1.20 ± 0.08). Labium length 1.60 ±
661   0.18 (1.38 ± 0.08), width 1.88 ± 0.25 (1.52 ± 0.08). Sternum length 4.11 ± 0.40 (3.57 ± 0.31),
662   width 4.34 ± 0.48 (3.73 ± 0.29). *Dolomedes kalanoro* has two different coloration morphs: the
663   dark morph (Fig 22A–B, 23A, 24A) has only light colored but indistinct carapace margin that
664   fades in the anterior carapace and in the abdomen; the white banded morph (Fig 22G–H) is more
665   brownish with very distinct, but thin, white lateral bands that do not expand to the edge of the
666   carapace. The former is more abundant in the surveyed region.
667   **Natural history.** Large sized wandering spider. Inhabiting rivers with open canopy and streams
668   with dense canopy (Fig 17, Table 2). Although spiders can be seen both day and night, they are
669   more active at night. Spiders hide in cracks of river banks, gaps between roots of trees, and
670   among dead tree trunks during day times (Fig 22A–B & C–H).
671   **Remark.** The male *Dolomedes* found in the eastern humid forest of Madagascar fits the original
672   descriptions of *D. kalanoro* by Silva and Griswold (2013a) although the type specimens were
673   collected in the western and the southern dry or subhumid forest of the island (Fig 16A). We
674   therefore consider these *Dolomedes* in Eastern Madagascar to be conspecific with *D. kalanoro*.
675   The female *D. kalanoro* is very similar to *D. straeleni* Roewer, 1955 collected and described
676   from the Upemba Lake, Congo after re-examining the type series deposited at the RMCA
677   (Holotype female, MT_119613) and the Senckenberg Natural History Museum, Frankfurt (SMF)
678   (Paratype female, SMF_10547) (Yu et al. in prep.). Considering the lack of any male
679   descriptions and molecular data available for detailed analyses and the historical biogeographic
680   separation between Madagascar and Congo, our best hypothesis is that these are separate species.
681   **Distribution.** Western and southern dry and subhumid forests (Silva & Griswold, 2013a) and
682   eastern humid forests of Madagascar (see Fig 16A).
683
684   ### *Dolomedes gregoric* Yu & Kuntner sp. nov.
685   (Fig 16B, 18B & G, 19B, 20B & E, 21B, 22C–D & I, 25, 26)
686   ZooBank id: urn:lsid:zoobank.org:act:075EEA19-43F1-4B65-97CC-5E014CE4D22C
687   **Holotype.** MADAGASCAR: Toamasina Province: 1 male, the stream along the trail Chute
688   Sacree, Parc national d'Andasibe-Mantadia (18°49'30.7"S, 48°26'5.3"E, 976 m), 12 IV 2022,
689   KPY leg., USNMENT01580825 (USNM).

690 **Paratype.** 1 female, same collecting information as the Holotype, USNMENT01580826
691 (USNM).
692 **Other material examined.** 2 females and 1 male, same collecting information as the Holotype,
693 KPARA00248, 00250, 00254 (NIB).
694 **Diagnosis.** Male *D. gregoric* **sp. nov.** differs from the other two *Dolomedes* species of the
695 "Kalanoro" group by i) the MA with a narrow base and expands distinctly at the middle (Fig
696 18B, 25C & E); ii) the long Eb with a wide base (Fig 18B, 19B, 25C & E); and iii) the LA with a
697 narrow ventral tip but without a straight basal section at the dorsal edge (Fig 19B). Female *D.
698 gregoric* **sp. nov.** can be separated from the other two *Dolomedes* species of the "Kalanoro"
699 group by i) the narrow MF without a horn extension (Fig 20E, 26C); ii) the shorter EF (Fig 20E,
700 26C); and iii) the long and ventrally bent CD (Fig 20B, 26D).
701 **Description. Male (Holotype, USNMENT01580825).** Total length 16.43: carapace length 8.27,
702 width 7.39, anterior height 2.90, posterior height 3.80; abdomen length 8.16, width 4.65. Length
703 of palp and legs: palp 14.84 (5.93, 2.40, 3.00, 3.51); leg I 47.24 (12.01, 4.55, 11.95, 11.56, 7.17);
704 leg II 46.39 (12.16, 4.46, 11.81, 11.38, 6.58); leg III 40.71 (11.07, 3.99, 10.01, 10.15, 5.49); leg
705 IV 47.74 (12.49, 4.25, 11.51, 12.62, 6.87). Leg formula 4123. Carapace pear-shaped, brownish
706 bearded with dense black short setae that form series of radial black markings pointing towards
707 the distinct fovea (Fig 25A). A pair of triangular black markings positioned anterior to the fovea
708 (Fig 25A). Lateral carapace with two distinct, thin white lateral bands formed by dense white
709 setae that do not expand to the edge of the carapace (Fig 25A). Eight eyes ringed with black (Fig
710 25B). Eyes arranged in two rows. AER weakly recurved while PER strongly recurved. MOA
711 dark brown with several black setae (Fig 25B). Diameters of AME 0.41, ALE 0.30, PME 0.57,
712 PLE 0.61; MOA length 1.21, anterior width of MOA 0.84, posterior width of MOA 1.32;
713 interval of AMEs 0.13, interval of PMEs 0.21, interval between AME and ALE 0.12, interval
714 between PME and PLE 0.45. Clypeus 1.04, brown covered with dark short setae (Fig 25B).
715 Chelicerae length 3.18, chestnut-brown covered with black long setae (Fig 25B). The right
716 chelicera with four promarginal and five retromarginal teeth whereas the left chelicera with three
717 and four teeth respectively. Both fang and marginal teeth black. Endite length 2.61, width 1.19;
718 labium length 1.17, width 1.56; sternum near round, length 3.63, width 3.84; all endite, labium,
719 and sternum light brown. Abdomen long oval with a distinct brownish cardiac mark; dorsum
720 bearded with dense, dark brown short setae (Fig 25A). Lateral abdomen covered with white short
721 setae that form distinct lateral bands (Fig 25A). Venter abdomen brown. Legs yellowish-brown,
722 covered with dark blackish setae in different densities, regions with sparser setae form light-
723 colored linear markings (Fig 25A). Palp tibia with a highly sclerotized RTA which divided into a
724 sharp, larger ventral lobe and a blunt, smaller dorsal lobe (Fig 21B). Basal retrolateral edge of
725 the ventral Cy with an oval shaped BCA (Fig 18B, 25C & E). T sclerotized with a membranous
726 upper edge, the prolateral side attached to the DTP and the retrolateral side attached to the
727 membranous Co (Fig 18B, 25C & E). T + DTP + Co forms a "U" shaped tegular ring (Fig 18B,
728 25C & E). A highly sclerotized Sa sits at the lower center of the ring, attached to the T (Fig 18B,
729 25C & E). MA sits retrolaterally to the Sa, hook-shaped with a narrow base and expands

730 distinctly at the middle (Fig 18B, 25C & E). Fu hook shaped, retrolateral side with a narrow and
731 distinct lateral lobe (Fig 18B, 25C & E). Ventral edge of the Fu folded and forms a groove that
732 contains the long, broad-based, and curved Eb (Fig 18G, 19B, 25D & F). LA trapezoid with a
733 blunt and narrow tip (Fig 19B). All Fu, Eb, and LA originated from the DST (Fig 19B).
734 **Female (Paratype, USNMENT01580826).** Total length 17.02: carapace length 9.16, width
735 7.93, anterior height 3.16, posterior height 3.83; abdomen length 7.86, width 5.40. Length of
736 palp and legs: palp 13.58 (4.67, 1.96, 2.81, 4.14); leg I 40.21 (10.67, 4.27, 10.85, 9.34, 5.08); leg
737 II 41.35 (11.46, 4.53, 10.88, 9.38, 5.10); leg III 38.72 (10.90, 4.33, 9.53, 9.40, 4.56); leg IV
738 45.58 (11.70, 4.29, 11.38, 12.17, 6.04). Leg formula 4213. Diameters of AME 0.49, ALE 0.32,
739 PME 0.65, PLE 0.63; MOA length 1.37, anterior width of MOA 1.02, posterior width of MOA
740 1.47; interval of AMEs 0.27, interval of PMEs 0.28, interval between AME and ALE 0.16,
741 interval between PME and PLE 0.57. Clypeus 1.26. Chelicerae length 3.24. Chelicerae with
742 three promarginal and four retromarginal teeth. Endite length 2.67, width 1.53; labium length
743 1.48, width 1.58; sternum near round, length 3.44, width 3.99. Female similar to male, but larger,
744 darker in the coloration with indistinct light-colored carapace edge, and with relatively shorter
745 legs. (Fig 26A–B). Epigynum pentagon shaped, longer than wide and highly sclerotized; divided
746 into two LLs by the narrow rectangular MF with two small and distinct membranous windows
747 (Fig 20E, 26C). CD long and ventrally bent (Fig 20B, 26D). AB small, knob-shaped, and
748 laterally positioned (Fig 20B, 26D). FD begins with a coiled and tubular part; ended with a
749 spindle flake (Fig 20B, 26D).
750 **Variation.** Given as variation of two females followed by variation of three males in
751 parentheses. Total length 17.22 ± 0.58 (15.43 ± 1.42): carapace length 8.72 ± 0.42 (7.95 ± 0.46),
752 width 7.68 ± 0.41 (7.15 ± 0.35), anterior height 3.04 ± 0.11 (2.77 ± 0.18), posterior height 3.58 ±
753 0.25 (3.64 ± 0.23); abdomen length 8.50 ± 0.67 (7.48 ± 0.96), width 5.84 ± 0.53 (4.46 ± 0.28).
754 Palp 12.90 ± 0.60 (14.30 ± 0.77); leg I 38.86 ± 1.24 (44.61 ± 3.72); leg II 40.22 ± 1.03 (43.69 ±
755 3.83); leg III 37.32 ± 1.98 (38.56 ± 3.04); leg IV 43.87 ± 1.50 (45.82 ± 2.72). Diameters of AME
756 0.43 ± 0.06 (0.40 ± 0.02), ALE 0.31 ± 0.02 (0.29 ± 0.01), PME 0.58 ± 0.06 (0.54 ± 0.04), PLE
757 0.60 ± 0.03 (0.59 ± 0.04); Clypeus 1.17 ± 0.08 (0.98 ± 0.08). Chelicerae length 3.42 ± 0.15 (3.21
758 ± 0.23). All the specimens have three promarginal and four retromarginal teeth on both
759 chelicerae except the Holotype male has asymmetrical number of the cheliceral marginal teeth.
760 Endite length 2.61 ± 0.23 (2.49 ± 0.18), width 1.50 ± 0.07 (1.17 ± 0.04). Labium length 1.45 ±
761 0.09 (1.18 ± 0.01), width 1.68 ± 0.13 (1.43 ± 0.19). Sternum length 3.41 ± 0.09 (3.38 ± 0.36),
762 width 3.79 ± 0.24 (3.53 ± 0.44). Male *D. gregoric* **sp. nov.** has two different coloration morphs:
763 the dark morph (Fig 22D) has only light colored but indistinct carapace edge that fades in the
764 anterior carapace and in the lateral abdomen; and the white banded morph (Fig 22I, 25A) with
765 very distinct, but thin, white lateral bands that do not expand to the edge of the carapace. We did
766 not find such color variations in the female *D. gregoric* **sp. nov.** Considering the white banded
767 morph of is in general less abundant in the surveyed regions and we found only two females, it is
768 possible that the coloration variations also present in female *D. gregoric* **sp. nov.**

Natural history. Large sized wandering spider but slightly smaller, albeit not significant (see Result), than the other two close related *Dolomedes* species. Known inhabits only the steep forest stream with several waterfalls along trail Chute Sacree, Parc national d'Andasibe-Mantadia. Active at night, found on the edge between roots or tree trunks that grow into the water. (Fig 22C–D & I). Population size much smaller than the coexisted *D. bedjanic* **sp. nov.**

Etymology. The species is named after our colleague Matjaž Gregorič who organized the field trip and contributed to the discovery of this species. The species epithet is a noun in apposition.

Distribution. Known only from the type localities (see Fig 16B)

Dolomedes bedjanic Yu & Kuntner sp. nov.
(Fig 16C, 18C & H, 19C, 20C & F, 21C, 22E–F, 27, 28)
ZooBank id: urn:lsid:zoobank.org:act:081004EB-ED43-4BA1-9AB9-C7DCE95BB338

Holotype. MADAGASCAR: Antsiranana Province: 1 male, the 4th stream below Mantella Camp, on the trail toward Mandena village, Parc National de Marojejy (14°26'38.4"S, 49°47'0.9"E, 366 m), 25 III 2022, KPY leg., USNMENT01580827 (USNM).

Paratype. 1 female, same collecting locality as the Holotype, 29 III 2022, KPY leg., USNMENT01580828 (USNM).

Other material examined. MADAGASCAR: Antsiranana Province: 1 female and 1 male, the 1st stream below Mantella Camp, on the trail toward Mandena village, Parc National de Marojejy (14°26'22.4"S, 49°46'38.8"E, 463 m), 25–30 III 2022, KPY leg., KPARA00129, 00166 (NIB); 2 females and 1 juvenile, the 3rd stream below Mantella Camp, on the trail toward Mandena village, Parc National de Marojejy (14°26'29.5"S, 49°46'48.2"E, 412 m), 25–30 III 2022, KPY leg., KPARA00131, 00154 (NIB); 1 female, same collecting information as the Holotype, KPARA00132 (NIB); 1 female, the 5th stream below Mantella Camp, on the trail toward Mandena village, Parc National de Marojejy (14°26'47.3"S, 49°47'6.5"E, 342 m), 25 III 2022, KPY leg., KPARA00133 (NIB); 2 females and 5 juveniles, the stream on the trail toward Cascade de Humbert, Parc National de Marojejy (14°26'3.72"S, 49°46'21.8"E, 546 m), 28 III 2022, KPY leg., KPARA00144–146, 00159–162 (NIB). Toamasina Province: 3 females and 2 males, the streams around Lac Vert, Reserve Analamazoatra (18°56'14.2"S, 48°25'12.5"E, 939 m), 4–8 IV 2022, KPY leg., KPARA00192, 00194, 00227, 00232–233 (NIB); 1 juvenile, the stream around Orchid Lake, Parc Mitsinjo (18°55'58.2"S, 48°24'48.9"E, 935 m), 7 IV 2022, KPY leg., KPARA00226 (NIB); 2 males, the slow flowing stream and swamps along trail Kalanoro, next to Vakona Lodge (18°53'16.9"S, 48°26'4.5"E, 987 m), 10 IV 2022, KPY leg., KPARA00234–235 (NIB); 4 females and 1 male, the stream along the trail Chute Sacree, Parc national d'Andasibe-Mantadia (18°49'30.7"S, 48°26'5.3"E, 976 m), 6 & 12 IV 2022, KPY leg. KPARA00202, 00247, 00251–252, 00255 (NIB).

Diagnosis. Male *D. bedjanic* **sp. nov.** differs from the other two *Dolomedes* species of the "Kalanoro" group by i) the long palp that is twice longer than the carapace width (Fig 2H); ii) the RTA positioned near dorsally (Fig 18H, 27D & F) with only a sharp ventral lobe (Fig 21C); iii) the Cy shorter than the palp tibia (Fig 5B); iii) the MA expands gradually from a relatively

809   broader base to the middle (Fig 18C, 27C & E); and v) the short Eb with a wide base (Fig 18C,
810   19C, 27C & E). Female *D. bedjanic* **sp. nov.** can be separated from the other two *Dolomedes*
811   species of the "Kalanoro" group by i) the wide MF without a horn extension (Fig 20F, 28C); and
812   ii) the short CD that does not bend ventrally (Fig 20C, 28D).
813   **Description. Male (Holotype, USNMENT01580827).** Total length 15.89: carapace length 8.69,
814   width 7.88, anterior height 3.03, posterior height 4.12; abdomen length 7.20, width 4.02. Length
815   of palp and legs: palp 17.07 (7.09, 2.65, 3.72, 3.61); leg I 47.61 (12.66, 4.63, 12.65, 11.80, 5.87);
816   leg II 46.92 (12.55, 4.69, 12.20, 11.44, 6.04); leg III 41.88 (11.44, 4.19, 10.62, 10.54, 5.09); leg
817   IV 43.35 (12.28, 4.38, 12.22, 12.94, NA). Leg formula 1243. Carapace pear-shaped, brownish
818   bearded with dense black short setae that form series of radial black markings pointing towards
819   the distinct fovea (Fig 27A). A pair of triangular black markings positioned anterior to the fovea
820   (Fig 27A). Edge of the carapace bearded with sparse greyish setae that form indistinct light-
821   colored bands (Fig 27A). Eight eyes ringed with black (Fig 27B). Eyes arranged in two rows.
822   AER weakly recurved while PER strongly recurved. MOA dark brown with several black setae
823   (Fig 27B). Diameters of AME 0.39, ALE 0.29, PME 0.51, PLE 0.59; MOA length 1.09, anterior
824   width of MOA 0.89, posterior width of MOA 1.34; interval of AMEs 0.14, interval of PMEs
825   0.23, interval between AME and ALE 0.14, interval between PME and PLE 0.42. Clypeus 1.14,
826   brown covered with dark short setae (Fig 27B). Chelicerae length 3.5, chestnut-brown covered
827   with black long setae (Fig 25B). The right chelicera with four promarginal and six retromarginal
828   teeth whereas the left chelicera with three and four teeth respectively. Both fang and marginal
829   teeth black. Endite length 2.68, width 1.27; labium length 1.51, width 1.54; sternum near round,
830   length 3.63, width 3.59; all endite, labium, and sternum yellowish-brown. Abdomen long oval
831   with a distinct yellowish cardiac mark; dorsum bearded with dense, dark brown short setae (Fig
832   27A). Yellowish setae cover the lateral and the dorsal abdomen that forms indistinct light-
833   colored lateral bands and dorsal patches (Fig 27A). Venter abdomen brown. Legs brown,
834   covered with dark blackish setae in different densities, regions with sparser setae form light-
835   colored linear markings. Palp long, twice longer than the carapace width (Fig 2H). Tibia with a
836   highly sclerotized RTA positioned near dorsally (Fig 18H, Fig 27D & F) with only a sharp
837   ventral lobe (Fig 21C). Cy shorter that the palp tibia (Fig 5B). Basal retrolateral edge of the
838   ventral Cy with an oval shaped BCA (Fig 18C, Fig 27C & E). T sclerotized with a membranous
839   upper edge, the prolateral side attached to the DTP and the retrolateral side attached to the
840   membranous Co. T + DTP + Co forms a "U" shaped tegular ring (Fig 18C, 27C & E). A highly
841   sclerotized Sa sits at the lower center of the ring, attached to the T (Fig 18C, 27C & E). MA sits
842   retrolaterally to the Sa, hook-shaped with a relatively broad base and expands gradually to the
843   middle (Fig 18C, 27C & E). Fu hook shaped, retrolateral side with a small but distinct lateral
844   lobe (Fig 18C, 27C & E). Ventral edge of the Fu folded and forms a groove that contains the
845   short, broad-based, and curved Eb (Fig 18H, 19C, 27D & F). LA trapezoid with a blunt and
846   broad ventral tip (Fig 19C). All Fu, Eb, and LA originated from the DST (Fig 19C).
847   **Female (Paratype, USNMENT01580828).** Total length 21.55: carapace length 10.66, width
848   9.44, anterior height 3.62, posterior height 4.03; abdomen length 10.89, width 7.58. Length of

849 palp and legs: palp 13.58 (4.67, 1.96, 2.81, 4.14); leg I 40.21 (10.67, 4.27, 10.85, 9.34, 5.08); leg
850 II 41.35 (11.46, 4.53, 10.88, 9.38, 5.10); leg III 38.72 (10.90, 4.33, 9.53, 9.40, 4.56); leg IV
851 45.58 (11.70, 4.29, 11.38, 12.17, 6.04). Leg formula 4213. Diameters of AME 0.50, ALE 0.33,
852 PME 0.63, PLE 0.65; MOA length 1.38, anterior width of MOA 1.11, posterior width of MOA
853 1.61; interval of AMEs 0.17, interval of PMEs 0.27, interval between AME and ALE 0.18,
854 interval between PME and PLE 0.61. Clypeus 1.37. Chelicerae length 4.47. Chelicerae with
855 three promarginal and four retromarginal teeth. Endite length 3.15, width 1.67; labium length
856 1.74, width 1.95; sternum near round, length 4.09, width 4.45. Female similar to the male, but
857 larger, darker in the coloration, and with relatively shorter legs. A series of white spots and lines
858 distributed on the dorsal abdomen (Fig 28A–B). Epigynum pentagon shaped, longer than wide
859 and highly sclerotized; divided into two LLs by the wide rectangular MF with two small and
860 distinct membranous windows (Fig 20F, 28C). CD short, curved, while does not bend ventrally
861 (Fig 20C, 28D). AB small, horn-shaped and anteriorly positioned (Fig 20C, 28D). FD begins
862 with a coiled and tubular part; ended with a triangular flake (Fig 20C, 28D).
863 **Variation.** Given as variation of 14 females followed by variation of seven males in parentheses.
864 Total length 21.21 ± 2.10 (16.99 ± 1.11): carapace length 10.61 ± 0.84 (8.59 ± 0.44), width 9.34
865 ± 0.86 (7.66 ± 0.38), anterior height 3.52 ± 0.32 (3.03 ± 0.16), posterior height 4.04 ± 0.45 (3.78
866 ± 0.26); abdomen length 10.60 ± 1.39 (8.40 ± 0.88), width 6.57 ± 1.38 (4.75 ± 0.68). Palp 15.63
867 ± 1.29 (16.33 ± 0.68); leg I 45.28 ± 3.75 (46.03 ± 2.19); leg II 45.86 ± 3.63 (44.60 ± 2.14); leg
868 III 42.41 ± 3.53 (39.15 ± 2.15); leg IV 49.16 ± 4.05 (44.32 ± 1.08). Diameters of AME 0.45 ±
869 0.04 (0.39 ± 0.02), ALE 0.31 ± 0.02 (0.27 ± 0.02), PME 0.60 ± 0.05 (0.52 ± 0.02), PLE 0.64 ±
870 0.06 (0.57 ± 0.03); Clypeus 1.47 ± 0.16 (1.12 ± 0.05). Chelicera length 4.39 ± 0.43 (3.45 ± 0.21).
871 All the specimens have three promarginal and four retromarginal teeth on both chelicerae except
872 the Paratype female has asymmetrical number of the cheliceral marginal teeth. Endite length
873 3.16 ± 0.29 (2.54 ± 0.16), width 1.67 ± 0.09 (1.29 ± 0.03). Labium length 1.76 ± 0.18 (1.42 ±
874 0.08), width 1.90 ± 0.18 (1.46 ± 0.09). Sternum length 4.18 ± 0.42 (3.55 ± 0.17), width 4.43 ±
875 0.43 (3.63 ± 0.22). Although *D. bedjanic* **sp. nov.** has relatively larger population in the
876 investigated regions compare to the other two species of the "Kalanoro" group, no white banded
877 morph is found.
878 **Natural history.** Large sized wandering spider. Inhabiting water bodies, both flowing or
879 standing, with dense canopy coverage. Active at night, found on surfaces near or on water (Fig
880 22C–D). One individual (KPARA00251) was sitting on a riverside tree trunk away from the
881 water. An individual (KPARA00202) was found resting in holes on the river bank during day
882 time.
883 **Etymology.** The species is named after our colleague Matjaž Bedjanič who participated in the
884 aquatic collecting work and contributed to the discovery of this species. The species epithet is a
885 noun in apposition.
886 **Distribution.** Northern and eastern humid forests of Madagascar (see Fig 23C)
887
888 **Species group "Hydatostella"**

889 **Diagnosis.** *Dolomedes* species of the species groups can be distinguished from all the other
890 known *Dolomedes*, except the Madagascar *Dolomedes* species of the group "Kalanoro", by the
891 combination of the following characters:
892 Male: The presence of a lateral lobe at the retrolateral edge of the Fu in the ventral view (Fig 18,
893 29, black arrows; see also species descriptions).
894 Female: i) epigynum longer than wide, without lateral extensions at the posterior edges (Fig
895 20F–J); ii) two fully separated, medially positioned, relatively small, and triangular or square-
896 shaped MF windows (Fig 20 F–J); iii) CD wider than the first loop of the FD, or similar in the
897 width (Fig 20A–E); and iv) FD simply and vertically coiled without any contrary flexure or
898 horizontal spiral (Fig 20A–E).
899   *Dolomedes* of the group "Hydatostella" can be diagnosed from those of the "Kalanoro"
900 group by i) the smaller body size, ii) the relatively shorter legs, and iii) the dark brownish to
901 blackish coloration with very distinct white lateral bands that expand to the edge of the carapace.
902 **Composition.** *Dolomedes hydatostella* **sp. nov.**, *D. rotundus* **sp. nov.**
903
904 ### *Dolomedes hydatostella* Yu & Kuntner sp. nov.
905 (Fig 16D, 18D & I, 19D, 20D & I, 21D, 22J–K, 29, 30)
906 ZooBank id: urn:lsid:zoobank.org:act:6C524835-816A-42F8-8700-BF1A597F8ED9
907 **Holotype.** MADAGASCAR: Antsiranana Province: 1 male, the 2th muddy stream and swamp
908 below Mantella Camp, on the trail toward Mandena village, Parc National de Marojejy
909 (14°26'26.8"S, 49°46'44.6"E, 433 m), 30 III 2022, KPY leg., USNMENT01580829 (USNM;
910 collected as sub adult).
911 **Paratype**. 1 female, same collecting information as the Holotype, USNMENT01580830
912 (USNM).
913 **Other material examined.** 4 females and 1 male, same collecting information as the Holotype,
914 KPARA00157–158, 00163–164, 00258 (NIB).
915 **Diagnosis.** Male *D. hydatostella* **sp. nov.** differs from *D. rotundus* **sp. nov.** by i) the similar
916 sized RTA dorsal and ventral lobes (Fig 21D); ii) the straight Eb retrolateral arc, in the ventral
917 view (Fig 18D, 29C & E); and iii) the LA with a distinct narrow base (Fig 19D). Female *D.*
918 *hydatostella* **sp. nov.** differs from *D. rotundus* **sp. nov.** by i) the pentagon shaped epigynum (Fig
919 20I, 30C); ii) the relatively longer posterior MF (Fig 20I, 30C); and ii) the shorter EF (Fig 20I,
920 30C).
921 **Description. Male (Holotype, USNMENT01580829).** Total length 11.63: carapace length 6.23,
922 width 5.88, anterior height 2.19, posterior height 2.49; abdomen length 5.40, width 2.91. Length
923 of palp and legs: palp 9.49 (3.69, 1.53, 1.85, 2.42); leg I 26.82 (7.11, 2.96, 7.10, 6.27, 3.38); leg
924 II 27.21 (7.42, 2.92, 7.10, 6.40, 3.37); leg III 24.53 (6.91, 3.83, 6.23, 5.71, 2.85); leg IV 29.29
925 (7.92, 3.07, 7.21, 7.37, 3.72). Leg formula 4213. Carapace pear-shaped, light brown bearded
926 with dense black short setae (Fig 29A). Fovea distinct, and extends posteriorly from the center
927 (Fig 29A). A pair of triangular black spots positioned anteriorly to the fovea. Lateral carapace
928 with dense white setae that form distinct wide lateral bands (Fig 29A). Lateral bands wider in the

929 first half of the carapace and gradually shrink to the posterior carapace (Fig 29A). Eight eyes
930 ringed with black. Eyes arranged in two rows. AER weakly recurved while PER strongly
931 recurved. MOA brown with several black setae (Fig 29B). Diameters of AME 0.35, ALE 0.20,
932 PME 0.42, PLE 0.44; MOA length 0.78, anterior width of MOA 0.71, posterior width of MOA
933 1.04; interval of AMEs 0.10, interval of PMEs 0.18, interval between AME and ALE 0.12,
934 interval between PME and PLE 0.3. Clypeus 0.74, light yellowish covered with dark short setae.
935 Chelicerae length 2.28, light brown covered with black long setae (Fig 29B). Chelicerae with
936 three promarginal and four retromarginal teeth. Both fang and marginal teeth chestnut brown.
937 Endite length 1.84, width 1.00; labium length 0.93, width 1.00; sternum near round, length 2.36,
938 width 2.65; all endite, labium, and sternum yellowish-brown. Abdomen long oval with a distinct
939 and greyish-brown cardiac mark; dorsum bearded with dense, dark brown short setae with a
940 series of white spot (Fig 29A). Lateral abdomen covered with white short setae that form distinct
941 and irregular lateral bands and patches (Fig 29A). Venter abdomen brownish. Legs light brown,
942 covered with dark blackish setae in different densities, regions with sparser setae form light-
943 colored linear markings (Fig 29A). Palp tibia with a highly sclerotized RTA (Fig 18I, 29D & F)
944 divided into two sharp lobes that are in similar sizes (Fig 21D). Basal retrolateral edge of the
945 ventral Cy with an oval shaped BCA (Fig 18D, 29C & E). T sclerotized with a membranous
946 upper edge, the prolateral side attached to the DTP and the retrolateral side attached to the
947 membranous Co (Fig 18D, 29C & E). T + DTP + Co forms a "U" shaped tegular ring (Fig 18D,
948 29C & E). A highly sclerotized Sa sits at the lower center of the ring, attached to the T (Fig 18D,
949 29C & E). MA sits retrolaterally to the Sa, hook-shaped and expand gradually from a narrow
950 base (Fig 18D, Fig 29C & E). Fu hook shaped, retrolateral side with a small but distinct lateral
951 lobe (Fig 18D, 29C & E). Ventral edge of the Fu folded and forms a groove that contains the
952 short, broad-based, and curved Eb (Fig 18I, 19D, 29D & F). From the ventral view, retrolateral
953 arc of the Eb strait (Fig 18D, 29C & E). LA trapezoid with round tips and a distinct narrow base
954 (Fig 19D). All Fu, Eb, and LA originated from the DST (Fig 19D).
955 **Female (Paratype, USNMENT01580830).** Total length 17.09: carapace length 7.18, width
956 6.58, anterior height 2.57, posterior height 3.15; abdomen length 9.91, width 6.23. Length of
957 palp and legs: palp 9.11(2.96, 1.37, 1.96, 2.82); leg I 23.69 (6.80, 2.91, 6.56, 5.11, 2.31); leg II
958 24.70 (7.36, 2.96, 6.70, 5.24, 2.44); leg III 23.07 (6.75, 2.74, 6.01, 5.10, 2.47); leg IV 27.65
959 (7.78, 2.83, 7.08, 6.92, 3.04). Leg formula 4213. Diameters of AME 0.38, ALE 0.24, PME 0.44,
960 PLE 0.50; MOA length 0.94, anterior width of MOA 0.79, posterior width of MOA 1.18;
961 interval of AMEs 0.11, interval of PMEs 0.24, interval between AME and ALE 0.15, interval
962 between PME and PLE 0.35. Clypeus 0.83. Chelicerae length 2.82. The right chelicera with three
963 promarginal and five retromarginal teeth whereas the left chelicera with three and four teeth
964 respectively. Endite length 1.87, width 1.10; labium length 0.98, width 1.31; sternum near round,
965 length 2.79, width 3.02. Female similar to male, but larger, much darker in the coloration, and
966 with relatively shorter legs (Fig 30A–B). Epigynum pentagon shaped, highly sclerotized, and
967 longer than wide; divided into two LLs by the near rectangular MF with two small and distinct
968 membranous windows and a relatively larger posterior part (Fig 20C, 30C). EF short and does

969 not extend the near the anterior margin of the epigynum (Fig 20I, 30C). CD short, curved, and
970 does not bend ventrally (Fig 20D, 30D). AB small, horn-shaped and laterally positioned (Fig
971 20D, 30D). FD begins with a coiled and tubular part and ended with a thin flake (Fig 20D, 30D).
972 **Variation.** Given as variation of five females followed by variation of two males in parentheses.
973 Total length 15.54 ± 1.41 (12.58 ± 1.34): carapace length 6.95 ± 0.34 (6.38 ± 0.21), width 6.43 ±
974 0.28 (6.03 ± 0.21), anterior height 2.61 ± 0.25 (2.26 ± 0.09), posterior height 2.91 ± 0.28 (2.70 ±
975 0.30); abdomen length 8.59 ± 1.34 (6.21 ± 1.14), width 5.48 ± 0.83 (3.64 ± 1.03). Palp 9.17 ±
976 0.37 (9.74 ± 0.35); leg I 23.69 ± 1.16 (27.54 ± 1.02); leg II 24.50 ± 1.38 (27.88 ± 0.95); leg III
977 23.02 ± 0.96 (24.84 ± 0.43); leg IV 27.96 ± 1.22 (29.60 ± 0.43). Diameters of AME 0.36 ± 0.03
978 (0.28 ± 0.11), ALE 0.36 ± 0.02 (0.21 ± 0.01), PME 0.23 ± 0.03 (0.41 ± 0.01), PLE 0.45 ± 0.03
979 (0.44 ± 0.01); Clypeus 0.48 ± 0.10 (0.77 ± 0.02). Chelicera length 2.71 ± 0.13 (2.37 ± 0.12).
980 Most of the specimens has three promarginal and four retromarginal teeth on both chelicerae
981 while two specimens have asymmetrical number of the cheliceral marginal teeth. Endite length
982 1.86 ± 0.08 (1.81 ± 0.70), width 1.11 ± 0.05 (0.97 ± 0.34). Labium length 0.95 ± 0.09 (0.94 ±
983 0.42), width 1.22 ± 0.10 (1.01 ± 0.41). Sternum length 2.78 ± 0.17 (2.50 ± 0.84), width 3.01 ±
984 0.19 (2.76 ± 0.82).
985 **Natural history.** Median-sized wandering spider inhabiting shallow standing water bodies or
986 very slow-flowing parts of streams with dense canopy coverage. Active at night, found holding
987 on to leaf litter or grass emerging from the water surface (Fig 22I).
988 **Etymology.** The species epithet "hydatostella" is a compound noun in apposition. The first half
989 "hydatos-" is a Latinized Greek, "ὕδωρ (hydōr)", refering to "water". The second half "-stella" is
990 a Latin word refering to "stars". Together the species epithet means "stars on water".
991 **Distribution.** Known only from the type locality (see Fig 23D)
992
993 ***Dolomedes rotundus* Yu & Kuntner sp. nov.**
994 (Fig 16D, 18E & J, 19E–F, 20E & J, 21E, 22L–M, 31, 32)
995 ZooBank id: urn:lsid:zoobank.org:act:03ADE51C-2B73-4F7F-B2BD-61755461912C
996 **Holotype.** MADAGASCAR: Toamasina Province: 1 male, the slow flowing stream and swamps
997 along trail Kalanoro, next to Vakona Lodge (18°53'16.9"S, 48°26'4.5"E, 987 m), 10 IV 2022,
998 KPY leg., USNMENT01580831 (USNM).
999 **Paratype.** 1 female, same collecting information as the Holotype, USNMENT01580832
1000 (USNM).
1001 **Other material examined.** MADAGASCAR: Toamasina Province: 2 juveniles, slow flowing
1002 part of the streams around Lac Vert, Reserve Analamazoatra, Toamasina Province
1003 (18°56'14.2"S, 48°25'12.5"E, 939 m), 4–8 IV 2022, KPY leg., KPARA00229–230 (NIB); 2
1004 females, 4 males, and 3 juveniles, same collecting information as the Holotype, KPARA00236–
1005 239, 00241, 00243, 00244 (NIB); 1 male, forêt Analalava, Foulpointe, Tamatave, I 1995, Pauly
1006 A. leg., MT_207084 (RMCA).
1007 **Diagnosis.** Male *D. rotundus* **sp. nov.** differs from *D. hydatostella* **sp. nov.** by i) the round
1008 ventral RTA lobe which is larger than the dorsal lobe (Fig 21E); ii) the bent retrolateral arc of the

1009   Eb, in the ventral view (Fig 18E, 31C & E); and iii) the LA with a broad base (Fig 19E & F).

1010   Female *D. rotundus* **sp. nov.** differs from *D. hydatostella* **sp. nov.** by i) the triangular or round-

1011   shaped epigynum (Fig 20J, 32C); ii) the relatively shorter posterior MF (Fig 20J, 32C); and iii)

1012   the longer EF extending to near the anterior edge of the epigynum (Fig 20J, 32C).

1013   **Description. Male (Holotype, USNMENT01580831).** Total length 13.15: carapace length 6.47,

1014   width 5.80, anterior height 2.19, posterior height 2.85; abdomen length 6.68, width 4.38. Length

1015   of palp and legs: palp 9.88 (3.93, 1.55, 1.98, 2.42); leg I 26.74 (7.25, 2.90, 7.10, 6.07, 3.42); leg

1016   II 26.80 (7.49, 2.85, 7.12, 6.09, 3.25); leg III 24.56 (7.08, 2.67, 6.20, 5.72, 2.89); leg IV 29.12

1017   (7.94, 2.83, 7.08, 7.41, 3.86). Leg formula 4213. Carapace pear-shaped, light yellowish bearded

1018   with dense black short setae (Fig 31A). Fovea distinct, and extends posteriorly from the center

1019   (Fig 31A). A pair of triangular black spots positioned anteriorly to the fovea (Fig 31A). First half

1020   of the lateral carapace with dense white setae that form distinct wide lateral patches (Fig 31A).

1021   The dense white setae coverages distinctly sparser at the middle of the carapace edge, and

1022   become thin and fading (Fig 31A). Eight eyes ringed with black. Eyes arranged in two rows.

1023   AER weakly recurved while PER strongly recurved (Fig 31B). MOA brownish with several

1024   black setae (Fig 31B). Diameters of AME 0.37, ALE 0.24, PME 0.41, PLE 0.44; MOA length

1025   0.90, anterior width of MOA 0.74, posterior width of MOA 1.01; interval of AMEs 0.11, interval

1026   of PMEs 0.13, interval between AME and ALE 0.10, interval between PME and PLE 0.38.

1027   Clypeus 0.67, light yellowish covered with sparse dark short setae (Fig 31B). Chelicerae length

1028   2.56, yellowish covered with black long setae (Fig 31B). Chelicerae with three promarginal and

1029   four retromarginal teeth. Fangs and marginal teeth dark brown. Endites length 1.73, width 0.97;

1030   labium length 0.89, width 1.00; sternum near round, length 2.50, width 2.88; Endite, labium, and

1031   sternum light yellowish (Fig 31A). Abdomen long oval with a distinct and greyish-brown cardiac

1032   mark; dorsum bearded with dense, dark brown short setae with a series of white spot (Fig 31A).

1033   Lateral abdomen covered with white short setae that form distinct and irregular lateral bands and

1034   patches (Fig 31A). Venter abdomen brownish. Legs brownish covered with blackish short setae

1035   in different densities, regions with sparser setae form light-colored linear markings (Fig 31A).

1036   Palp tibia with a highly sclerotized RTA (Fig 18J, 21E, 31D & F) which divided into a sharp

1037   ventral lobe and a larger, round-tipped dorsal lobe (Fig 21D). Basal retrolateral edge of the

1038   ventral Cy with an oval shaped BCA (Fig 18E, 31 C & E), T sclerotized with a membranous

1039   upper edge, the prolateral side attached to the DTP and the retrolateral side attached to the

1040   membranous Co (Fig 18E, 31 C & E). T + DTP + Co forms a "U" shaped tegular ring (Fig 18E,

1041   31 C & E). A highly sclerotized Sa sits at the lower center of the tegular ring, attached to the T

1042   (Fig 18E, 31 C & E). MA sits retrolaterally to the Sa, hook-shaped and expands gradually from a

1043   narrow base (Fig 18E, 31 C & E). Fu hook shaped, retrolateral side with a small lateral lobe (Fig

1044   18E, 31 C & E). Ventral edge of the Fu folded and forms a groove that contains curved Eb (Fig

1045   18J, 19E–F, 31D & F). In the ventral view, retrolateral arc of the Eb bent (Fig 18E, 31 C & E).

1046   LA trapezoid with round tips with a broad base (Fig 19E & F). All Fu, Eb, and LA originated

1047   from the DST (Fig 19E & F).

Female (Paratype, USNMENT01580832). Total length 16.05: carapace length 6.56, width 6.00, anterior height 2.21, posterior height 2.47; abdomen length 9.49, width 6.36. Length of palp and legs: palp 8.36 (2.81, 1.26, 1.82, 2.47); leg I 21.44 (6.21, 2.58, 5.93, 4.47, 2.25); leg II 22.26 (6.74, 2.59, 5.97, 4.65, 2.31); leg III 20.44 (6.10, 2.53, 5.42, 4.46, 1.93); leg IV 25.14 (7.08, 2.82, 6.43, 6.24, 2.57). Leg formula 4213. Diameters of AME 0.29, ALE 0.23, PME 0.43, PLE 0.43; MOA length 0.87, anterior width of MOA 0.70, posterior width of MOA 1.06; interval of AMEs 0.12, interval of PMEs 0.21, interval between AME and ALE 0.13, interval between PME and PLE 0.41. Clypeus 0.74. Chelicerae length 2.71. Chelicerae with three promarginal and four retromarginal teeth. Endite length 1.69, width 1.02; labium length 0.89, width 1.11; sternum near round, length 2.61, width 2.83. Female similar to male, but larger, darker the in coloration, and with relatively shorter legs (Fig 32A–B). Epigynum round or triangle shaped, highly sclerotized and longer than wide; divided into two LLs by the near oval MF with two small and distinct membranous windows and a relatively small posterior part (Fig 20J, 32C). EF long, extends to near the anterior edge of the epigynum (Fig 20J, 32C). CD short, curved, and do not bend ventrally (Fig 20E, 32D). AB small, knob-shaped, and laterally positioned (Fig 20E, Fig 32D). FD begins with a coiled and tubular part and ended with a thin flake (Fig 20E, Fig 32D).

Variation. Given as variation of five females followed by variation of two males in parentheses. Total length 14.68 ± 1.23 (12.11 ± 1.10): carapace length 6.77 ± 0.27 (6.05 ± 0.45), width 6.20 ± 0.23 (5.56 ± 0.40), anterior height 2.28 ± 0.16 (2.13 ± 0.12), posterior height 2.64 ± 0.16 (2.74 ± 0.15); abdomen length 7.91 ± 1.38 (6.07 ± 0.67), width 5.08 ± 1.16 (3.82 ± 0.72). Palp 8.96 ± 0.35 (12.56 ± 0.54); leg I 22.30 ± 1.09 (25.49 ± 1.54); leg II 23.19 ± 0.97 (25.72 ± 1.70); leg III 21.61 ± 1.19 (23.30 ± 1.45); leg IV 26.45 ± 1.62 (27.41 ± 1.56). Diameters of AME 0.33 ± 0.03 (0.31 ± 0.04), ALE 0.22 ± 0.01 (0.22 ± 0.02), PME 0.43 ± 0.01 (0.40 ± 0.02), PLE 0.45 ± 0.02 (0.44 ± 0.02); Clypeus 0.48 ± 0.10 (0.77 ± 0.02). Chelicera length 2.61 ± 0.15 (2.42 ± 0.14). Most of the specimens has three promarginal and four retromarginal teeth on both chelicerae while one specimen has asymmetrical number of the cheliceral marginal teeth. Endite length 1.82 ± 0.13 (1.66 ± 0.18), width 1.04 ± 0.03 (0.89 ± 0.10). Labium length 0.96 ± 0.07 (0.84 ± 0.10), width 0.96 ± 0.07 (0.84 ± 0.10). Sternum length 2.64 ± 0.03 (2.46 ± 0.21), width 2.89 ± 0.08 (2.74 ± 0.24). The specimen from Tamatave (MT_207084) has a slightly different MA with a sharp dorsal tip (Fig 19F)

Natural history. Median-sized wandering spider inhabiting habitats similar to *D. hydatostella* **sp. nov.** Active at night, found floating on water, or holding on to leaf litter or vegetation emerging from the water surface (Fig 22L–M).

Remark. Specimens of the "Hydatostella" group from the north and the east of the island are very similar and are nearly identical in the habitus. However, the differences between the two populations are constant and receive strong support in both morphological and phylogenetic analyses. The poor dispersal abilities and geological separation can as well explain the limitation of gene flow between the populations (see Results and Discussion). We hence separate *D. rotundus* **sp. nov.** as a new species.

Etymology. The species epithet is a masculine adjective, referring to the major diagnostic characteristics of the species: round shaped female epigynum and male RTA dorsal lobe.

Distribution. Known from limited areas of eastern humid forests of Madagascar (see Fig 23D)

Acknowledgements

We sincerely thank Tiana Vololona, Rhina Harin' Hala Rasolondalao, and the staff at Madagascar's Institute for the Conservation of Tropical Ecosystems (MICET) for their help in the transportation and obtaining the research permits. We would like to express our thanks the local students Annie Rasoanoeliarimanana, and Jeremia Ravelojaona for their help in the field. We are thankful to the local guides and the porters who supported our fieldwork in the remote forests. We acknowledge our colleagues Matjaž Gregorič and Matjaž Bedjanič for their help in organizing the field trip. We thank Peter Jäger at SMF and Arnaud Henrard at RMCA for loaning the specimens, and Peter Michalik for the suggestions in the integrative taxonomy. We also thank Rok Kuntner for etymological advice.

References

Adams DC, Otárola-Castillo E. 2013. Geomorph: An r package for the collection and analysis of geometric morphometric shape data. *Methods in Ecology and Evolution* 4:393–399. DOI: 10.1111/2041-210X.12035.

Agnarsson I, Jencik BB, Veve GM, Hanitriniaina S, Agostini D, Goh SP, Pruitt J, Kuntner M. 2015. Systematics of the Madagascar *Anelosimus* spiders: Remarkable local richness and endemism, and dual colonization from the Americas. *ZooKeys* 2015:13–52. DOI: 10.3897/zookeys.509.8897.

Agnarsson I, Kuntner M. 2005. Madagascar: An unexpected hotspot of social *Anelosimus* spider diversity (Araneae: Theridiidae). *Systematic Entomology* 30:575–592. DOI: 10.1111/j.1365-3113.2005.00289.x.

Albo MJ, Bidegaray-Batista L, Bechsgaard J, Silva ELC da, Bilde T, Pérez-Miles F. 2017. Molecular phylogenetic analyses show that Trechaleidae and Lycosidae are sister groups. *Arachnology* 17:169–176. DOI: 10.13156/arac.2017.17.4.169.

Ali JR, Aitchison JC. 2008. Gondwana to Asia: Plate tectonics, paleogeography and the biological connectivity of the Indian sub-continent from the middle Jurassic through latest Eocene (166-35 Ma). *Earth-Science Reviews* 88:145–166. DOI: 10.1016/j.earscirev.2008.01.007.

Antonelli A, Smith RJ, Perrigo AL, Crottini A, Hackel J, Testo W, Farooq H, Torres Jiménez MF, Andela N, Andermann T, Andriamanohera AM, Andriambololonera S, Bachman SP, Bacon CD, Baker WJ, Belluardo F, Birkinshaw C, Borrell JS, Cable S, Canales NA, Carrillo JD, Clegg R, Clubbe C, Cooke RSC, Damasco G, Dhanda S, Edler D, Faurby S, de Lima Ferreira P, Fisher BL, Forest F, Gardiner LM, Goodman SM, Grace OM, Guedes TB, Henniges MC, Hill R, Lehmann CER, Lowry PP, Marline L, Matos-Maraví P, Moat J, Neves B, Nogueira MGC, Onstein RE, Papadopulos AST, Perez-Escobar OA, Phelps LN,

1128   Phillipson PB, Pironon S, Przelomska NAS, Rabarimanarivo M, Rabehevitra D,
1129   Raharimampionona J, Rajaonah MT, Rajaonary F, Rajaovelona LR, Rakotoarinivo M,
1130   Rakotoarisoa AA, Rakotoarisoa SE, Rakotomalala HN, Rakotonasolo F, Ralaiveloarisoa
1131   BA, Ramirez-Herranz M, Randriamamonjy JEN, Randriamboavonjy T, Randrianasolo V,
1132   Rasolohery A, Ratsifandrihamanana AN, Ravololomanana N, Razafiniary V, Razanajatovo
1133   H, Razanatsoa E, Rivers M, Sayol F, Silvestro D, Vorontsova MS, Walker K, Walker BE,
1134   Wilkin P, Williams J, Ziegler T, Zizka A, Ralimanana H. 2022. Madagascar's extraordinary
1135   biodiversity: Evolution, distribution, and use. *Science* 378:962. DOI:
1136   10.1126/science.abf0869.

1137   Blandin P. 1979. Etudes sur les Pisauridae afrícaines XI. Genres peu connus ou nouveaux des
1138   Iles Canaries, du Continent africaín et de Madagascar. *Revue Zoologique Africaine* 93:347–
1139   375.

1140   Bleckmann H, Bender M. 1987. Water surface waves generated by the male Pisaurid spider
1141   *Dolomedes triton* (Walckenaer) during courtship behavior. *Journal of Arachnology* 15:363–
1142   369.

1143   Bond JE, Godwin RL, Colby JD, Newton LG, Zahnle XJ, Agnarsson I, Hamilton CA, Kuntner
1144   M. 2022. Improving taxonomic practices and enhancing its extensibility—an example from
1145   araneology. *Diversity* 14:5. DOI: 10.3390/d14010005.

1146   Bösenberg W, Strand E. 1906. Japanische Spinnen. *Abhandlungen der Senckenbergischen*
1147   *Naturforschenden Gesellschaft* 30:93–422.

1148   Brown JL, Cameron A, Yoder AD, Vences M. 2014. A necessarily complex model to explain the
1149   biogeography of the amphibians and reptiles of Madagascar. *Nature Communications* 5:1–
1150   10. DOI: 10.1038/ncomms6046.

1151   Buerki S, Devey DS, Callmander MW, Phillipson PB, Forest F. 2013. Spatio-temporal history of
1152   the endemic genera of Madagascar. *Botanical Journal of the Linnean Society* 171:304–329.

1153   Cardini A, Elton S. 2007. Sample size and sampling error in geometric morphometric studies of
1154   size and shape. *Zoomorphology* 126:121–134. DOI: 10.1007/s00435-007-0036-2.

1155   Carico JE. 1973. The Nearctic Species of the Genus *Dolomedes* (Araneae: Pisauridae). *Bulletin*
1156   *of the Museum of Comparative Zoology* 144:435–488.

1157   Chamberlin R V. 1924. Descriptions of new American and Chinese spiders, with notes on other
1158   Chinese species. *Proceedings of the United States National Museum* 63:1–38.

1159   Chen F, Xue G, Wang Y, Zhang H, He J, Chen J, Xie P. 2021. Evolution of the Yangtze River
1160   reconstructed by the largest molecular phylogeny of Cyprinidae. *Research Square*:1–14.

1161   Clerck C. 1757. *Svenska spindlar : uti sina hufvud-slägter indelte samt under några och sextio*
1162   *särskildte arter beskrefne : och med illuminerade Figr uplyste. Stockholmiae*: Sweden:
1163   Literis Laur. Salvii, MDCCLVII.

1164   Davies VT, Raven RJ. 1980. *Megadolomedes* nov. gen. (Araneae: Pisauridae) with a description
1165   of the male of the type-species, *Dolomedes australianus* Koch 1865. *Memoirs of The*
1166   *Queensland Museum* 20:135–141.

1167 Dayrat B. 2005. Towards integrative taxonomy. *Biological Journal of the Linnean Society*
1168   85:407–415.
1169 Dias MS, Cornu JF, Oberdorff T, Lasso CA, Tedesco PA. 2013. Natural fragmentation in river
1170   networks as a driver of speciation for freshwater fishes. *Ecography* 36:683–689. DOI:
1171   10.1111/j.1600-0587.2012.07724.x.
1172 Duffey E. 2012. *Dolomedes plantarius* (Clerck, 1757) (Araneae: Pisauridae): A reassessment of
1173   its ecology and distribution in Europe, with comments on its history at Redgrave and
1174   Lopham Fen, England. *Bulletin of the British Arachnological Society* 15:285–292. DOI:
1175   10.13156/arac.2012.15.1.285.
1176 Folmer O, Black M, Hoeh W, Lutz R, Vrijenhoek R. 1994. DNA primers for amplification of
1177   mitochondrial cytochrome c oxidase subunit I from diverse metazoan invertebrates.
1178   *Molecular Marine Biology and Biotechnology* 3:294–299.
1179 Gering RL. 1953. Structure and function of the genitalia in some American agelenid spiders.
1180   *Smithsonian Miscellaneous Collections* 121:1–84.
1181 Gertsch WJ. 1934. Further notes on American spiders. *American Museum Novitates* 726:1–26.
1182 Griffiths D. 2006. Pattern and process in the ecological biogeography of European freshwater
1183   fish. *Journal of Animal Ecology* 75:734–751. DOI: 10.1111/j.1365-2656.2006.01094.x.
1184 Griswold CE. 1993. Investigations into the Phylogeny of the Lycosoid Spiders and Their Kin
1185   (Arachnida: Araneae: Lycosoidea). *Smithsonian Contributions to Zoology* 539:1–39.
1186 Griswold CE, Ubick D, Ledford J, Polotow D. 2022. A revision of the Malagasy crack-leg
1187   spiders of the genus *Uduba* Simon, 1880 (Araneae, Udubidae), with description of 35 new
1188   species from Madagascar. *Proceedings of the California Academy of Science* 67:1–193.
1189 Hedin MC, Maddison WP. 2001. A combined molecular approach to phylogeny of the jumping
1190   spider subfamily Dendryphantinae (Araneae: Salticidae). *Molecular Phylogenetics and*
1191   *Evolution* 18:386–403. DOI: 10.1006/mpev.2000.0883.
1192 Hedin M, Milne MA. 2023. New species in old mountains: integrative taxonomy reveals ten new
1193   species and extensive short-range endemism in *Nesticus* spiders (Araneae, Nesticidae) from
1194   the southern Appalachian Mountains. *ZooKeys* 1145:1–130. DOI:
1195   10.3897/zookeys.1145.96724.
1196 Huang J-P, Lin C-P. 2011. Lineage-specific late Pleistocene expansion of an endemic subtropical
1197   gossamer-wing damselfly, *Euphaea formosa*, in Taiwan. *BMC Evolutionary Biology* 11:11–
1198   94. DOI: 10.1186/1471-2148-11-94.
1199 Huelsenbeck JP, Ronquist F. 2001. MRBAYES: Bayesian inference of phylogenetic trees.
1200   *Bioinformatics Applications Note* 17:754–755.
1201 Jäger P. 2020. *Thunberga* gen. nov., a new genus of huntsman spiders from Madagascar
1202   (Araneae: Sparassidae: Heteropodinae). *Zootaxa* 4790:245–260. DOI:
1203   10.11646/zootaxa.4790.2.3.
1204 Johnson JC. 2001. Sexual cannibalism in fishing spiders (*Dolomedes triton*): An evaluation of
1205   two explanations for female aggression towards potential mates. *Animal Behaviour* 61:905–
1206   914. DOI: 10.1006/anbe.2000.1679.

1207   Johnson JC, Sih A. 2007. Fear, food, sex and parental care: a syndrome of boldness in the fishing
1208   spider, *Dolomedes triton*. Animal Behaviour 74:1131–1138. DOI:
1209   10.1016/j.anbehav.2007.02.006.

1210   Kimura M. 1980. A simple method for estimating evolutionary rates of base substitutions
1211   through comparative studies of nucleotide sequences. *Journal of Molecular Evolution*
1212   16:111–120.

1213   Klingenberg CP. 2016. Size, shape, and form: concepts of allometry in geometric
1214   morphometrics. *Development Genes and Evolution* 226:113–137. DOI: 10.1007/s00427-
1215   016-0539-2.

1216   Kralj-Fišer S, Čandek K, Lokovšek T, Čelik T, Cheng R-C, Elgar MA, Kuntner M. 2016. Mate
1217   choice and sexual size dimorphism, not personality, explain female aggression and sexual
1218   cannibalism in raft spiders. *Animal Behaviour* 111:49–55. DOI:
1219   10.1016/j.anbehav.2015.10.013.

1220   Kramer RA, Richter DD, Pattanayak S, Sharma NP. 1997. Ecological and economic analysis of
1221   watershed protection in eastern Madagascar. *Journal of Environmental Management*
1222   49:277–295.

1223   Kuntner M, Cheng R-C, Kralj-Fišer S, Liao C-P, Schneider JM, Elgar MA. 2016. The evolution
1224   of genital complexity and mating rates in sexually size dimorphic spiders. *BMC*
1225   *Evolutionary Biology* 16:1–9. DOI: 10.1186/s12862-016-0821-y.

1226   Kuntner M, Coddington JA, Schneider JM. 2009. Intersexual arms race? Genital coevolution in
1227   nephilid spiders (Araneae, Nephilidae). *Evolution* 63:1451–1463. DOI: 10.1111/j.1558-
1228   5646.2009.00634.x.

1229   Lapinski W, Walther P, Tschapka M. 2015. Morphology reflects microhabitat preferences in an
1230   assemblage of neotropical wandering spiders. *Zoomorphology* 134:219–236. DOI:
1231   10.1007/s00435-015-0257-8.

1232   Latreille PA. 1804. Tableau methodique des Insectes. *Nouveau Dictionnaire d'Histoire Naturelle*
1233   *Paris* 24:129–295.

1234   Leroy B, Paschetta M, Canard A, Bakkenes M, Isaia M, Ysnel F. 2013. First assessment of
1235   effects of global change on threatened spiders: Potential impacts on *Dolomedes plantarius*
1236   (Clerck) and its conservation plans. *Biological Conservation* 161:155–163. DOI:
1237   10.1016/j.biocon.2013.03.022.

1238   Murphy JA, Roberts MJ. 2015. *Spider families of the world : and their spinnerets*. York, UK:
1239   British Arachnological Society.

1240   Pearson RG, Raxworthy CJ. 2009. The evolution of local endemism in Madagascar: Watershed
1241   versus climatic gradient hypotheses evaluated by null biogeographic models. *Evolution*
1242   63:959–967. DOI: 10.1111/j.1558-5646.2008.00596.x.

1243   Petrunkevitch A. 1928. System Aranearum. *Transactions of The Connecticut Academy of Arts*
1244   *and Sciences* 29:1–271.

1245 Piacentini LN, Ramírez MJ. 2019. Hunting the wolf: A molecular phylogeny of the wolf spiders
1246   (Araneae, Lycosidae). *Molecular Phylogenetics and Evolution* 136:227–240. DOI:
1247   10.1016/j.ympev.2019.04.004.
1248 Platnick NI, Forster RR. 1993. A revision of the New Caledonian spider genus *Bradystichus*
1249   (Araneae, Lycosoidea). *American Museum Novitates* 3075:1–14.
1250 Polotow D, Carmichael A, Griswold CE. 2015. Total evidence analysis of the phylogenetic
1251   relationships of Lycosoidea spiders (Araneae, Entelegynae). *Invertebrate Systematics*
1252   29:124–163. DOI: 10.1071/IS14041.
1253 Posada D. 2008. jModelTest: Phylogenetic model averaging. *Molecular Biology and Evolution*
1254   25:1253–1256. DOI: 10.1093/molbev/msn083.
1255 Poy D, Piacentini LN, Michalik P, Lin SW, Ramírez MJ. 2023. MicroCT analysis unveils the
1256   role of inflatable female genitalia and male tibial complex in the genital coupling in the
1257   spider genus *Aysha* (Anyphaenidae, Araneae). *Journal of morphology* 284:e21586. DOI:
1258   10.1002/jmor.21586.
1259 Puillandre N, Brouillet S, Achaz G. 2021. ASAP: assemble species by automatic partitioning.
1260   *Molecular Ecology Resources* 21:609–620. DOI: 10.1111/1755-0998.13281.
1261 QGIS.org. 2023. QGIS Geographic Information System.
1262 de Queiroz K. 2005. A unified concept of species and its consequences for the future of
1263   taxonomy. In: *Proceedings of the California Academy of Sciences*. San Francisco,
1264   California, U.S.A.: California Academy of Sciences, 196–215.
1265 de Queiroz K. 2007. Species concepts and species delimitation. *Systematic Biology* 56:879–886.
1266   DOI: 10.1080/10635150701701083.
1267 R Core Team. 2022. R: A language and environment for statistical computing. In: *R Foundation*
1268   *for Statistical Computing*. Vienna, Austria.
1269 Raharimalala FN, Ravaomanarivo LH, Ravelonandro P, Rafarasoa LS, Zouache K, Tran-Van V,
1270   Mousson L, Failloux AB, Hellard E, Moro CV, Ralisoa BO, Mavingui P. 2012.
1271   Biogeography of the two major arbovirus mosquito vectors, *Aedes aegypti* and *Aedes*
1272   *albopictus* (Diptera, Culicidae), in Madagascar. *Parasites and Vectors* 5:56. DOI:
1273   10.1186/1756-3305-5-56.
1274 Ralimanana H, Perrigo AL, Smith RJ, Borrell JS, Faurby S, Rajaonah MT, Randriamboavonjy T,
1275   Vorontsova MS, Cooke RSC, Phelps LN, Sayol F, Andela N, Andermann T,
1276   Andriamanohera AM, Andriambololonera S, Bachman SP, Bacon CD, Baker WJ, Belluardo
1277   F, Birkinshaw C, Cable S, Canales NA, Carrillo JD, Clegg R, Clubbe C, Crottini A,
1278   Damasco G, Dhanda S, Edler D, Farooq H, de Lima Ferreira P, Fisher BL, Forest F,
1279   Gardiner LM, Goodman SM, Grace OM, Guedes TB, Hackel J, Henniges MC, Hill R,
1280   Lehmann CER, Lowry PP, Marline L, Matos-Maraví P, Moat J, Neves B, Nogueira MGC,
1281   Onstein RE, Papadopulos AST, Perez-Escobar OA, Phillipson PB, Pironon S, Przelomska
1282   NAS, Rabarimanarivo M, Rabehevitra D, Raharimampionona J, Rajaonary F, Rajaovelona
1283   LR, Rakotoarinivo M, Rakotoarisoa AA, Rakotoarisoa SE, Rakotomalala HN,
1284   Rakotonasolo F, Ralaiveloarisoa BA, Ramirez-Herranz M, Randriamamonjy JEN,

1285   Randrianasolo V, Rasolohery A, Ratsifandrihamanana AN, Ravololomanana N, Razafiniary
1286   V, Razanajatovo H, Razanatsoa E, Rivers M, Silvestro D, Testo W, Torres Jiménez MF,
1287   Walker K, Walker BE, Wilkin P, Williams J, Ziegler T, Zizka A, Antonelli A. 2022.
1288   Madagascar's extraordinary biodiversity: Threats and opportunities. *Science* 378:963. DOI:
1289   10.1126/science.adf1466.

1290 Raven R, Hebron W. 2018. A review of the water spider family Pisauridae in Australia and New
1291   Caledonia with descriptions of four new genera and 23 new species. *Memoirs of the*
1292   *Queensland Museum Nature* 60:233–381.

1293 Roewer CF. 1955. Araneae Lycosaeformia I. (Agelenidae, Hahniidae, Pisauridae) mit
1294   Berücksichtigung aller Arten der äthiopischen Region. *Exploration du Parc National de*
1295   *l'Upemba, Mission G. F. de Witte* 30:1–420.

1296 Sanmartín I, Ronquist F. 2004. Southern hemisphere biogeography inferred by event-based
1297   models: Plant versus animal patterns. *Systematic Biology* 53:216–243. DOI:
1298   10.1080/10635150490423430.

1299 Santos AJ. 2007. A phylogenetic analysis of the nursery-web spider family Pisauridae, with
1300   emphasis on the genera *Architis* and *Staberius* (Araneae: Lycosoidea). *Zoologica Scripta*
1301   36:489–507. DOI: 10.1111/j.1463-6409.2007.00291.x.

1302 Schlick-Steiner BC, Steiner FM, Seifert B, Stauffer C, Christian E, Crozier RH. 2010. Integrative
1303   taxonomy: A multisource approach to exploring biodiversity. *Annual Review of Entomology*
1304   55:421–438. DOI: 10.1146/annurev-ento-112408-085432.

1305 Schneider CA, Rasband WS, Eliceiri KW. 2012. NIH Image to ImageJ: 25 years of image
1306   analysis. *Nature Methods* 9:671–675. DOI: 10.1038/nmeth.2089.

1307 Schneider CJ, Smith TB, Larison B, Moritz C. 1999. A test of alternative models of
1308   diversification in tropical rainforests: Ecological gradients vs. rainforest refugia.
1309   *Proceedings of the National Academy of Sciences* 96:13869–13873.

1310 Schwartz SK, Wagner WE, Hebets EA. 2013. Spontaneous male death and monogyny in the
1311   dark fishing spider. *Biology Letters* 9:20130113. DOI: 10.1098/rsbl.2013.0113.

1312 Sierwald P. 1989. Morphology and ontogeny of female copulatory organs in American
1313   Pisauridae, with special reference to homologous features (Arachnida: Araneae).
1314   *Smithsonian Contributions to Zoology* 484:1–24.

1315 Sierwald P. 1990. Morphology and homologous features in the male palpal organ in Pisauridae
1316   and other spider families, with notes on the taxonomy of Pisauridae (Arachnida: Araneae).
1317   Nemouria, *Occasional Papers of the Delaware Museum of Natural History* 35:1 – 59.

1318 Silva ELC da, Gibbons A, Sierwald P. 2015. Description of the male of *Dolomedes raptoroides*
1319   Zhang, Zhu & Song, 2004 (Araneae: Lycosoidea: Pisauridae). *Zootaxa* 3946:139–145. DOI:
1320   10.11646/zootaxa.3946.1.8.

1321 Silva ELC da, Griswold CE. 2013a. A new species of *Dolomedes* Latreille, 1804 (Araneae:
1322   Lycosoidea: Pisauridae) from Madagascar. *Zootaxa* 3691:461–466. DOI:
1323   10.11646/zootaxa.3691.4.5.

1324 Silva ELC da, Griswold CE. 2013b. The first record and the description of a new species of
1325   *Dendrolycosa* Doleschall, 1859 (Araneae: Pisauridae: Pisaurinae) from Madagascar.
1326   *Zootaxa* 3682:572–578. DOI: 10.11646/zootaxa.3682.4.8.
1327 Silva ELC da, Sierwald P. 2013. On three monotypic nursery web spider genera from
1328   Madagascar with first description of the male of *Tallonia picta* Simon, 1889 and
1329   redescription of the type-species of *Paracladycnis* Blandin, 1979 and *Thalassiopsis* Roewer,
1330   1955 (Araneae: Lycosoidea: Pisauridae). Zootaxa 3750:277–288. DOI:
1331   10.11646/zootaxa.3750.3.7.
1332 Simon E. 1884. Description d'une nouvelle famille de l'ordre des Araneae (Bradystichidae).
1333   *Annales de la Société Entomologique de Belgique* 28:297–301.
1334 Simon E. 1898. *Histoire naturelle des araignées. Deuxième édition, tome second*. Paris, France:
1335   Roret.
1336 Smith H. 2000. The status and conservation of the fen raft spider (*Dolomedes plantarius*) at
1337   Redgrave and Lopham Fen National Nature Reserve, England. *Biological Conservation*
1338   95:153–164.
1339 Smith TB, Wayne RK, Girman DJ, Bruford MW. 1997. A role for ecotones in generating
1340   rainforest biodiversity. *Science* 276:1855–1857.
1341 Stamatakis A. 2014. RAxML version 8: A tool for phylogenetic analysis and post-analysis of
1342   large phylogenies. *Bioinformatics* 30:1312–1313. DOI: 10.1093/bioinformatics/btu033.
1343 Strand E. 1907. Diagnosen neuer Spinnen aus Madagaskar und Sansibar. *Zoologischer Anzeiger*
1344   31:725–748.
1345 Sukumaran J, Holder MT. 2010. DendroPy: A Python library for phylogenetic computing.
1346   *Bioinformatics* 26:1569–1571. DOI: 10.1093/bioinformatics/btq228.
1347 Sukumaran J, Holder MT. 2015. SumTrees: phylogenetic tree summarization. 4.0. 0.
1348 Suter RB. 1999. Cheap transport for fishing spiders (Araneae, Pisauridae): The physics of sailing
1349   on the water surface. *Journal of Arachnology* 27:489–496.
1350 Suter RB, Gruenwald J. 2000. Spider size and locomotion on the water surface (Araneae,
1351   Pisauridae). *Journal of Arachnology* 28:300–308. DOI: 10.1636/0161-
1352   8202(2000)028[0300:SSALOT]2.0.CO;2.
1353 Suter RB, Stratton GE, Miller PR. 2004. Taxonomic variation among spiders in the ability to
1354   repel water: Surface adhesion and hair density. *Journal of Arachnology* 32:11–21. DOI:
1355   10.1636/M02-74.
1356 Tanikawa A. 2003. Two new species and two newly recorded species of the spider family
1357   Pisauridae (Arachnida: Araneae) from Japan. *Acta Arachnologica* 52:35–42.
1358 Tanikawa A, Miyashita T. 2008. A revision of Japanese spiders of the genus *Dolomedes*
1359   (Araneae: Pisauridae) with its phylogeny based on mt-DNA. *Acta Arachnologica* 57:19–35.
1360 Vink CJ, Dupérré N. 2010. Pisauridae (Arachnida: Araneae). *Fauna of New Zealand* 64:1–60.
1361 Wheeler WC, Coddington JA, Crowley LM, Dimitrov D, Goloboff PA, Griswold CE, Hormiga
1362   G, Prendini L, Ramírez MJ, Sierwald P, Almeida-Silva L, Alvarez-Padilla F, Arnedo MA,
1363   Benavides Silva LR, Benjamin SP, Bond JE, Grismado CJ, Hasan E, Hedin M, Izquierdo

1364 MA, Labarque FM, Ledford J, Lopardo L, Maddison WP, Miller JA, Piacentini LN,
1365 Platnick NI, Polotow D, Silva-Dávila D, Scharff N, Szűts T, Ubick D, Vink CJ, Wood HM,
1366 Zhang J. 2017. The spider tree of life: phylogeny of Araneae based on target-gene analyses
1367 from an extensive taxon sampling. *Cladistics* 33:574–616. DOI: 10.1111/cla.12182.
1368 Wilmé L, Goodman SM, Ganzhorn JU. 2006. Biogeographic evolution of Madagascar's
1369 microendemic biota. *Science* 312:1063–1065. DOI: 10.1126/science.1084125.
1370 World Spider Catalog. 2023.World Spider Catalog. Version 24. Natural History Museum Bern.
1371 *Available at http://wsc.nmbe.ch.* DOI: 10.24436/2.
1372 Ye Z, Zhen Y, Damgaard J, Chen P, Zhu L, Zheng C, Bu W. 2018. Biogeography and
1373 diversification of Holarctic water striders: Cenozoic temperature variation, habitat shifting
1374 and multiple intercontinental dispersals. *Systematic Entomology* 43:19–30. DOI:
1375 10.1111/syen.12274.
1376 Zhang J, Kapli P, Pavlidis P, Stamatakis A. 2013. A general species delimitation method with
1377 applications to phylogenetic placements. *Bioinformatics* 29:2869–2876. DOI:
1378 10.1093/bioinformatics/btt499.
1379 Zhang J-X, Zhu M-S, Song D-X. 2004. A review of the Chinese nursery-web spiders (Araneae:
1380 Pisauridae). *Journal of Arachnology* 32:353–417.

Different types of evidence used (labeled as "Y") to diagnose *Dolomedes* species in recent regional reviews and in this paper.

BCA: basal cymbium apophysis; Cy: cymbium; DTP: distal tegular projection; Eb: embolus; EF: epigynal fold; Fu: fulcrum; LA: lateral subterminal apophysis; MA: median apophysis; MF: middle field; RTA: retrolateral tibial apophysis; Sa: saddle; T: tegulum.

1 Table 1:

2 **Different types of evidence used (labeled as "Y") to diagnose *Dolomedes* species in recent regional reviews and in this paper.**

3 BCA: basal cymbium apophysis; Cy: cymbium; DTP: distal tegular projection; Eb: embolus; EF: epigynal fold; Fu: fulcrum; LA:

4 lateral subterminal apophysis; MA: median apophysis; MF: middle field; RTA: retrolateral tibial apophysis; Sa: saddle; T: tegulum.

Literature	Region	Morphology																	Molecular		Ecology
		Somatic		Male palp												Female epigynum					
		Coloration	Leg I	Total length	Tibia	Cym length	RTA	BCA	T	DTP	Sa	MA	Fu	Eb	LA	Margin	MF / EF	Vulva	COI	Actin 5C	Habitat
Zhang et al. 2004	China	Y					Y	Y	Y			Y	Y			Y	Y	Y			
Tanikawa 2003	Japan (Ryukyu)	Y		Y	Y	Y	Y										Y	Y			
Tanikawa & Miyashita 2008	Japan	Y	Y		Y		Y									Y	Y		Y		Y
Vink & Dupérré 2010	New Zealand	Y					Y									Y	Y		Y	Y	Y
Raven & Hebron 2018	Oceania	Y		Y	Y	Y	Y		Y	Y		Y				Y	Y	Y			
This paper	Madagascar	Y	Y	Y		Y	Y					Y	Y	Y	Y	Y	Y	Y	Y		Y

Habitat classification for each locality in Madagascar where *Dolomedes* specimens were collected and recorded; see Taxonomy for coordinates.

1 **Table 1:**

2 **Habitat classification for each locality in Madagascar where *Dolomedes* specimens were**

3 **collected and recorded; see Taxonomy for coordinates.**

Locality	Species recorded	Habitat Classification	
		Canopy	Velocity
The 2nd muddy stream and swamp below Mantella Camp, Marojejy	*hydatostella*	Dense	Standing
The slow flowing stream and swamp along trail Kalanoro, Vakona Lodge, Andasibe-Mantadia	*bedjanic, rotundus*	Dense	Standing
Slow flowing part of the streams around Lac Vert, Analamazoatra	*rotundus*	Dense	Standing
The river next to Hotel Feon' ny Ala, Analamazoatra	*kalanoro*	Open	Flowing
The river along trail Circuit Tsakoka, Andasibe-Mantadia	*kalanoro*	Open	Flowing
The 1st, 3rd–5th stream below Mantella Camp, Marojejy	*bedjanic*	Dense	Flowing
The stream on the trail toward Cascade de Humbert, Marojejy	*bedjanic*	Dense	Flowing
The streams around Lac Vert, Analamazoatra	*kalanoro, bedjanic*	Dense	Flowing
The stream along trail Chute Sacree, Andasibe-Mantadia	*gregoric, bedjanic*	Dense	Flowing

Figure 1

The integrative taxonomic model applied in this study.
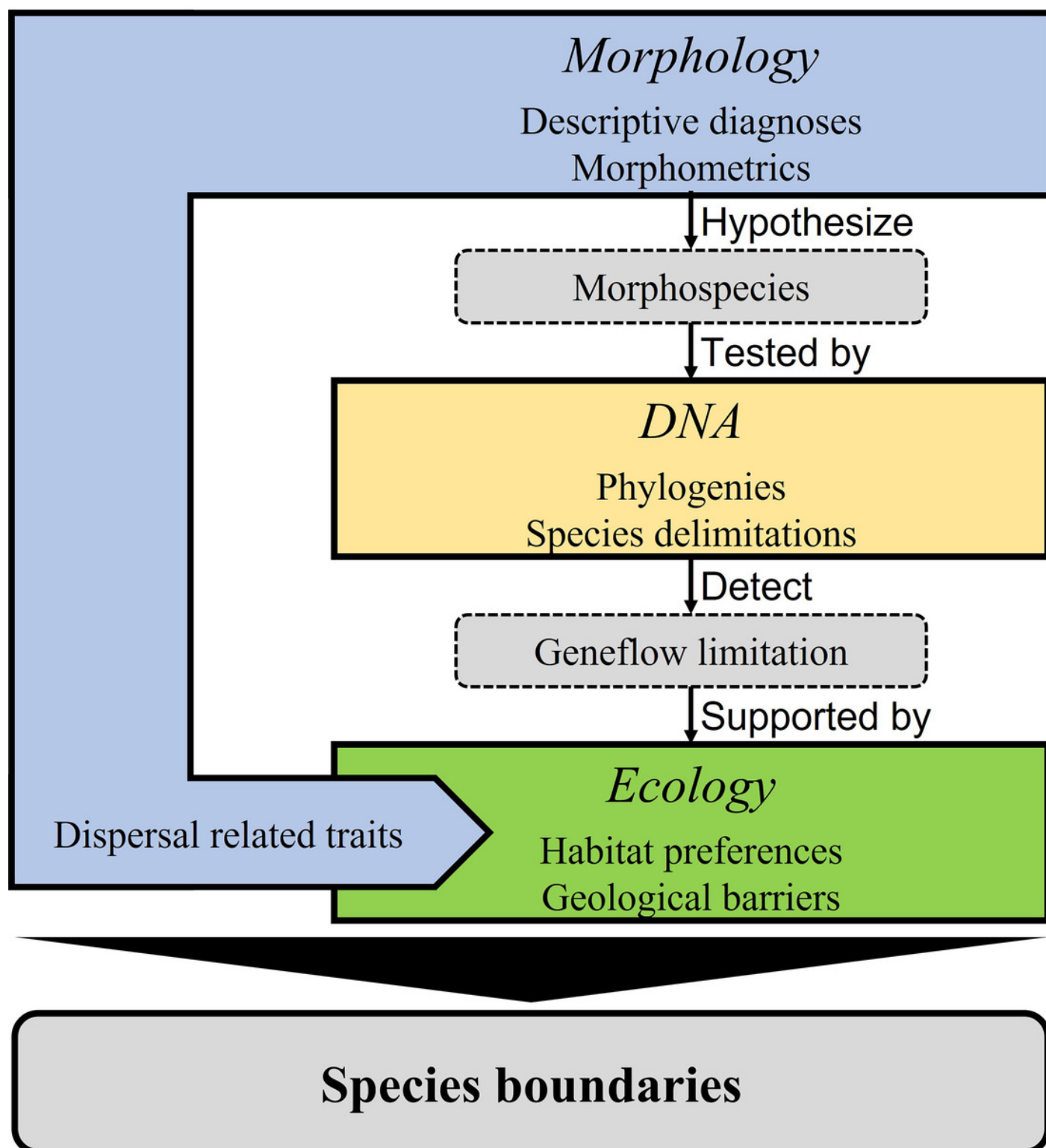
Figure 2

Size comparisons of the selected somatic characters among the five morphospecies.

(A–B) Carapace width. (C–D) Relative length of leg I. (E–F) Relative length of tarsus I. (G–H) Relative length of palp. Bold line: median, upper margin of the box: first quantile (Q_1), lower margin of the box: third quantile (Q_3), upper whisker: the maximum or $Q_1 + 1.5 \times$ interquartile range (IQR), lower whisker: the minimum or $Q_3 - 1.5 \times$ IQR of each group of data.
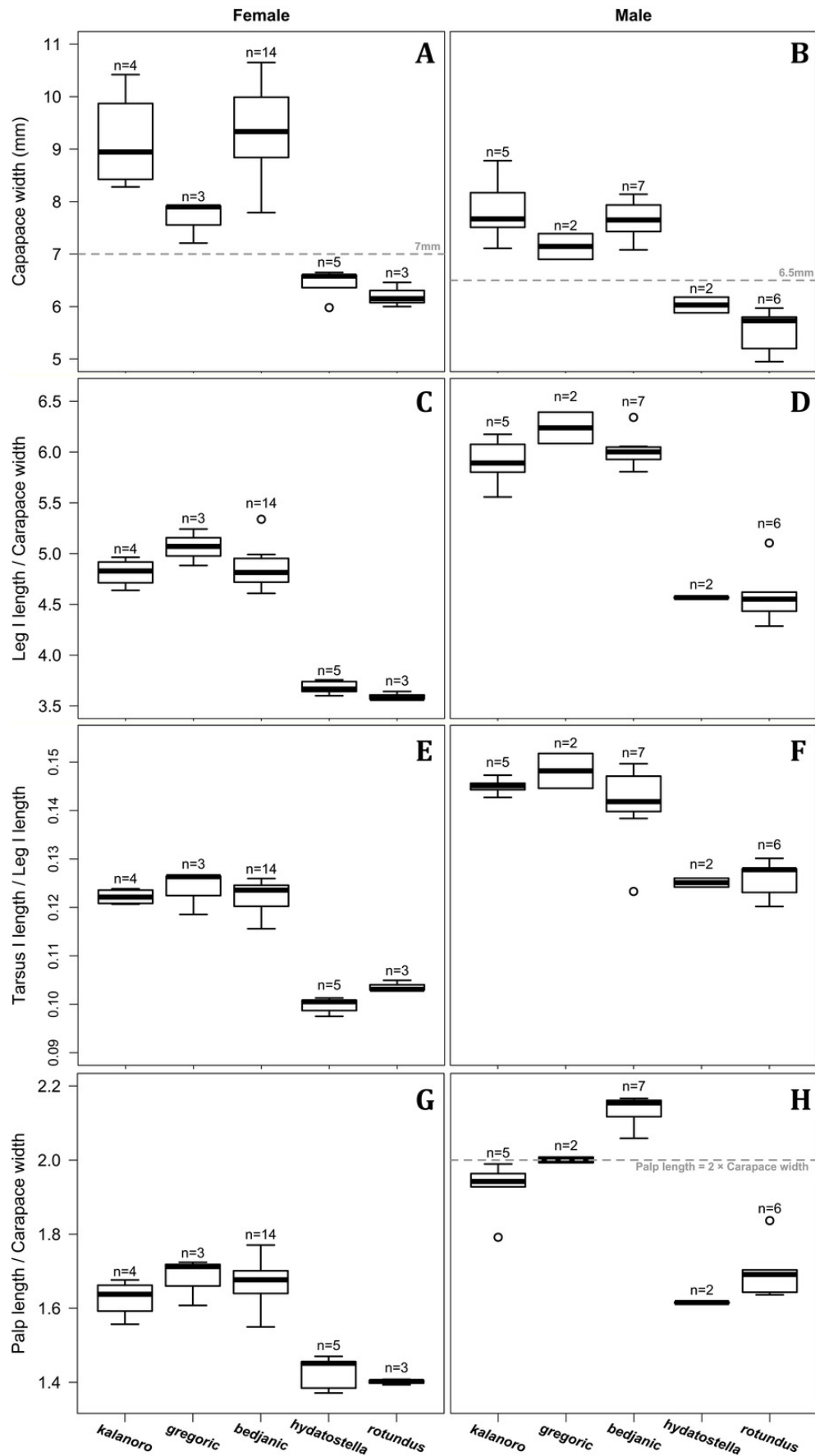
Figure 3

Shape component projections of retrolateral view of the right lateral subterminal apophysis on the first two principal component (PC) axes.

(A) "Kalanoro" group. (B) "Hydatostella" group. The symbols outside of the axes show how shapes change along each PC axis. Gray lines: the shape consensus at the maximum (S_M) or minimum (S_m) of the PC axes; grey points: landmarks of the mean shape consensus of all specimens; black arrows: vectors showing landmarks movement from the mean shape consensus to S_M or S_m.
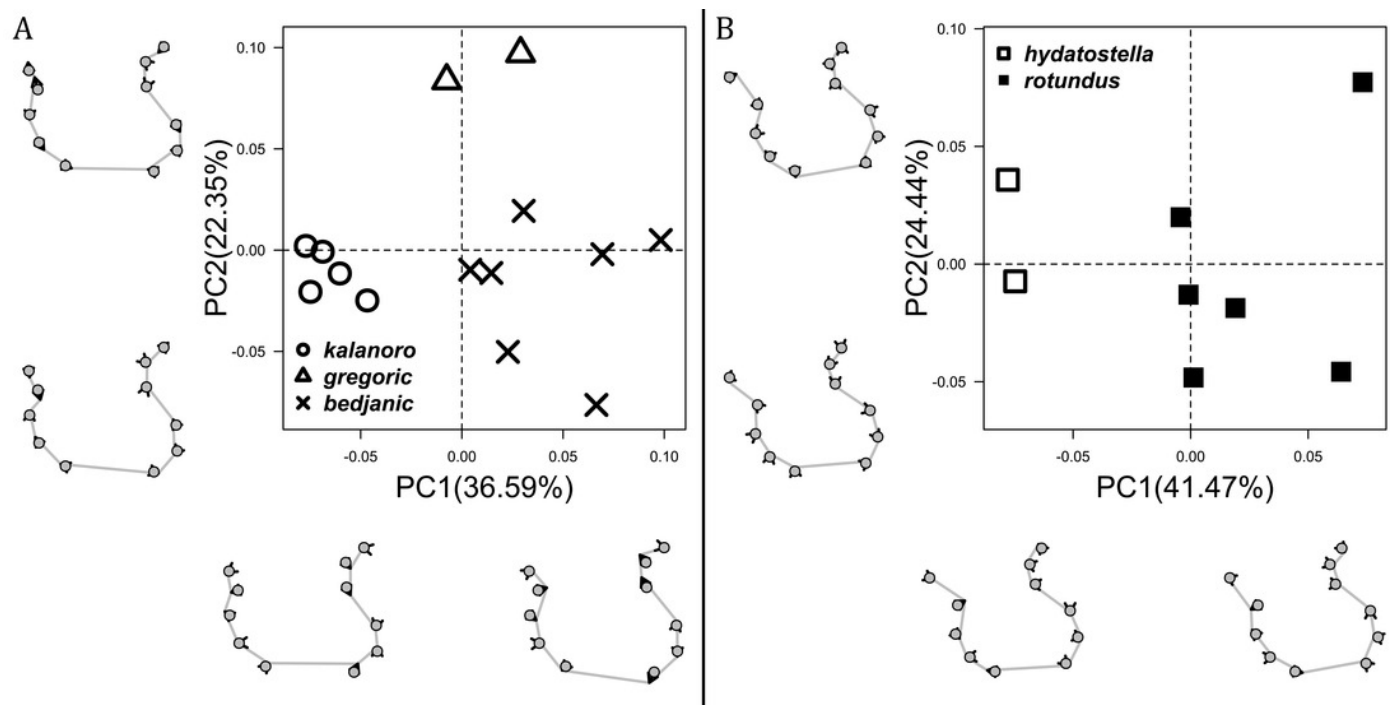
Figure 4

Shape component projections of the male embolus on the first two principal component (PC) axes.

(A–B) Ventral view of the left embolus: (A) "Kalanoro" group; (B) "Hydatostella" group. (C–D) Retrolateral view of the right embolus: (C) "Kalanoro" group; (D) "Hydatostella" group. The symbols outside of the axes show how shapes change along each PC axis. Gray lines: the shape consensus at the maximum (S_M) or minimum (S_m) of the PC axes; grey points: landmarks of the mean shape consensus of all specimens; black arrows: vectors showing landmarks movement from the mean shape consensus to S_M or S_m.

A

PC1(59.32%)
PC2(20.75%)
○ kalanoro
△ gregoric
✕ bedjanic

B

PC1(62.50%)
PC2(13.29%)
□ hydatostella
■ rotundus

C

PC1(84.00%)
PC2(9.56%)
○ kalanoro
△ gregoric
✕ bedjanic

D

PC1(65.39%)
PC2(15.85%)
□ hydatostella
■ rotundus
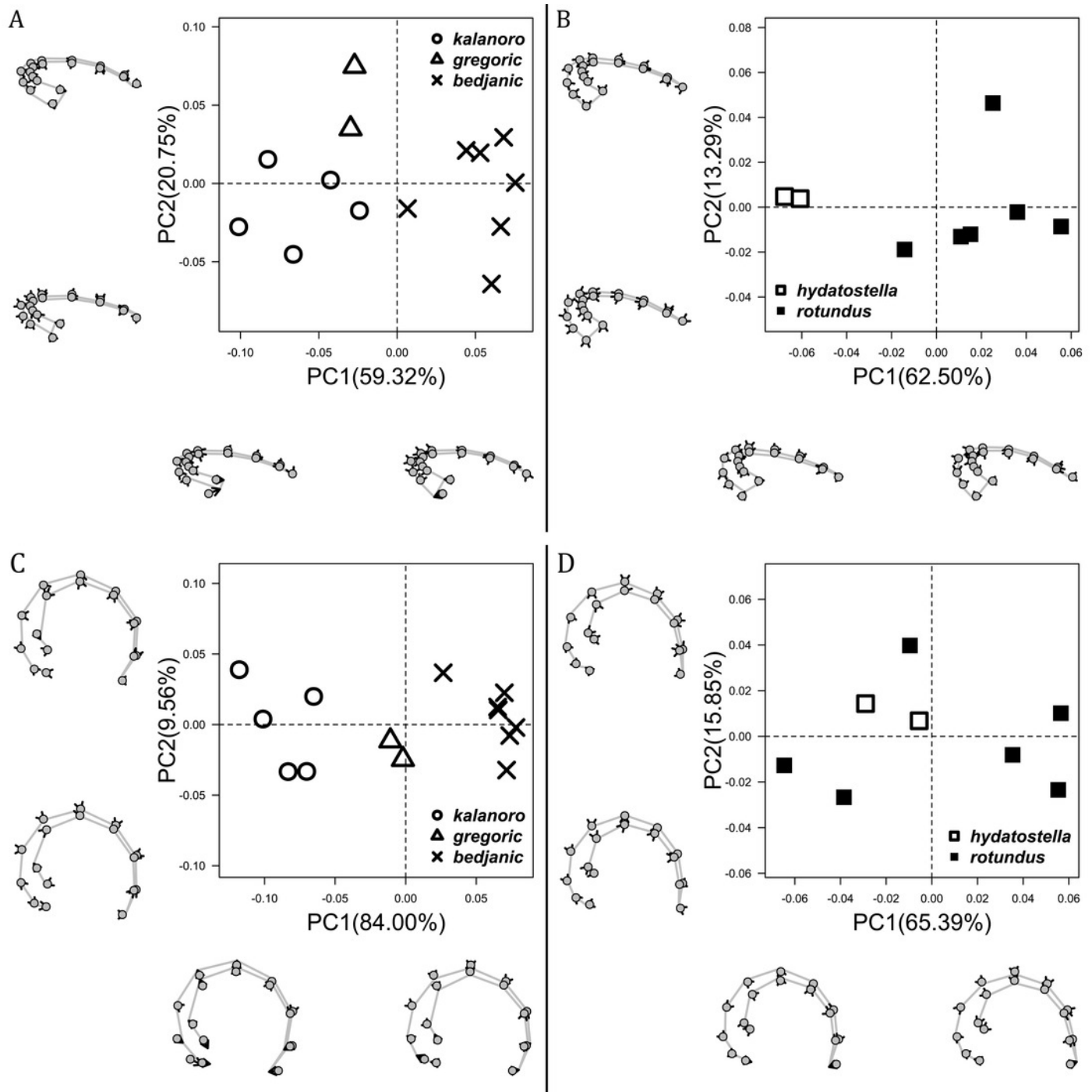
Figure 5

Size comparisons of the selected male genital characters among the five morphospecies.

(A) Diameter of embolic ring. (B) Relative length of cymbium. Bold line: median, upper margin of the box: first quantile (Q_1); lower margin of the box: third quantile (Q_3); upper whisker: the maximum or $Q_1 + 1.5 \times$ interquartile range (IQR); lower whisker: the minimum or $Q_3 - 1.5 \times$ IQR.
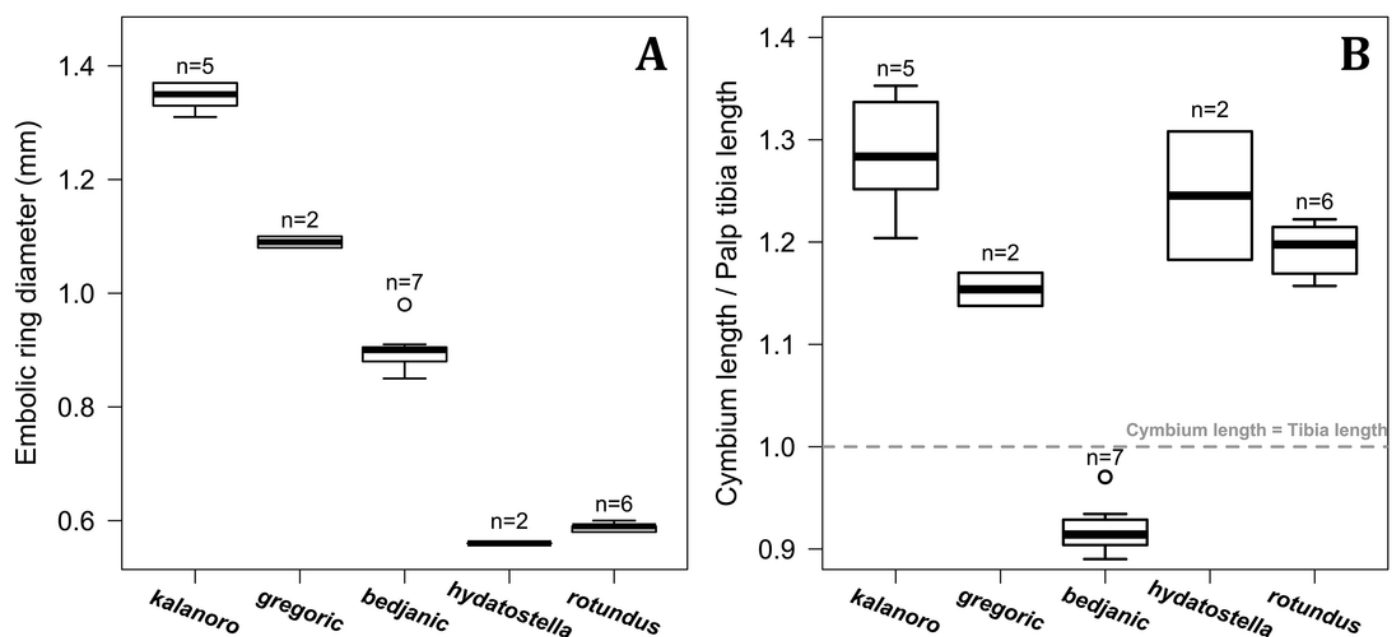
Figure 6

Shape component projections of ventral view of the left median apophysis on the first two principal component (PC) axes.

(A) "Kalanoro" group. (B) "Hydatostella" group. The symbols outside of the axes show how shapes change along each PC axis. Gray lines: the shape consensus at the maximum (S_M) or minimum (S_m) of the PC axes; grey points: landmarks of the mean shape consensus of all specimens; black arrows: vectors showing landmarks movement from the mean shape consensus to S_M or S_m.
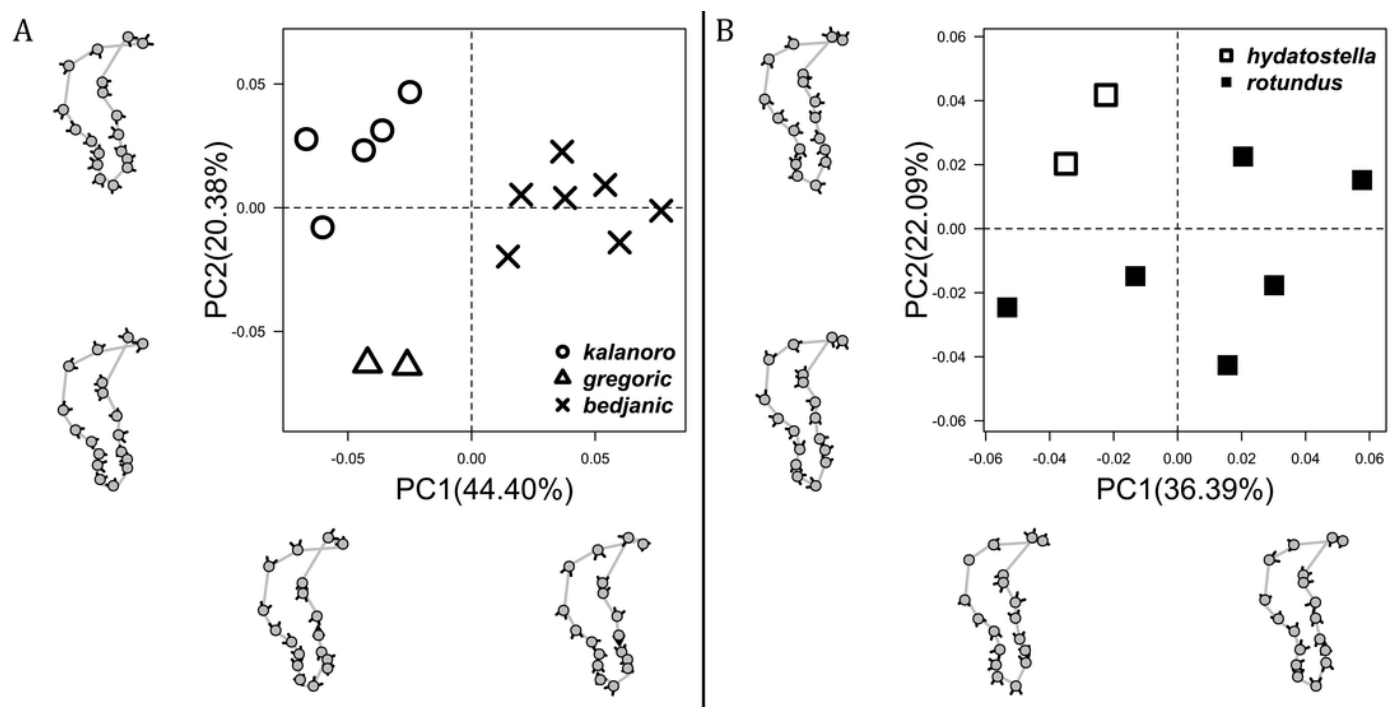
Figure 7

Shape component projections of the male fulcrum on the first two principal component (PC) axes.

(A–B) ventral view of the left fulcrum: (A) "Kalanoro" group; (B) "Hydatostella" group. (C–D) retrolateral view of the right fulcrum: (C) "Kalanoro" group; (D) "Hydatostella" group. The symbols outside of the axes show how shapes change along each PC axis. Gray lines: the shape consensus at the maximum (S_M) or minimum (S_m) of the PC axes; grey points: landmarks of the mean shape consensus of all specimens; black arrows: vectors showing landmarks movement from the mean shape consensus to S_M or S_m.
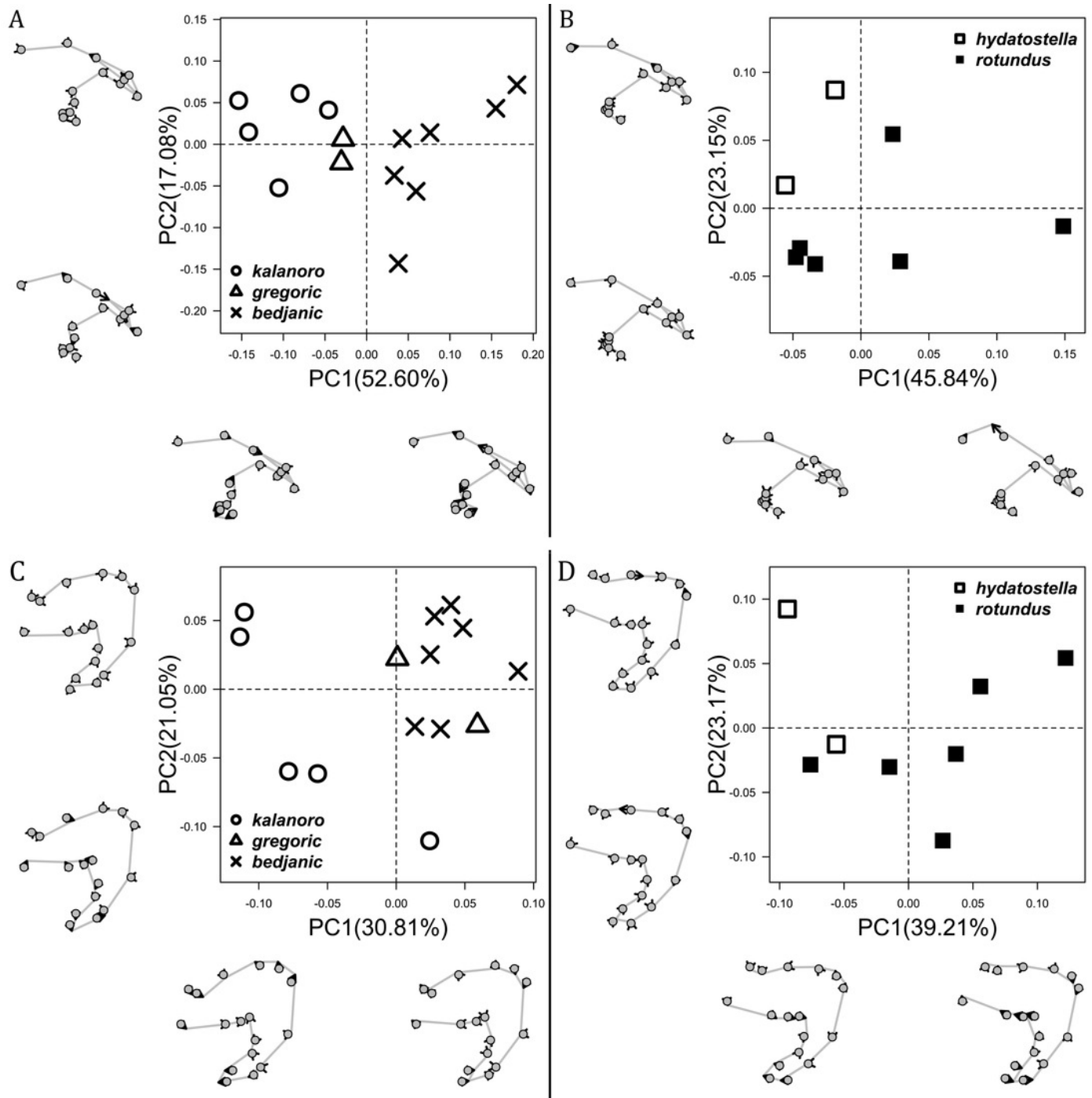
Figure 8

Shape component projections of the posterolateral view of the left retroalteral tibial apophysis on the first two principal component (PC) axes.

(A) "Kalanoro" group. (B) "Hydatostella" group. The symbols outside of the axes show how shapes change along each PC axis. Gray lines: the shape consensus at the maximum (SM) or minimum (Sm) of the PC axes; grey points: landmarks of the mean shape consensus of all specimens; black arrows: vectors showing landmarks movement from the mean shape consensus to S_M or S_m.
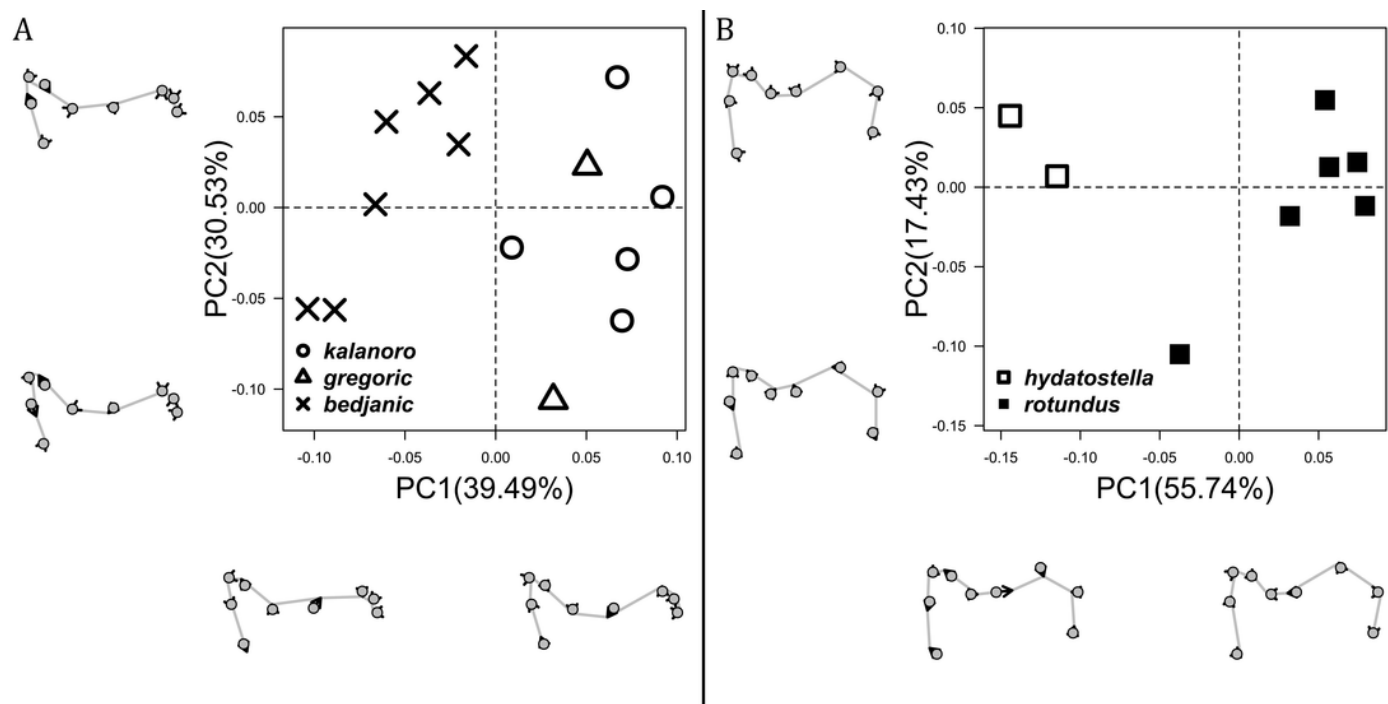
Figure 9

Shape component projections of ventral view of the epigynal middle field on the first two principal component (PC) axes.

(A) "Kalanoro" group. (B) "Hydatostella" group. The symbols outside of the axes show how shapes change along each PC axis. Gray lines: the shape consensus at the maximum (S_M) or minimum (S_m) of the PC axes; grey points: landmarks of the mean shape consensus of all specimens; black arrows: vectors showing landmarks movement from the mean shape consensus to S_M or S_m.
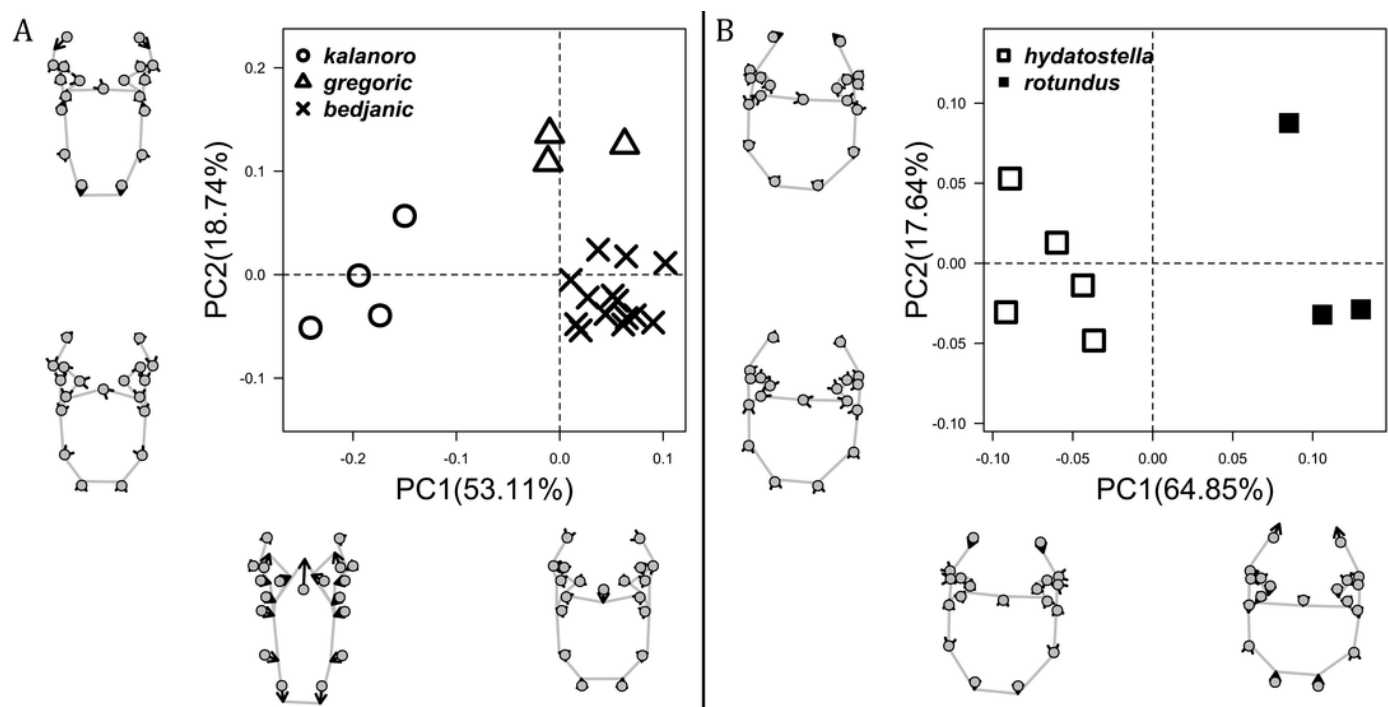
Figure 10

Shape component projections of ventral view of the epigynal margin on the first two principal component (PC) axes.

(A) "Kalanoro" group. (B) "Hydatostella" group. The symbols outside of the axes show how shapes change along each PC axis. Gray lines: the shape consensus at the maximum (S_M) or minimum (S_m) of the PC axes; grey points: landmarks of the mean shape consensus of all specimens; black arrows: vectors showing landmarks movement from the mean shape consensus to S_M or S_m.
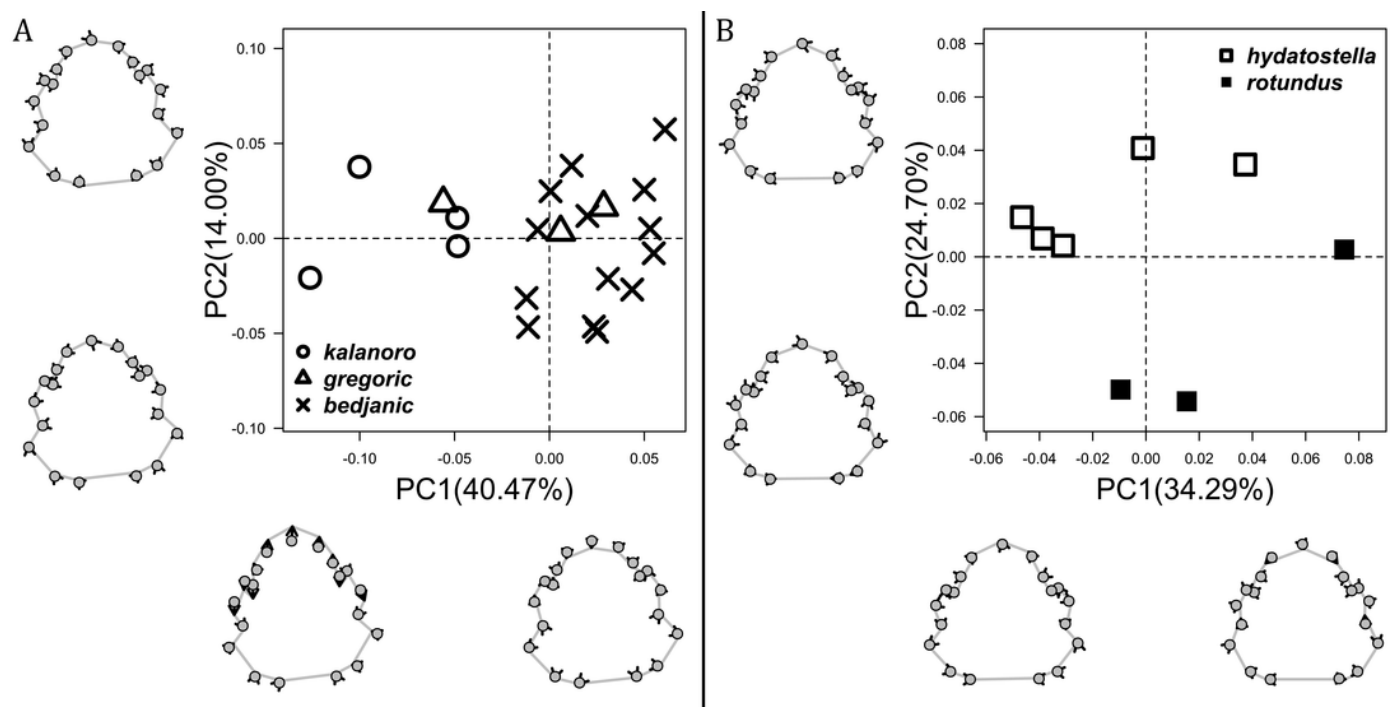
Figure 11

Shape component projections of ventral view of the vulva arrangement on the first two principal component (PC) axes.

(A) "Kalanoro" group. (B) "Hydatostella" group. The symbols outside of the axes show how shapes change along each PC axis. Gray lines: the shape consensus at the maximum (S_M) or minimum (S_m) of the PC axes; grey points: landmarks of the mean shape consensus of all specimens; black arrows: vectors showing landmarks movement from the mean shape consensus to S_M or S_m. Note: The vulva of a female "bedjanic" (KPARA00144) was excluded from this analysis due to severe deformation caused by a Mantispidae larva parasitizing her epigastric furrow beneath the epygynal middle field (see Fig S5).
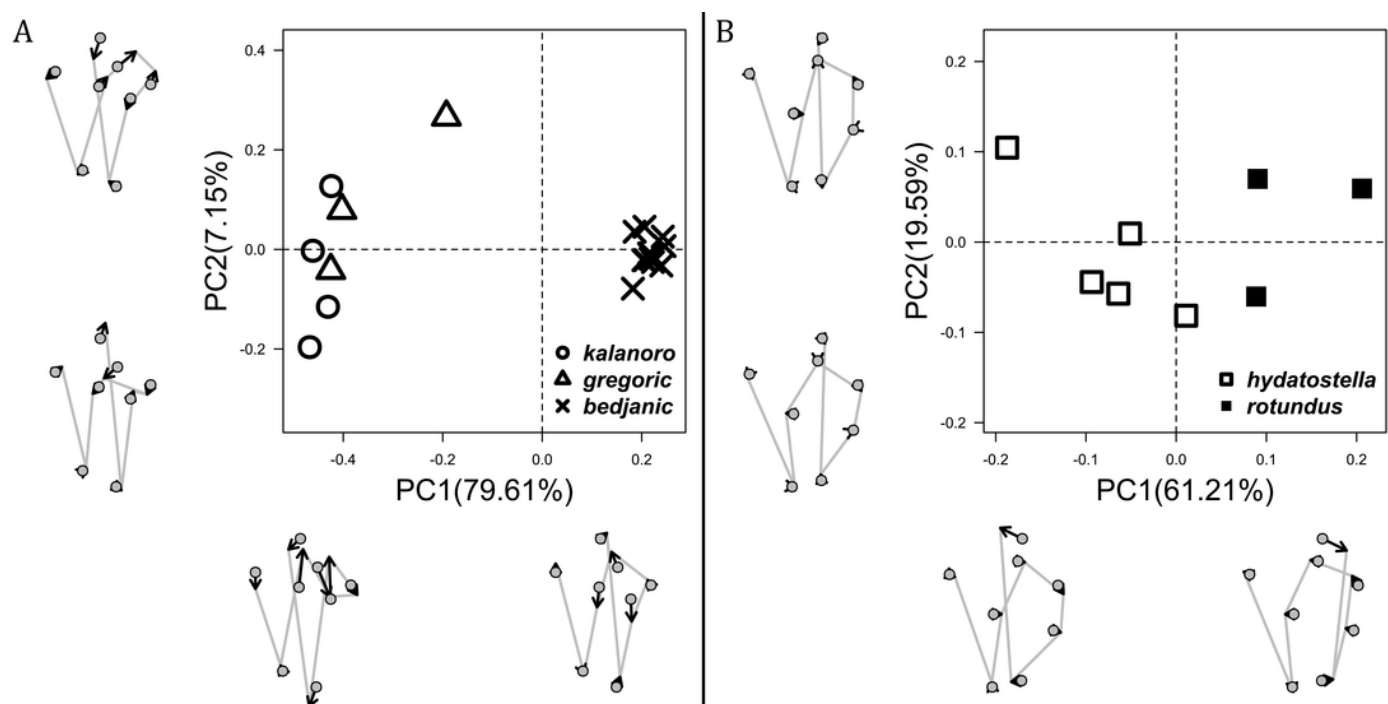
Figure 12

Shape consensuses of the retrolateral view of the embolus, fulcrum, and lateral subterminal apophysis of the expanded right male palp in each morphospecies.

Pairs of shapes covered in grey squares represent the differences in the shape components of the morphospecies do not distinctly separate on the first two principal component axes. The three morphospecies left to the black line belong to the "Kalanoro" group and the two right to the black line are the "Hydatostella" group.
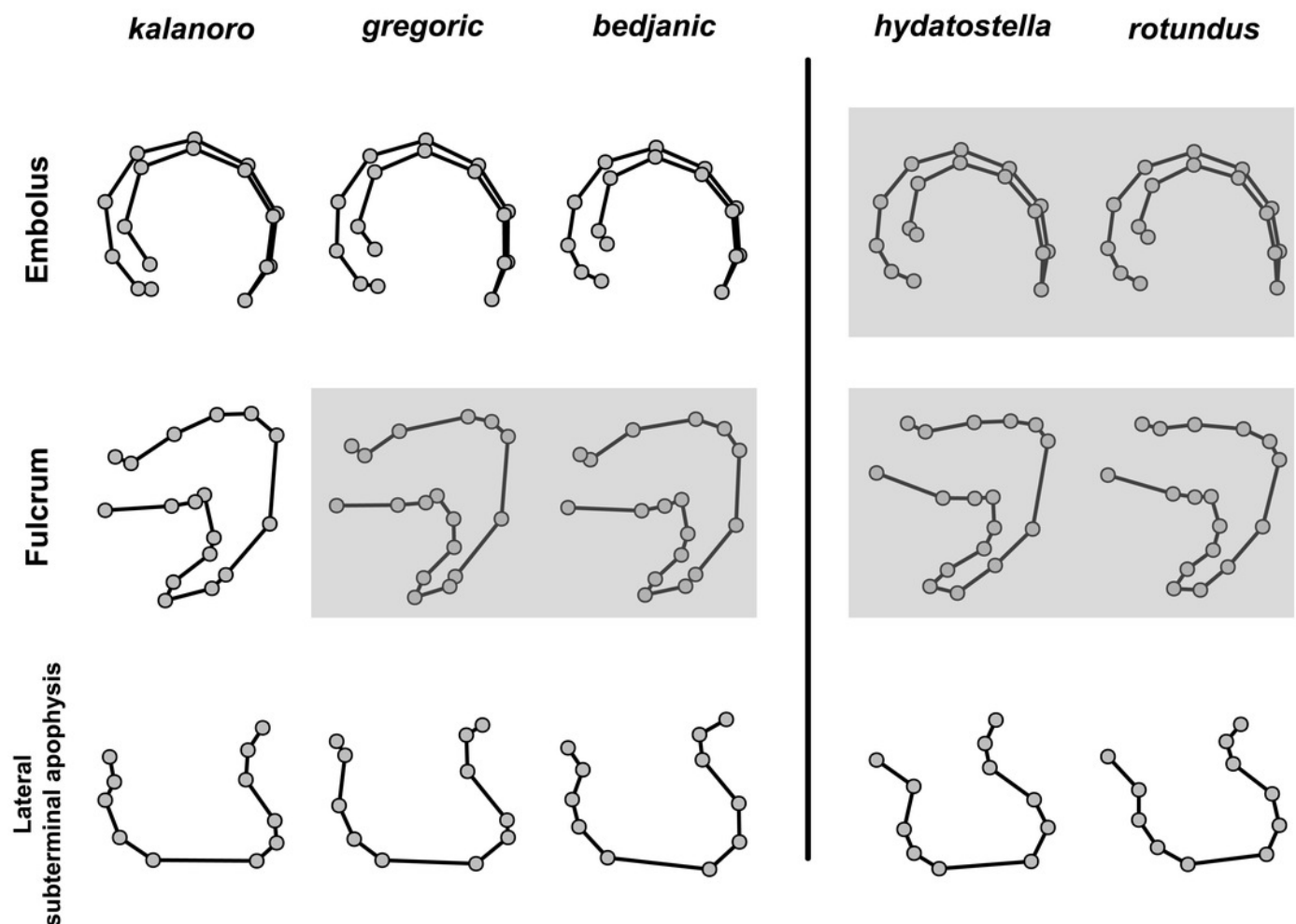
Figure 13

Shape consensuses of the ventral view of the median apophysis, embolus, fulcrum, and the posterolateral view of the retrolateral tibial apophysis of the left male palp in each morphospecies.

Pairs of shapes covered in grey squares represent the differences in the shape components of the morphospecies do not distinctly separate on the first two principal component axes. The three morphospecies left to the black line belong to the "Kalanoro" group and the two right to the black line are the "Hydatostella" group.
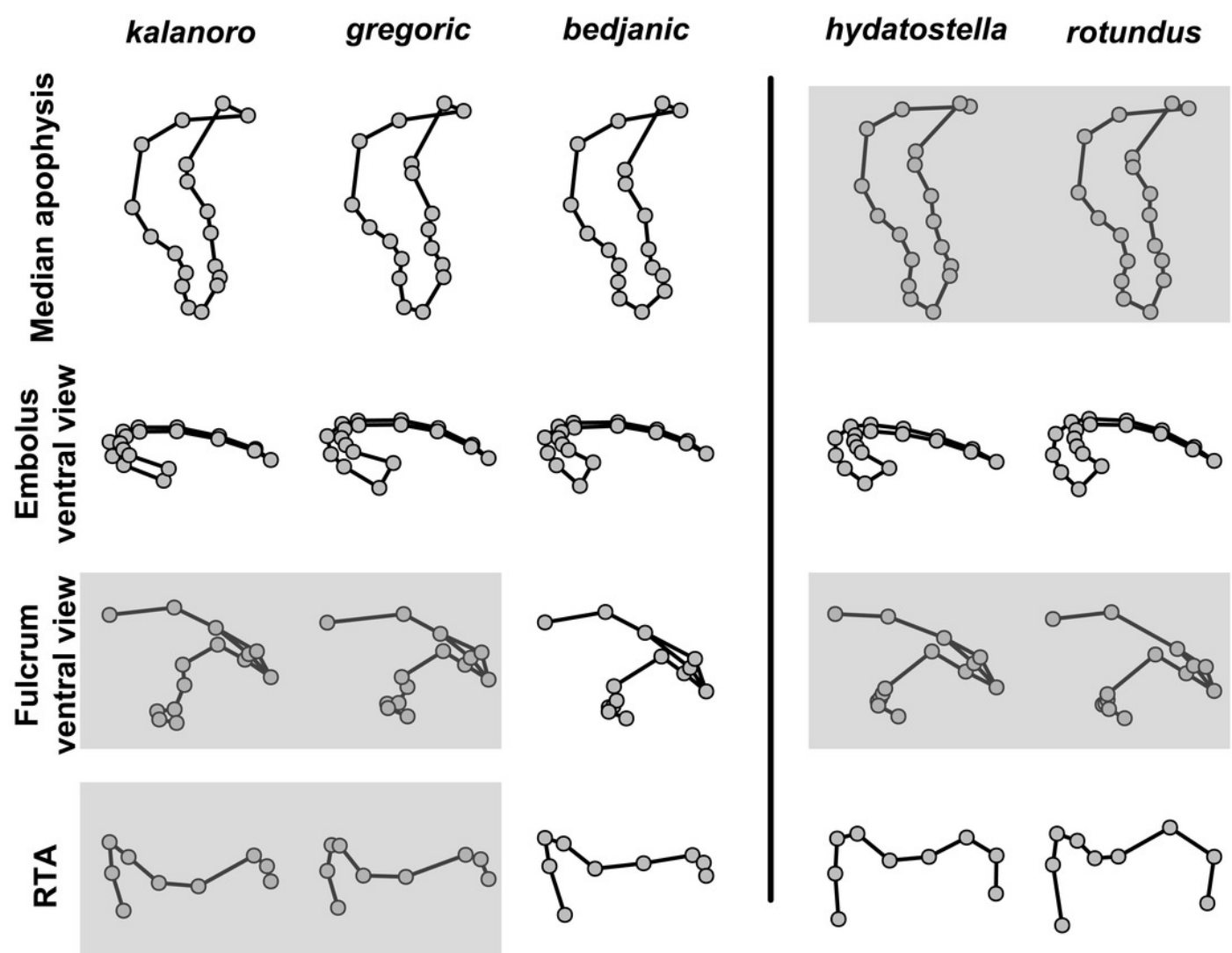
Figure 14

Shape consensuses of the ventral view of the margin of the epigynum, epigynal middle field, and the dorsal view of the vulva of the females in each morphospecies.

Pairs of shapes covered in grey squares represent the differences in the shape components of the morphospecies do not distinctly separate on the first two principal component axes. The three morphospecies left to the black line belong to the "Kalanoro" group and the two right to the black line are the "Hydatostella" group.
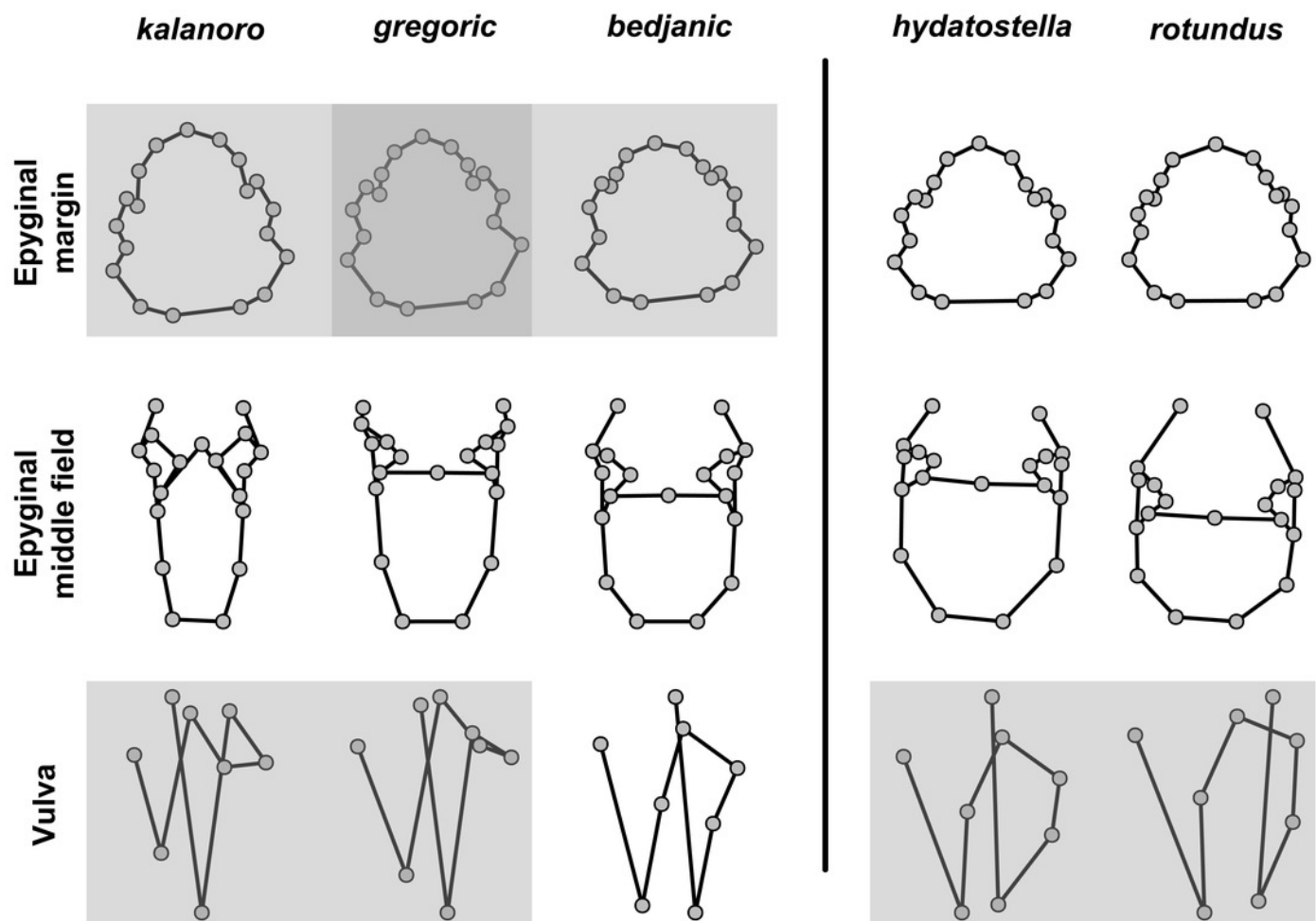
Figure 15

Summarized COI gene tree and species delimitations with nodes strongly supported by maximum likelihood and Bayesian inference analyses marked by solid circle and square, respectively.

The color-coded bars represent the separation of the species under different thresholds of genetic distance and species delimitation methods; ASAP: Assemble Species by Automatic Partitioning (Puillandre et al., 2021), bPTP: Bayesian implementation of the Poisson tree process model analysis (Zhang et al., 2013). Images A–E show the habitus of each species.
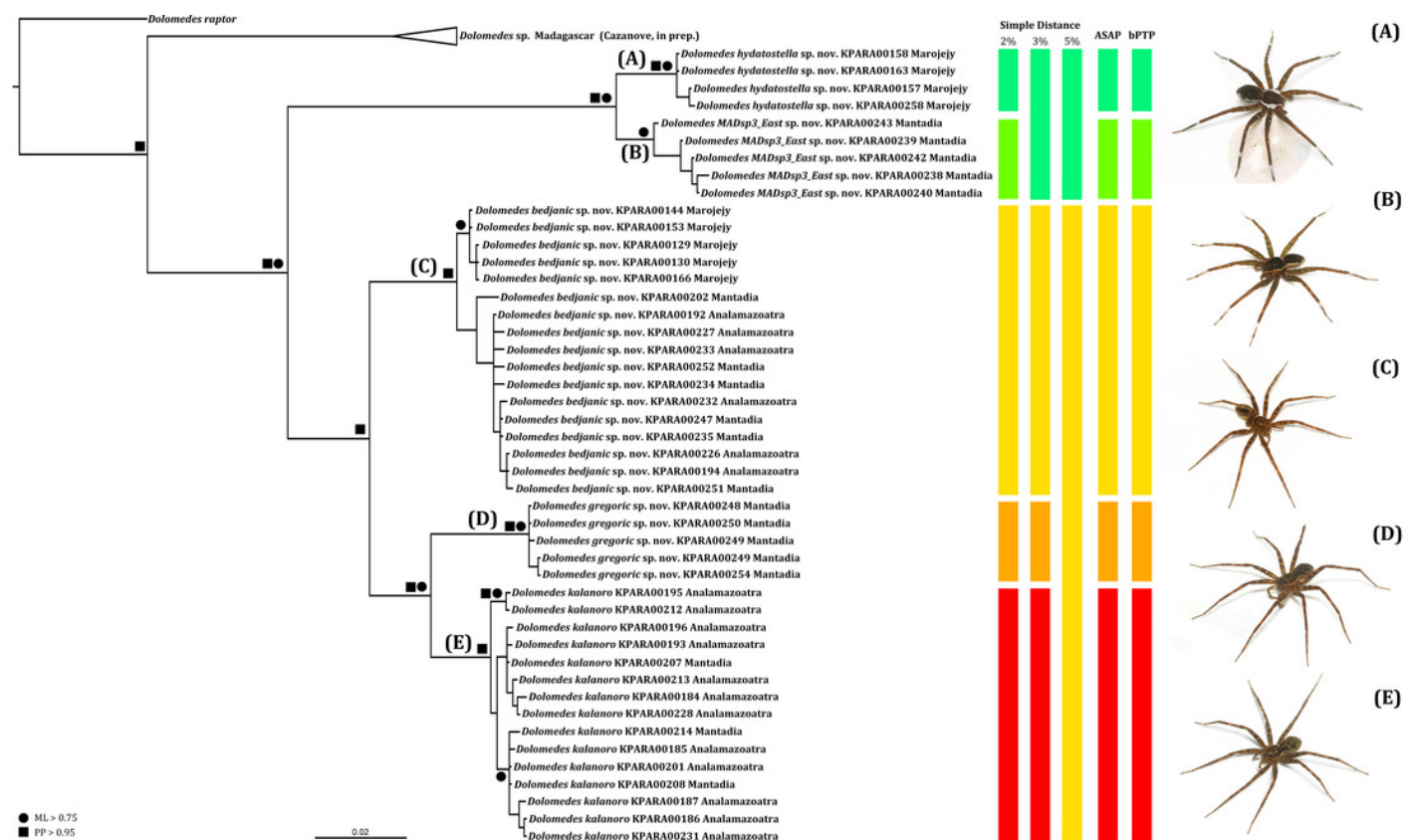
Figure 16

The collecting localities of the five *Dolomedes* species described in the study.

(A) *Dolomedes kalanoro* Silva & Griswold, 2013. (B) *D. gregoric* **sp. nov.** (C) *D. bedjanic* **sp. nov.** (D) *D. hydatostella* **sp. nov.** (hollow square) and *D. rotundus* sp. nov. (solid squares). Localities of the specimens shown in Silva and Griswold's (2013a) research and the specimen deposited at the Royal Museum for Central Africa are marked black whereas those collected in this study are in red.
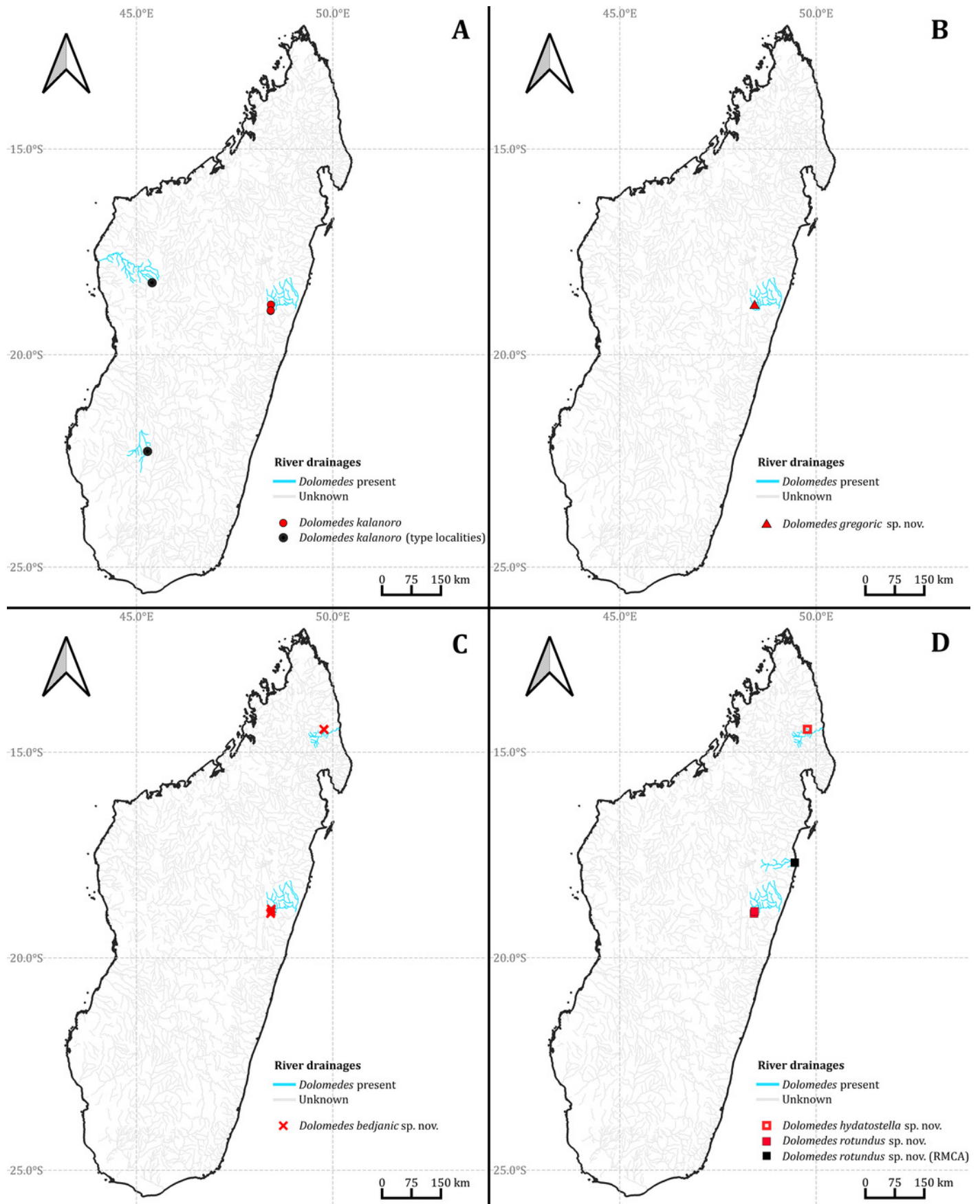
Figure 17

Estimated habitat preferences of the five *Dolomedes* species as summarized from Table 2.
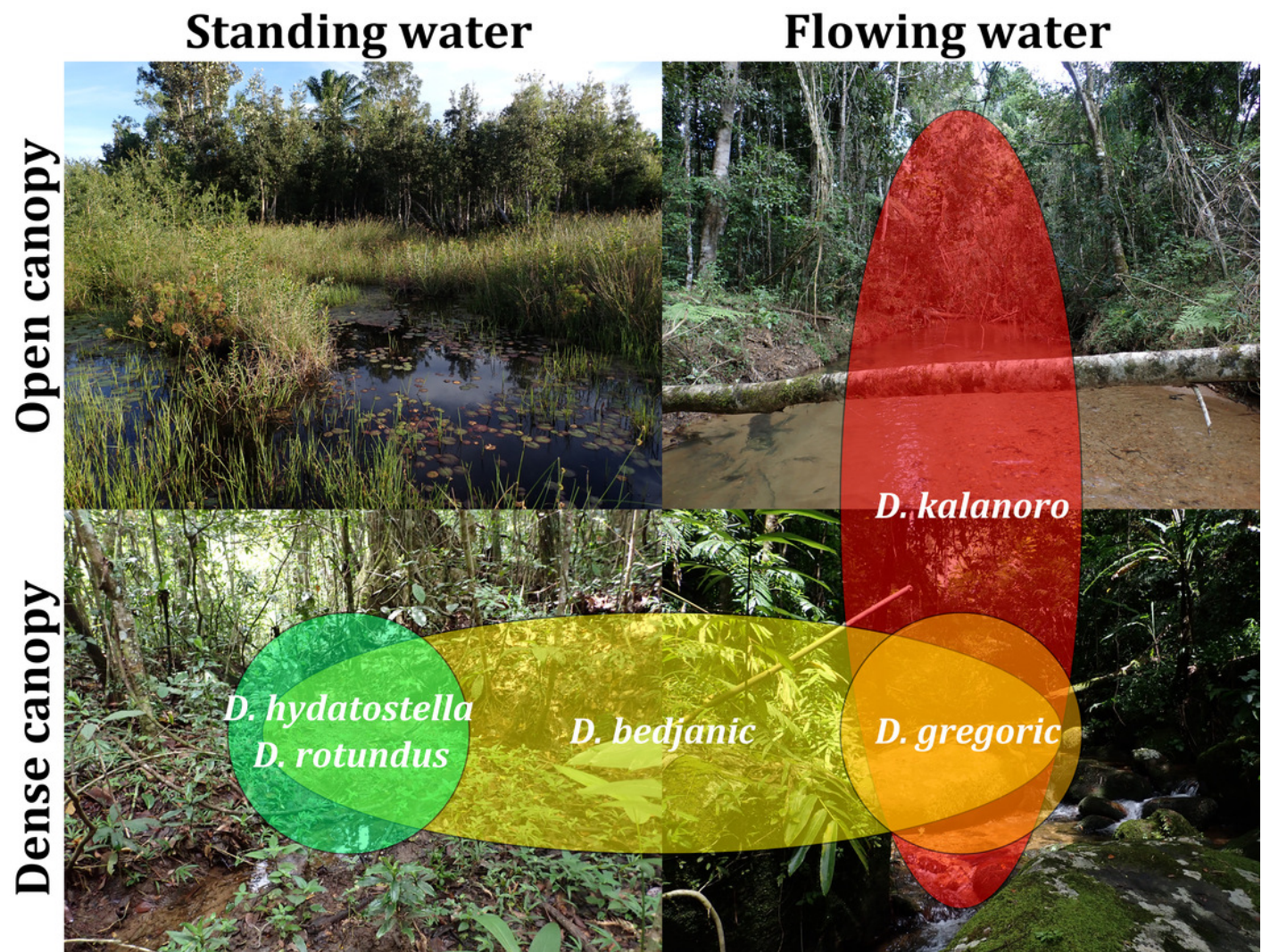
Figure 18

Comparisons of the male palps among the five *Dolomedes* species.

(A & F) *Dolomedes kalanoro* Silva & Griswold, 2013 (KPARA00185). (B & G) *D. gregoric* **sp. nov.** (Holotype male, USNMENT01580825). (C & H) *D. bedjanic* **sp. nov.** (Holotype male, USNMENT01580827). (D & I) *D. hydatostella* **sp. nov.** (Holotype male, USNMENT01580829). (E & J) *D. rotundus* **sp. nov.** (Holotype male, USNMENT01580831). (A–E) Ventral view. (F–J) Retrolateral view. Red arrows point to the saddle; black arrows show the lateral lobe on the fulcrum.
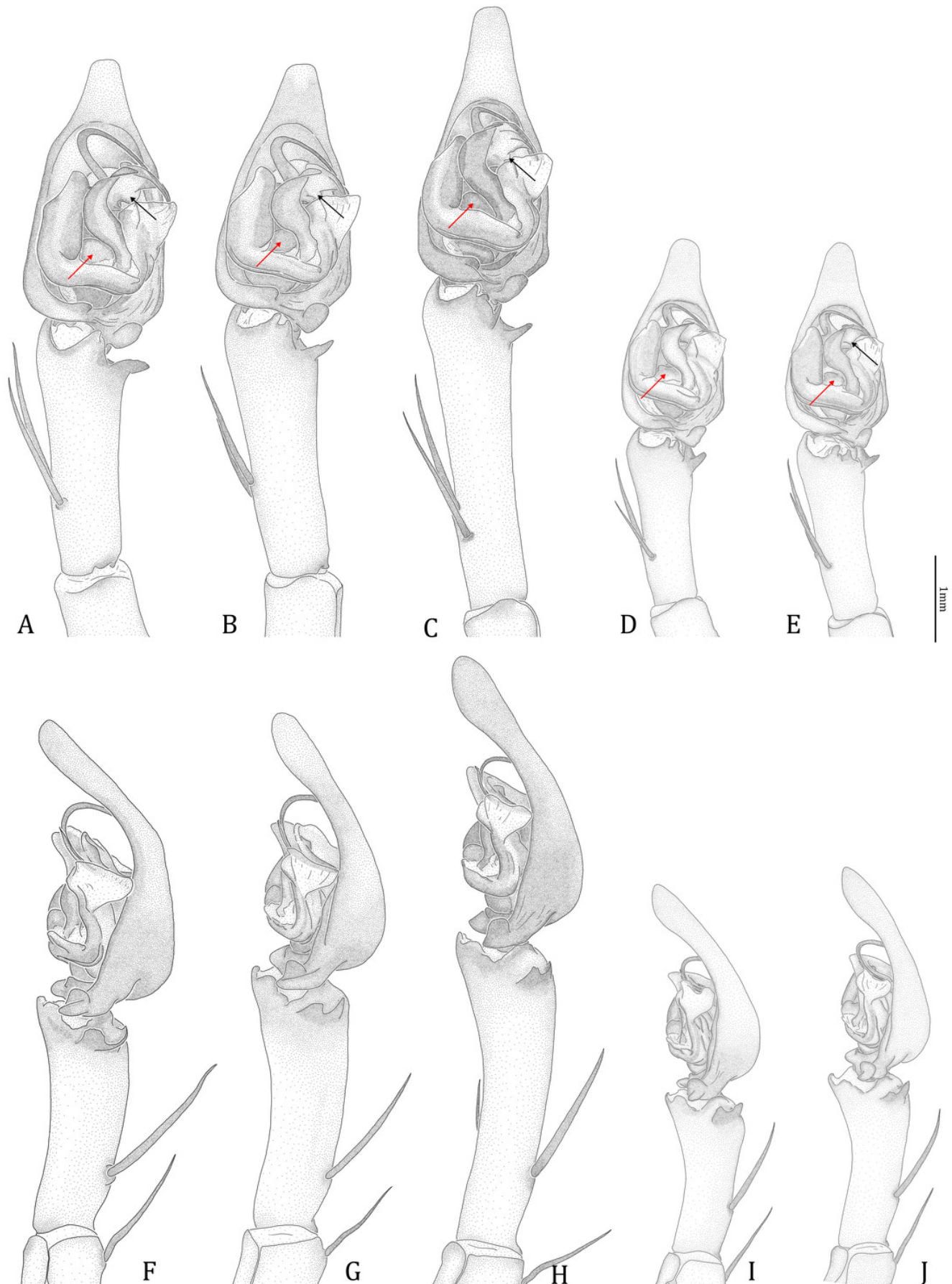
Figure 19

Retrolateral view of the right distal sclerotized tube of males of the five *Dolomedes* species.

(A) *Dolomedes kalanoro* Silva & Griswold, 2013 (KPARA00185). (B) *D. gregoric* **sp. nov.** (Holotype male, USNMENT01580825). (C) *D. bedjanic* **sp. nov.** (Holotype male, USNMENT01580827). (D) *D. hydatostella* **sp. nov.** (Holotype male, USNMENT01580829). (E–F) *D. rotundus* **sp. nov.**: (E) Holotype male (USNMENT01580831); (F) none type specimen (RMCA, MT_207084), showing the shape variation. The black arrow shows the dorsal direction. Eb: embolus; Fu: the fulcrum; LA: lateral subterminal apophysis.
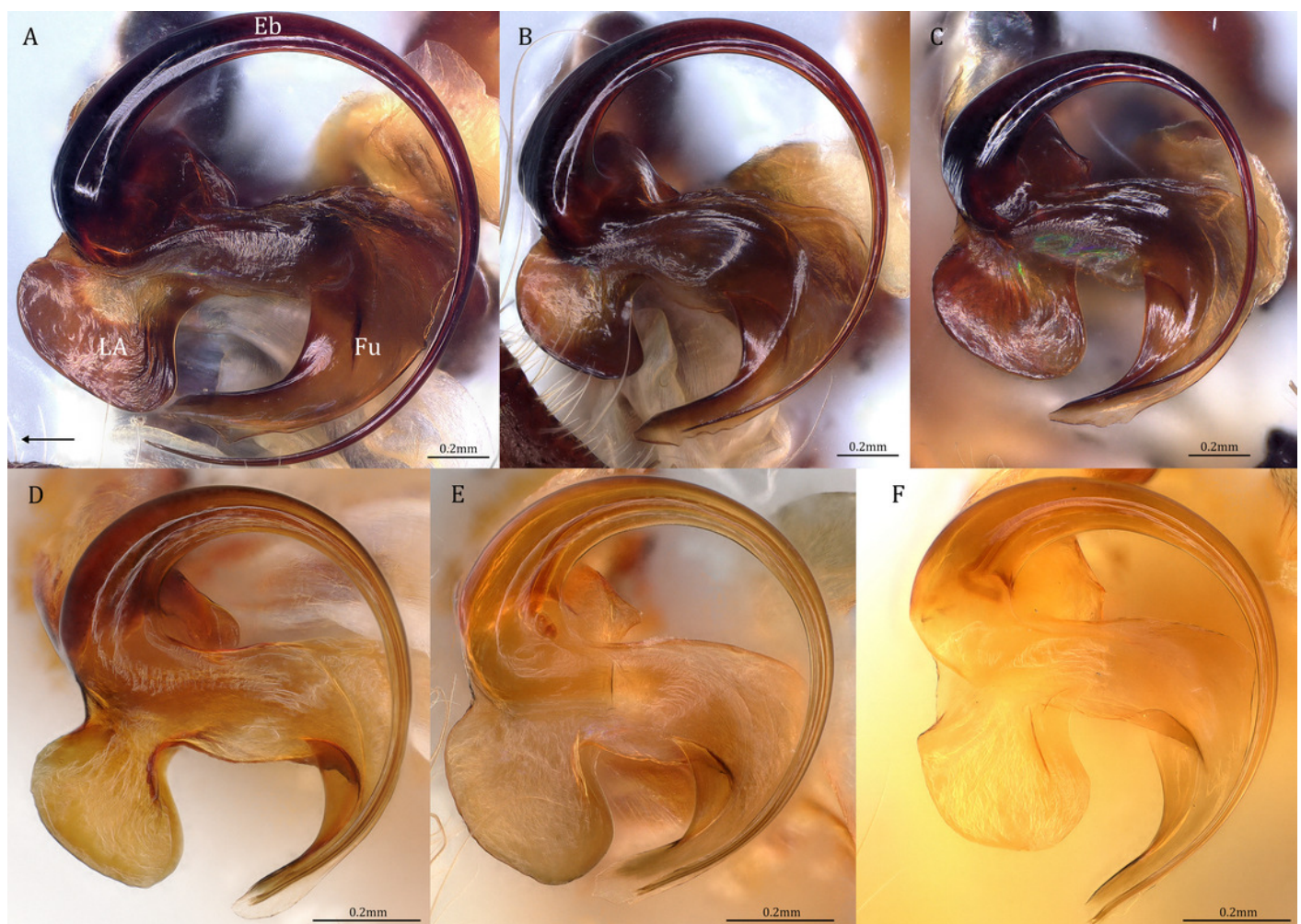
Figure 20

Comparisons of the female epigynum of the five *Dolomedes* species.

(A & F) *Dolomedes kalanoro* Silva & Griswold, 2013 (KPARA00193). (B & G) *D. gregoric* **sp. nov.** (Paratype female, USNMENT01580826). (C & H) *D. bedjanic* **sp. nov.** (Paratype female, USNMENT01580828). (D & I) *D. hydatostella* **sp. nov.** (Paratype female, USNMENT01580830). (E & J) *D. rotundus* **sp. nov.** (Paratype female, USNMENT01580832). (A–E) dorsal view with a line drawing showing the arrangement of the vulva, the circle represents the end of copulatory duct. (F– J) Ventral view, red arrows show the accessory bulb.
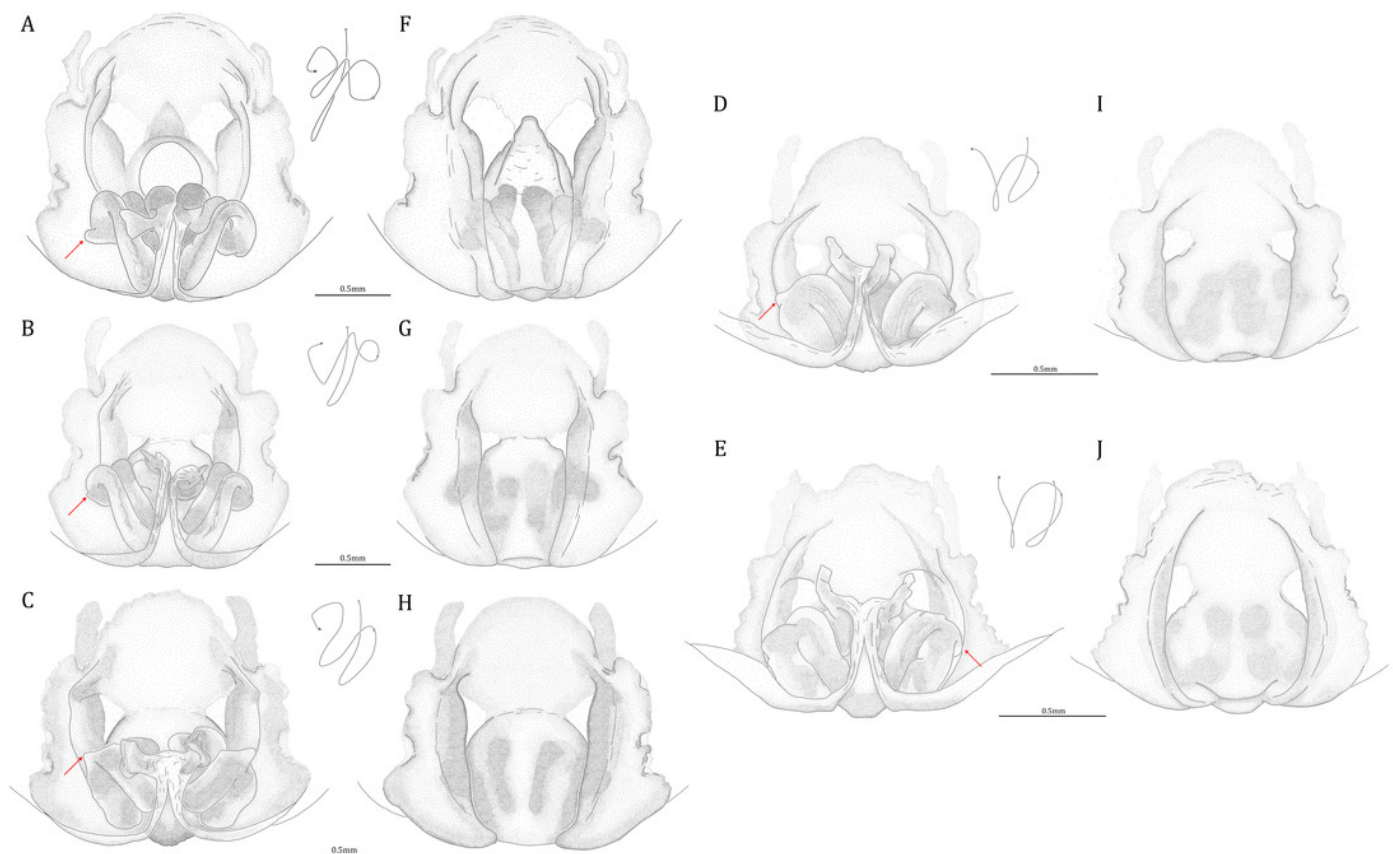
Figure 21

Posterolateral view of the left retrolateral tibial apophysis of the five *Dolomedes* species.

(A) *Dolomedes kalanoro* Silva & Griswold, 2013 (KPARA00185). (B) *D. gregoric* **sp. nov.** (Holotype male, USNMENT01580825). (C) *D. bedjanic* **sp. nov.** (Holotype male, USNMENT01580827). (D) *D. hydatostella* **sp. nov.** (Holotype male, USNMENT01580829). (E) *D. rotundus* **sp. nov.** (Holotype male, USNMENT01580831).
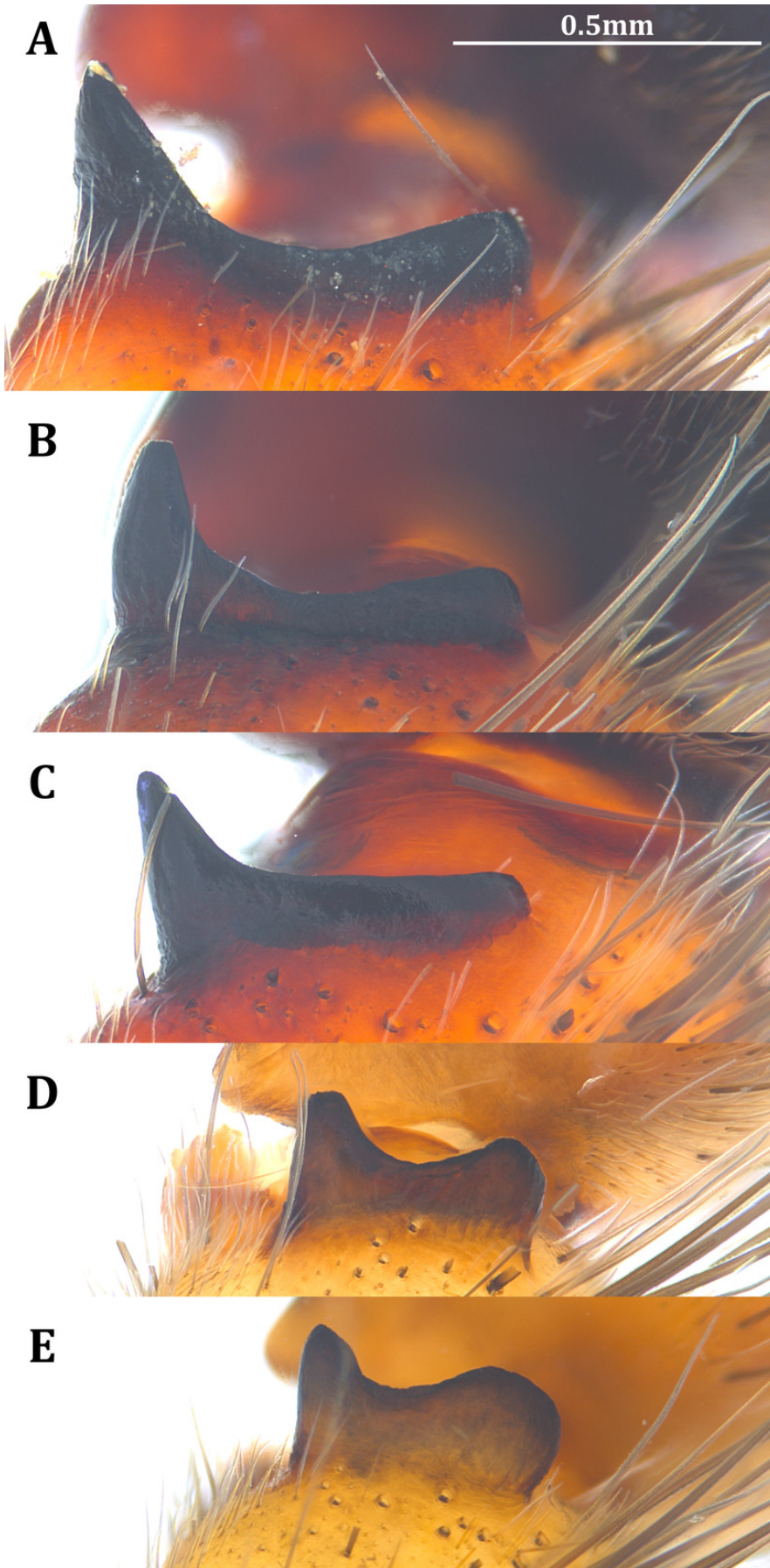
Figure 22

Dolomedes species collected from humid forests in the east and the north of Madagascar, showing the habitus coloration and variation.

(A–B) Dark morph *D. kalanoro* Silva & Griswold, 2013: (A) A female (KPARA00184) on a rock in a river; (B) a male (KPARA00185) at a river bank. (C–D) Dark morph *D. gregoric* **sp. nov.**: (C) A female (KPARA00250) in hunting pose on water; (D) a male (KPARA00248) placed on a white background. (E–F): *D. bedjanic* **sp. nov.**: (E) A female (KPARA00129) on a rock in a stream; (F) a male (KPARA00234) on shallow water under vegetation. (G–H) White banded morph *D. kalanoro*: (G) A male (KAPAR00227) hiding in a dead tree above a river during day time; (H) a female carrying an egg sac hiding in a tree trunk near a river during day time. (I) White banded morph *D. gregoric* **sp. nov.** (Holotype male, USNMENT01580825) on a tree trunk near a river. (J–K) *D. hydatostella* **sp. nov.**: (J) A female (KPARA00163) in a shallow understory swamp; (K) a male (KPARA00258) placed on a white background. (L–M) *D. rotundus* **sp. nov.**: (L) A female (KPARA00243), and (M) a male (KPARA00236) in a shallow, still part of a stream.

Figure 23

Male *Dolomedes kalanoro* Silva & Griswold, 2013 (KPARA00185).

(A) Dorsal view. (B) Anterior view. (C–D) Left palp: (C) Ventral view; (D) retrolateral view showing the length ration between cymbium and tibia. (E–F) Left palp: (E) Ventral view; (F) retrolateral view showing the detailed structure of male genital. BCA: basal cymbium apophysis; COp: conductor; Cy: cymbium; DTP: distal tegular projection; Eb: embolus; Fu: fulcrum; MA: median apophysis; RTA: retrolateral tibial apophysis; Sa: saddle; St: subtegulum; T: tegulum; VTA: ventral tibial apophysis.

Figure 24

Female *Dolomedes kalanoro* Silva & Griswold, 2013 (KPARA00193).

(A) Dorsal view. (B) Anterior view. (C–E) Epigynum: (C) ventral view; (D) lateral view, the arrow showing the horn extension; (E) dorsal view. CD: copulatory duct; COp: copulatory opening; EF: epigynal fold; FD: fertilization duct; LL: lateral lobe; MF: middle field.
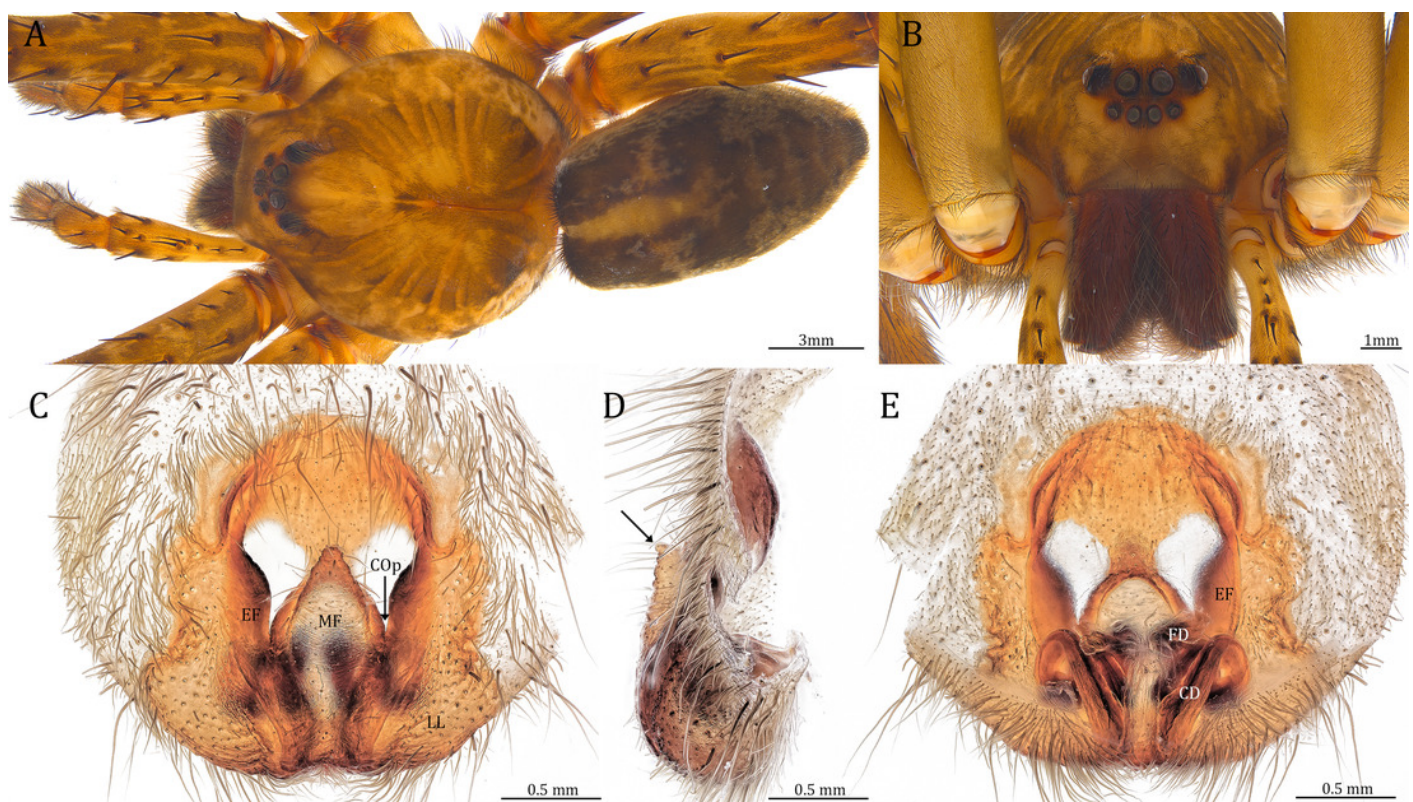
Figure 25

Male *Dolomedes gregoric* sp. nov. (Holotype, USNMENT01580825).

(A) Dorsal view. (B) Anterior view. (C–D) Left palp: (C) Ventral view; (D) retrolateral view showing the length ration between cymbium and tibia. (E–F) Left palp: (E) Ventral view; (F) retrolateral view showing the detailed structure of the male genital.

Figure 26

Female *Dolomedes gregoric* sp. nov. (Paratype, USNMENT01580826).

(A) Dorsal view. (B) Anterior view. (C–D) Epigynum: (C) Ventral view; (D) dorsal view.
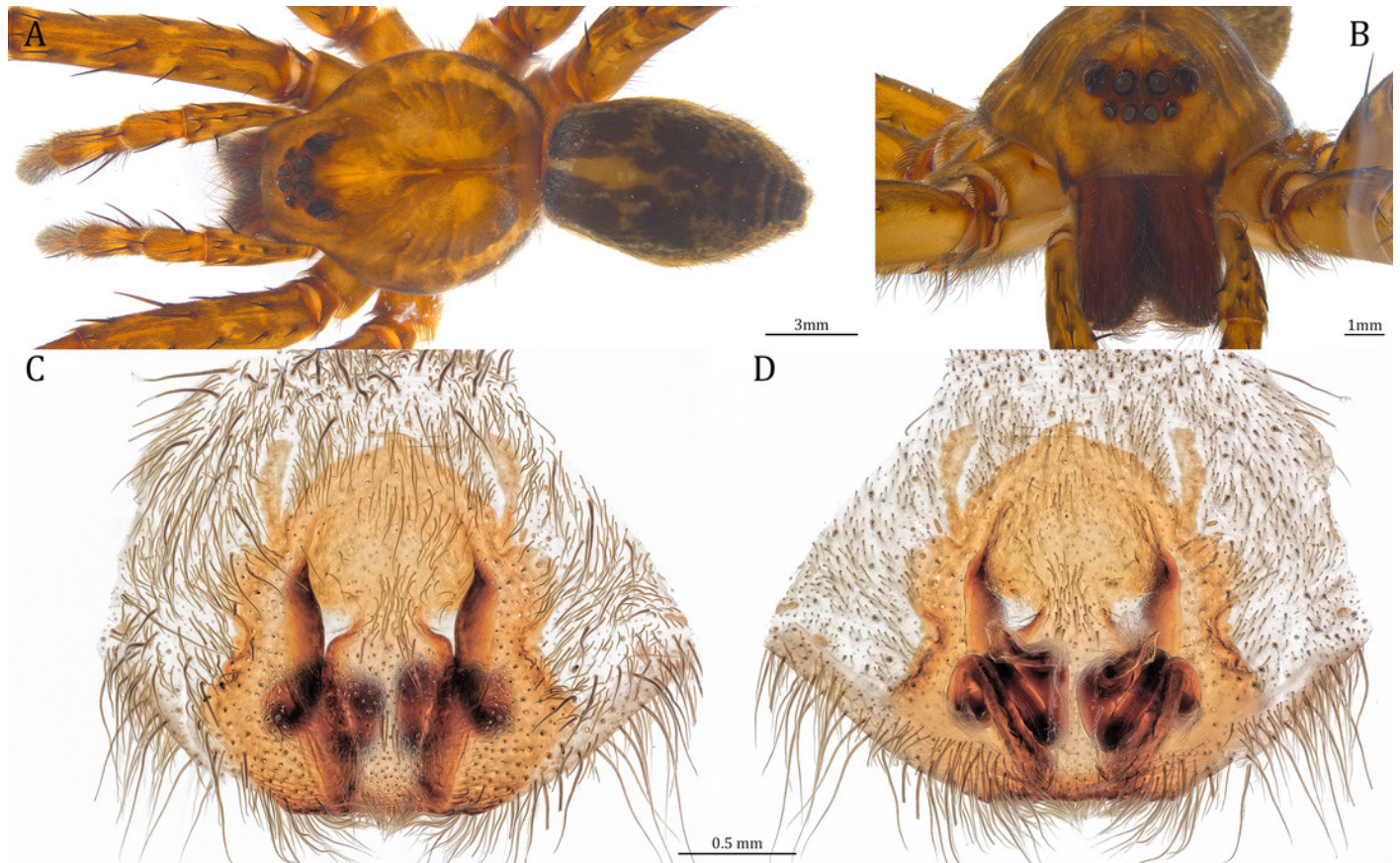
Figure 27

Male *Dolomedes bedjanic* sp. nov. (Holotype, USNMENT01580827).

(A) Dorsal view. (B) Anterior view. (C–D) Left palp: (C) Ventral view; (D) retrolateral view showing the length ration between cymbium and tibia. (E–F) Left palp: (E) Ventral view; (F) retrolateral view showing the detailed structure of the male genital.

Figure 28

Female *Dolomedes bedjanic* sp. nov. (Paratype, USNMENT01580828).

(A) Dorsal view. (B) Anterior view. (C–D) Epigynum: (C) Ventral view; (D) dorsal view.
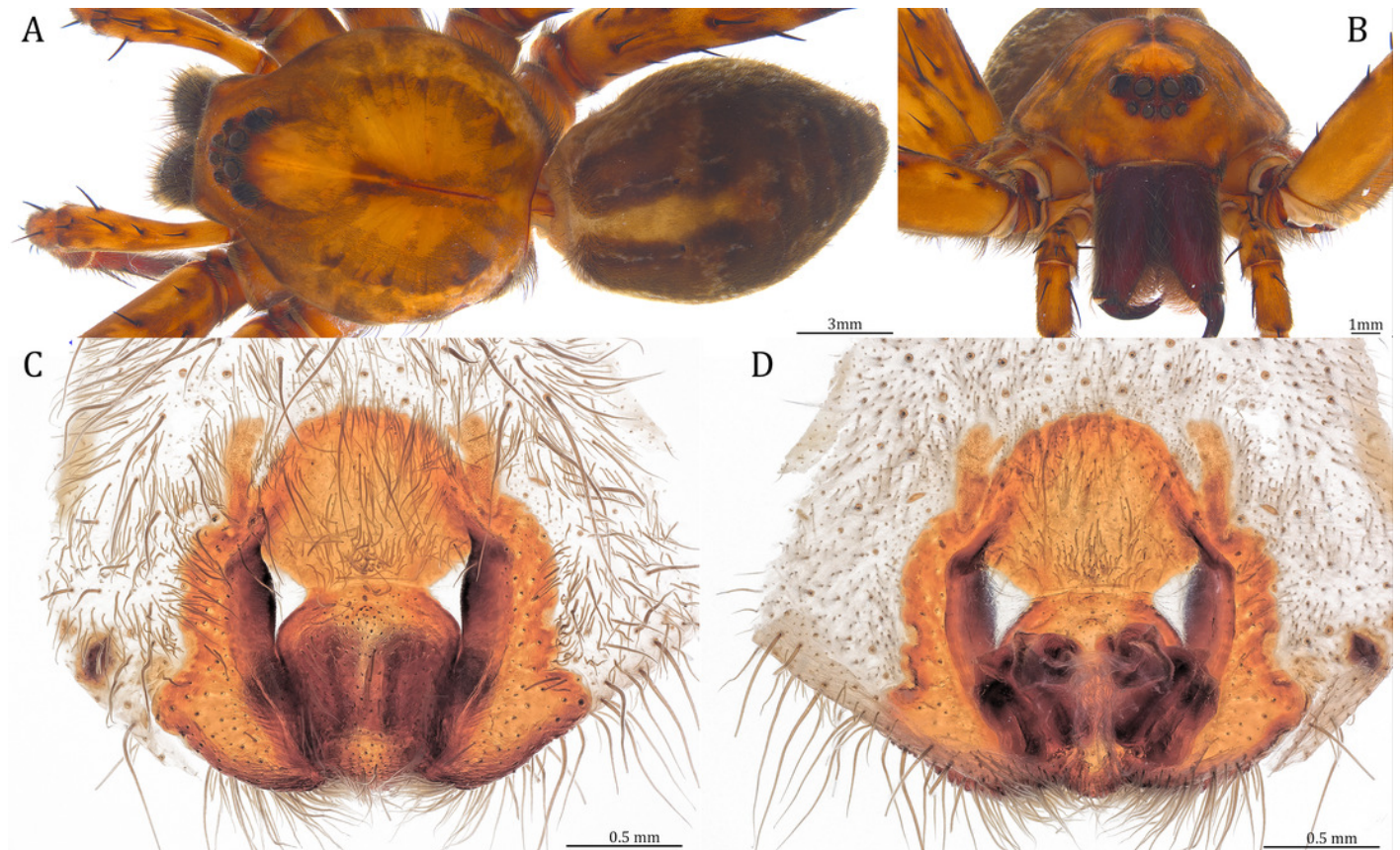
Figure 29

Male *Dolomedes hydatostella* sp. nov. (Holotype, USNMENT01580829).

(A) Dorsal view. (B) Anterior view. (C–D) Left palp: (C) Ventral view; (D) retrolateral view showing the length ration between cymbium and tibia. (E–F) Left palp: (E) Ventral view, the black arrow showing the lateral lobe on the fulcrum; (F) retrolateral view showing the detailed structure of the male genital.
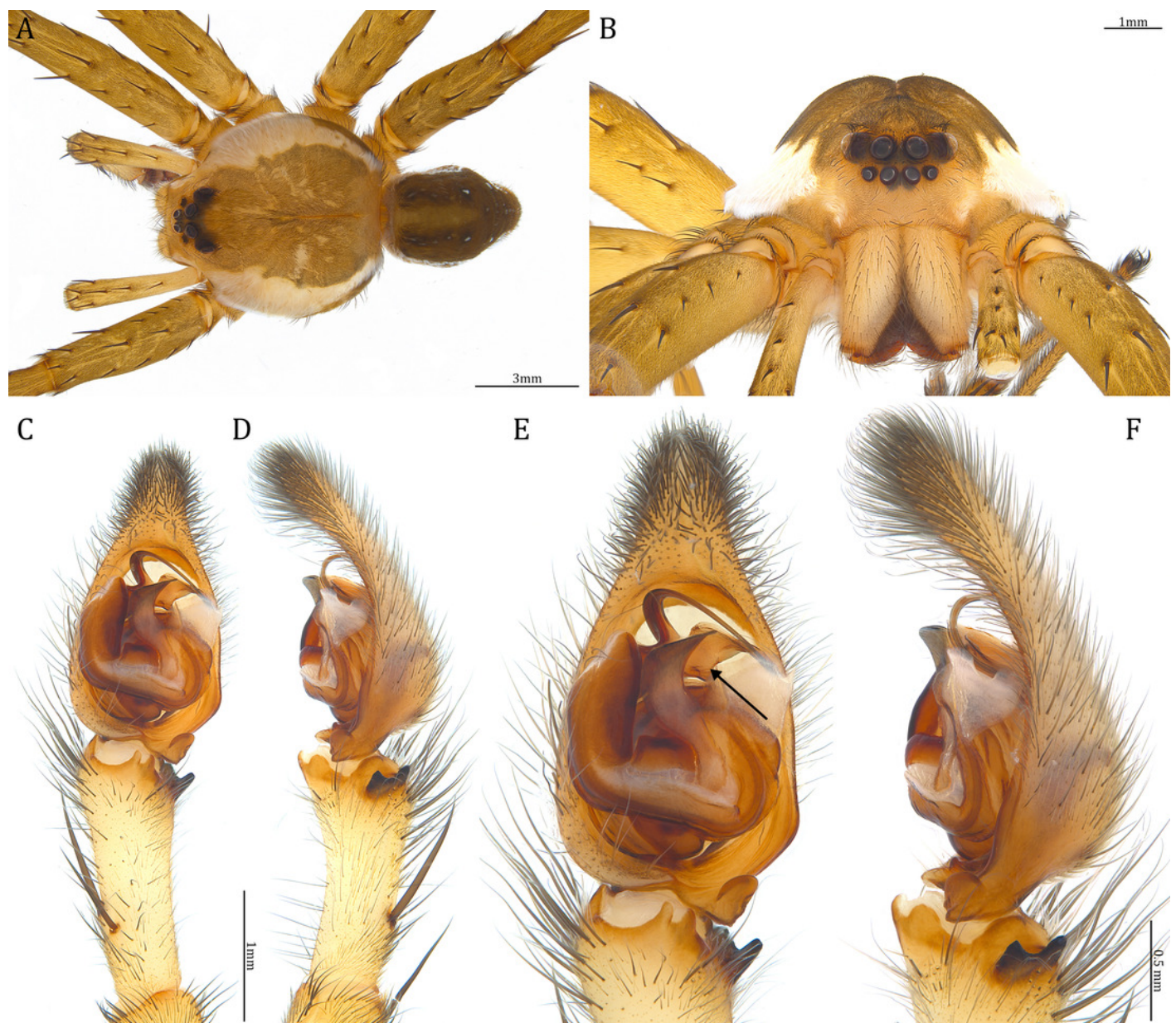
Figure 30

Female *Dolomedes hydatostella* sp. nov. (Paratype, USNMENT01580830).

(A) Dorsal view. (B) Anterior view. (C–D) Epigynum: (C) Ventral view; (D) dorsal view.
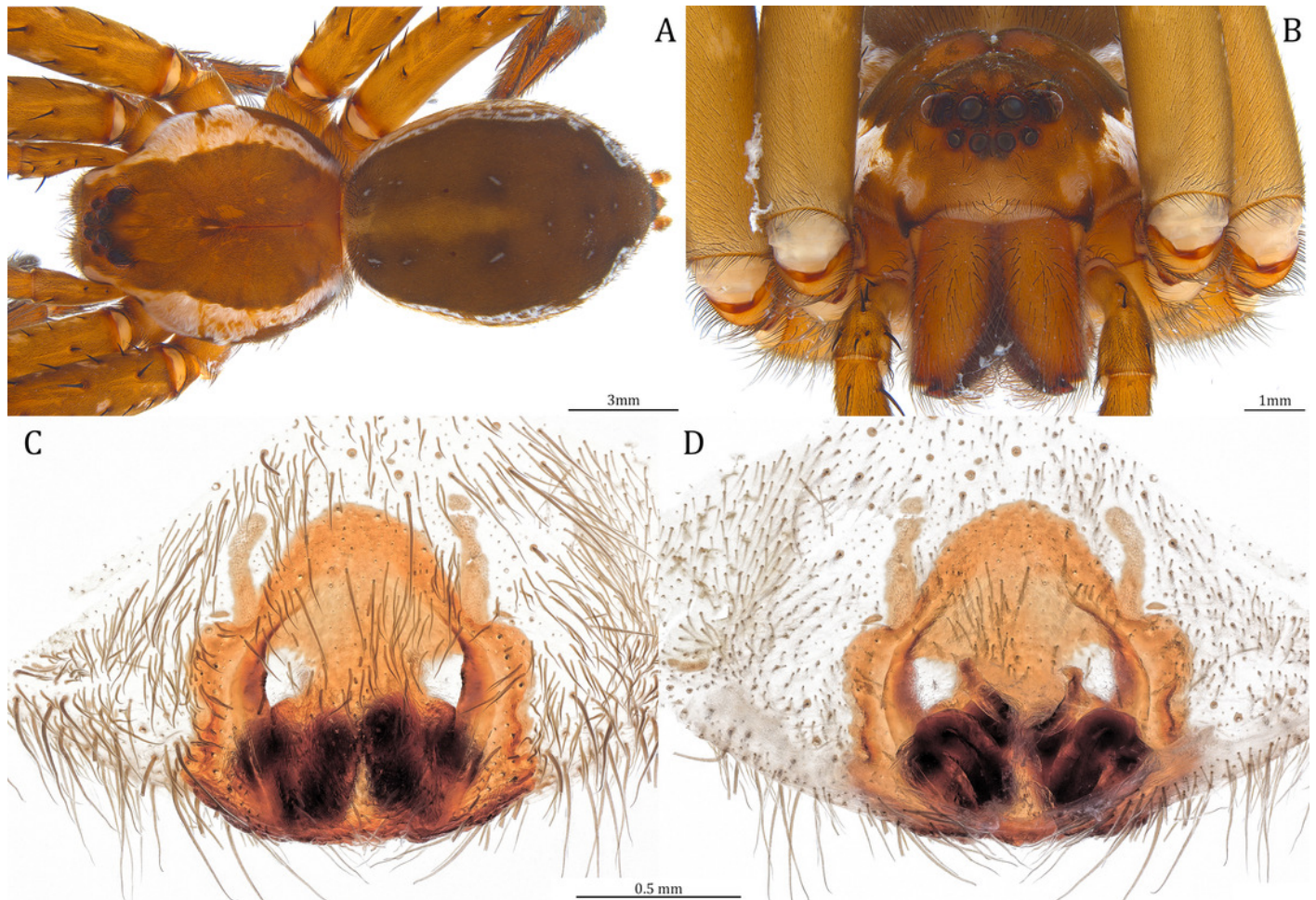
Figure 31

Male *Dolomedes rotundus* sp. nov. (Holotype, USNMENT01580831).

(A) Dorsal view. (B) Anterior view. (C–D) Left palp: (C) Ventral view; (D) retrolateral view showing the length ration between cymbium and tibia. (E–F) Left palp: (E) Ventral view; (F) retrolateral view showing the detailed structure of the male genital.

Figure 32

Female *Dolomedes rotundus* sp. nov. (Paratype, USNMENT01580832).

(A) Dorsal view. (B) Anterior view. (C–D) Epigynum: (C) Ventral view; (D) dorsal view.